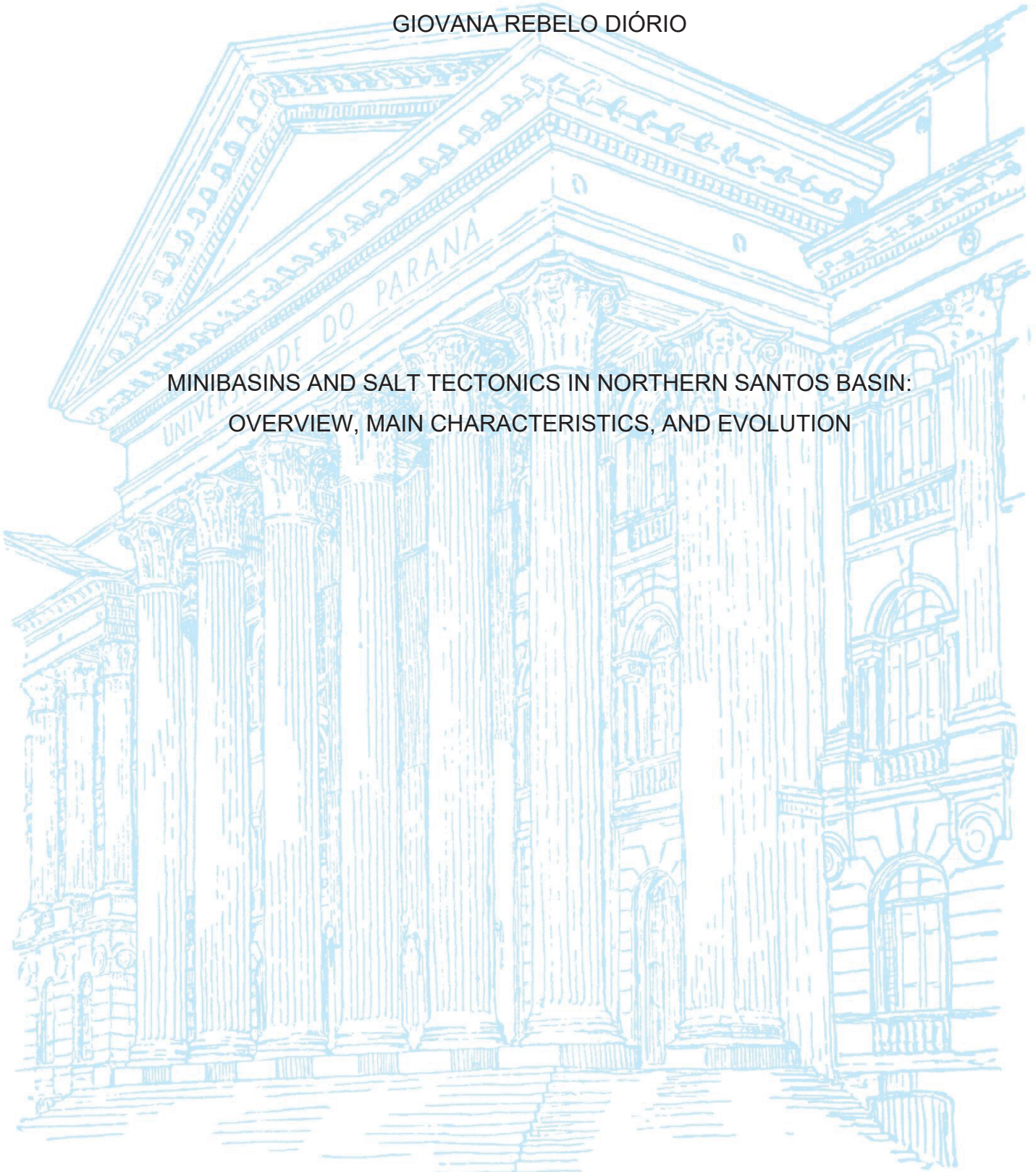UNIVERSIDADE FEDERAL DO PARANÁ

GIOVANA REBELO DIÓRIO

MINIBASINS AND SALT TECTONICS IN NORTHERN SANTOS BASIN:
OVERVIEW, MAIN CHARACTERISTICS, AND EVOLUTION

CURITIBA

2024

GIOVANA REBELO DIÓRIO

MINIBASINS AND SALT TECTONICS IN NORTHERN SANTOS BASIN:

OVERVIEW, MAIN CHARACTERISTICS, AND EVOLUTION

Dissertação apresentada ao Programa de Pós-Graduação em Geologia, Setor de Ciências da Terra, Universidade Federal do Paraná, como requisito à obtenção do título de Mestre em Geologia.

Orientadora: Profª. Drª. Barbara Trzaskos

CURITIBA

2024

TERMO DE APROVAÇÃO

Os membros da Banca Examinadora designada pelo Colegiado do Programa de Pós-Graduação GEOLOGIA da Universidade Federal do Paraná foram convocados para realizar a arguição da dissertação de Mestrado de **GIOVANA REBELO DIÓRIO** intitulada: **MINIBASINS AND SALT TECTONICS IN OFFSHORE NORTHERN SANTOS BASIN: OVERVIEW, MAIN CHARACTERISTICS, AND EVOLUTION**, sob orientação da Profa. Dra. BÁRBARA TRZASKOS, que após terem inquirido a aluna e realizada a avaliação do trabalho, são de parecer pela sua APROVAÇÃO no rito de defesa.

A outorga do título de mestra está sujeita à homologação pelo colegiado, ao atendimento de todas as indicações e correções solicitadas pela banca e ao pleno atendimento das demandas regimentais do Programa de Pós-Graduação.

CURITIBA, 26 de Abril de 2024.

Assinatura Eletrônica
27/04/2024 11:11:29.0
BÁRBARA TRZASKOS
Presidente da Banca Examinadora

Assinatura Eletrônica
30/04/2024 10:33:25.0
FERNANDO CESAR ALVES DA SILVA
Avaliador Externo (UNIVERSIDADE FEDERAL DO RIO GRANDE DO NORTE)

Assinatura Eletrônica
29/04/2024 11:26:13.0
LUCIANO PORTUGAL MAGNAVITA
Avaliador Externo (UNIVERSIDADE FEDERAL DO RIO DE JANEIRO)

DEPARTAMENTO DE GEOLOGIA-CENTRO POLITÉCNICO-UFPR - CURITIBA - Paraná - Brasil
CEP 81531-990 - Tel: (41) 3361-3365 - E-mail: posgeol@ufpr.br
Documento assinado eletronicamente de acordo com o disposto na legislação federal Decreto 8539 de 08 de outubro de 2015.
Gerado e autenticado pelo SIGA-UFPR, com a seguinte identificação única: 361019
**Para autenticar este documento/assinatura, acesse https://siga.ufpr.br/siga/visitante/autenticacaoassinaturas.jsp
e insira o codigo 361019**

Ministério da Educação
UNIVERSIDADE FEDERAL DO PARANÁ
Setor de Ciências da Terra
Programa de Pós-Graduação em Geologia

D E C L A R A Ç Ã O

Declaramos para os devidos fins que **GIOVANA REBELO DIÓRIO** realizou sua defesa de dissertação intitulada "**MINIBASINS AND SALT TECTONICS IN OFFSHORE NORTHERN SANTOS BASIN: OVERVIEW, MAIN CHARACTERISTICS, AND EVOLUTION**" em 26 de abril de 2024, no Programa de Pós-Graduação em Geologia da Universidade Federal do Paraná, área Geologia Exploratória, nível Mestrado, e que por sugestão da banca examinadora, o título foi alterado para "**MINIBASINS AND SALT TECTONICS IN NORTHERN SANTOS BASIN: OVERVIEW, MAIN CHARACTERISTICS, AND EVOLUTION**".

Curitiba, 22 de julho de 2024.

Prof. Dr. Leonardo Fadel Cury
Coord. Programa de Pós-Graduação em Geologia
Setor de Ciências da Terra
Universidade Federal do Paraná

RESUMO

A tectônica salífera relacionada ao sal Aptiano (Fm. Ariri) influenciou a evolução de minibacias (depressões sin-halocinéticas) na Bacia de Santos, cuja porção norte é a maior produtora de hidrocarbonetos do Brasil. Logo, este estudo realizou o mapeamento sismoestratigráfico do bloco sísmico 3D Franco-Iara, traçando cinco superfícies (base e topo do sal, Turoniano, topo do Cretáceo e fundo do mar), gerando quatro isópacas (Fm. Ariri, Fm. Camburi, Fm. Frade e Fm. Itamambuca), identificando estruturas e geometrias intra-sal e distinguindo as principais características das minibacias em planta e secção, e reconhecendo sistemas sedimentares de águas profundas. Corpos de sal autóctones (espessura de 340 a 3170 m) diminuem maturidade em direção à bacia (muralhas de sal, *salt stocks* e *welds* à NW e anticlinais de sal à SE). Para o nordeste, há muralhas e anticlinais de sal de direção E/W com dobras isoclinais, enquanto no sul prevalecem anticlinais N/S com cavalgamentos intra-sal. Na base do sal, rampas de alto ângulo (>5°) separam altos estruturais em dois *trends* (NW/SE e NE/SW). A muralha de sal de Itapu-Búzios é uma muralha assimétrica de direção E/W, de 20 km de largura, com anticlinais casco de tartaruga, grabens cristas proeminentes (deslocamentos de 350 m), falhas lístricas cenozoicas e falhas en *échelon* em suas extremidades. Minibacias são arredondadas a alongadas, com diâmetros de até 10 km e espessuras entre 2,5 e 1,8 km. A Fm. Camburi é a menos espessa (max. 800 m), depocentros são circulares ou alongados em E/W, com larguras de 3 km, e predominam depocentros verticalmente empilhados, seguidos por subbacias e depocentros migrantes. A Fm. Frade é a mais espessa (max. 2.2 km), com mudanças constantes nas larguras dos depocentros (até 10 km) e geometrias tanto em planta (circulares a alongadas N/S) quanto em seção (predominam depocentros migrantes, seguidos por empilhados, mas com mergulho). O Cenozoico é marcado por MTDs halocineticamente influenciados, que variam em extensão (25-58 km^2) e espessura (45-110 m). A Fm. Itamambuca possui os maiores depocentros (larguras de até 15 km), circulares, com predominância de depocentros migrantes, seguidos por empilhados verticalmente. A área de Franco-Iara registra a relação entre a evolução da tectônica salífera e minibacias. A Fm. Camburi registra uma fase inicial Albo-Cenomaniana de movimentação de sal radialmente convergente ao sul (formando corpos de sal e minibacias alongados em E/W), levando ao surgimento da muralha de Itapu-Búzios próximo a sub-bacias, além da formação de minibacias por diferença de densidade em áreas de baixo da base de sal. A Fm. Frade registra duas tendências do Cretáceo Superior: entrada sedimentar ao norte com propagação do sal para sul; e transladação do sal para leste formando minibacias alongadas N/S, *ramp syncline basins* e feições de contração em corpos de sal N/S, possivelmente relacionada à formação do Gap Albiano. A Fm. Itamambuca registra uma fase de declínio da tectônica salina (muralhas de sal colapsam e corpos de sal em altos da base do sal continuam a ascender), influenciados por ambientes sedimentares.

Palavras-chave: Mapeamento sismoestratigráfico; pós-sal; evolução tectonoestratigráfica; Formação Ariri.

ABSTRACT

Aptian salt (Ariri Fm.) underwent salt tectonics influencing the evolution of post-salt minibasins (synhalokinetic depressions) in Santos Basin. The northern part of this Basin is the most important Brazilian hydrocarbon producer, and studies there focus on the pre-salt rather than the intra-salt and post-salt. This study fills this gap by seismostratigraphically mapping the 3D Franco Iara seismic block. It emphasized five key-surfaces (salt-base, top-salt, Turonian, top of Cretaceous, seafloor) and four time-intervals isopaches (Aptian evaporitic Ariri Fm., Albian-Cenomanian Camburi Gr., Turonian-Maastrichian Frade Gr., Cenozoic Itamambuca Gr.), identifying intra-salt structures and geometries, minibasins' main characteristics in plan-view and cross-sections, and some deep-water sedimentary systems. Autochthonous salt bodies from Ariri Fm. (thickness ca. 340 to 3,170 m) decrease in maturity basinwards (NW salt walls, stocks and welds, and SE salt anticlines). Towards the north-east there are salt walls and anticlines with an E/W direction and intra isoclinal folds, whereas in the south N/S salt anticlines with intra-salt fold-and-thrust prevail. In the salt-base, higher (>5°) dipping angles separate structural highs in two main trends (NW/SE and NE/SW). Itapu-Búzios salt wall is a major (>20 km wide) E/W asymmetric salt wall with mock-turtle anticlines, prominent crestal grabens (offsets of ca. 350 m), Cenozoic listric faults and *en échelon* faults in its ends. Post-salt minibasins exhibit a rounded to N/S elongated shape, with diameters up to 10 km and maximum thicknesses between 2.5 to 1.8 km. Camburi Gr. is the least thick (max. ca. 800 m), depocenters are near-circular or E-W elongated in plan-view, with widths of ca. 3 km, and there is a predominance of vertically stacked depocenters, followed by subbasins and changing depocenters mainly in the northern and eastern areas. Frade Gr. is the thickest one (max. ca. 2.2 km), and there are constant changes in depocenters' widths (up to 10 km), and geometries both in plan-view (rounded-shaped to N-S elongated) and cross-section (predominance of changing depocenters, followed by stacked but dipping). The Cenozoic passage is marked hallokinetic-influenced MTDs aligned in a W/E trend, with varying areal extents (25-58 km^2) and thickness (45-110 m). Itamambuca Gr. presents the largest (widths up to 15 km) depocenters, which are predominantly rounded-shaped, with a predominance of changing depocenters, followed by vertically stacked ones. A further aspect in the Franco Iara area is that it records the relationship between the evolution of salt tectonics and minibasins. Camburi Gr. records an Albian-Cenomanian initial phase of radially convergent of salt movement towards the south (forming EW-oriented salt bodies and EW-elongated minibasins), leading to the rise of Itapu-Buzios salt wall nearby subbasins, and initiating density-driven minibasins in base-salt low-relief areas. Frade Gr. records two Upper Cretaceous trends: northern sedimentary input and salt spreading towards the south; and salt E-directed translation forming N-S elongated minibasins, ramp syncline basins and contraction-related features within N/S salt bodies, which might be related to the Albian Gap formation. Cenozoic Itamambuca Gr. records a phase of decreasing salt tectonics (mature salt walls collapse and salt bodies above salt-base high continue rising), increasingly influenced by sedimentary settings.

Keywords: Seismostratigraphic mapping; Post-salt; Tectonostratigraphic evolution; Ariri Formation.

*"Pensou que seria melhor se acostumar
logo ao conflito interno. Seu palpite
era de que a ambivalência perduraria até
o fim da viagem."*

(Julia Quinn)

*"E Coraline piange, Coraline ha l'ansia
Coraline vuole il mare, ma ha paura dell'acqua
e forse il mare è dentro di lei"*

(Coraline – Måneskin)

AGRADECIMENTOS

Se prepare - sou grata e emocionada (e, sinceramente, adoro algum motivo para brindar), logo essa seção será mais longa que o usual.

Primeiro, ao óbvio que precisa ser dito. À Barbara Trzaskos, minha orientadora e grande mentora geológica, em quem me inspiro de tantas formas. Não somente uma geóloga de mente questionadora, mas uma orientadora presente e uma pessoa de coração tão grande. Foi um imenso prazer ter você por perto em uma fase tão inicial e fundamental da minha vida profissional. Ao LABAP, que me acolheu, me forneceu os equipamentos necessários e virou um espaço que guardo com muito carinho. À UFPR, lar desde 2015, que me propiciou muito mais oportunidades e conhecimentos do que consigo mensurar, e ao Programa de Pós-graduação em Geologia pela oportunidade de me aprimorar mais nessa área que tanto amo. À PETROBRAS, pelas bolsas de estudo, fomentos e oportunidades através dos projetos Caruaçu e Trapas. À ANP por disponibilizar os dados usados nessa pesquisa. À DGB Earth Science pelo acesso ao OpendTect PRO. À Katalyst DM pelo acesso ao Geopost, e especialmente a Michele Reis pelo suporte. Ao Prof. Dr. Fernando Vesely pelos ensinamentos sempre tão divertidos e enriquecedores. À Paula Carolina Empinotti Pereira pelo auxílio em questões burocráticas. À minha banca de qualificação (Dr. Savio Garcia e PhD. Leonardo Muniz Pichel) e defesa (Dr. Luciano Magnavita e Prof. Dr. Fernando Cesar Silva), pelos importantes apontamentos e contribuições. À Geo Logica e ao Pedro Barreto pela oportunidade de participar da *3rd Salt Basins Technical Interest Group Field Trip: Salt Diapirism and Sediment Interactions in Portugal*, fundamental para a conclusão desse trabalho. À PROAP pelo auxílio financeiro essencial para a participação em eventos e treinamentos que fiz nesses dois anos. Aos que auxiliaram com revisões e discussões no artigo principal dessa dissertação: Barbara Trzaskos, Leonardo Pichel, Sérgio Dias e Vanessa Assis. E à Terra, sempre cheia de mistérios que se revelam aos poucos.

Em segundo, ao que está atrás do palco - desconhecido aos que apenas assistem, mas indispensável. Ao Guillan Fayad, que foi meu maior companheiro, apoiador e fonte de conforto nesses últimos dois anos, sempre paciente e sabendo quando e como estar presente (não teria conseguido sem você!). À Juliana Jubes (JuJu) e à Bruxa, filhas de coração, que eu vi crescer sem nunca deixarem de ser quem são e que me trouxeram tanto conforto, diversão, carinho e amor sem usar uma só palavra. À Carla e ao Chico, que me deram segurança e confiança para começar a traçar meus próprios caminhos. Às fiéis escudeiras do role de terça, Kaiana Mosko e Manuela Miquelito, que escutam sem julgamento, aconselham sem medo e sentem em sintonia. À Fernanda Reis, a melhor colega de casa e fonte inesgotável de memes com quem eu tenho o prazer de compartilhar momentos dos meus dias. Ao Sergio Leon Dias, que sente de forma tão semelhante à minha e com quem me uni no desespero para vencer prazos e inseguranças (e na alegria de aproveitar bons momentos, afinal você foi um presente que o mestrado me deu). À Vanessa Assis, que sabe enraizar meus pés no chão, tornar as coisas simples e leves e se animar para esquecer de coisas acadêmicas e falar de coisas banais. Ao Giordano Bruno Hurtado, que não teme nenhuma e acolhe todas as minhas facetas. Ao Gabriel Sereneski, por trazer alegria e ver o lado bom da vida. Ao Sebastião de Oliveira, Miguel Palú, Andreas Pauli, Kendra Souza, Nicole Calil, Maciel Rudnick e Winicius Silva, amigos de longa data, pela boa e acolhedora nostalgia que trazem às novidades inquietantes. Aos LABAPERS (Bruno Gomes, Gabriela Velasquez, Deise Silveira, Leonardo Barão, Ronaldo Kraft e Thammy Ellin), com quem compartilhei o cotidiano

e seus trabalhos, matérias, confraternizações, felicidades, angústias e aprendizados. À Mariana Lemos, Fernanda Avelar, Yara Mello e Edgar Sanches, que me ensinaram muito sobre pesquisa, confiaram em meu trabalho e me deram a oportunidade de crescer e aprender cientificamente. À Lara Lange, a primeira geóloga a me apresentar esse e outros mundos, e que ainda hoje me inspira. Ao meu pai Alan Diório e à minha mãe Fernanda Rebelo, que sempre torceram por mim e me deram asas para voar, mas sempre mantiveram um espaço no ninho para quando preciso voltar. Ao meu irmão, Alan Fernando Rebelo Diório, que me ensina calma na hora de priorizar e coragem na hora de ser quem somos. Aos Rebelo, meu sol, meu Norte, minha família que me moldou desde tão pequena, mas nesses dois anos agradeço especialmente Marcela, Carolina, Victor, Eduardo, Thiago, Paula, Herminia, Ana e Teresa, que estiveram presentes para me lembrar de minhas raízes, abraçar minhas dores e me incentivar. À toda a equipe da Influx Portão (em especial a Paty, Isadora, Flavia, Mari, Talita, Leticia, *Maestra* e Anaís), onde aprendi e me diverti muito ensinando. À equipe da UBT escalada Curitiba (em especial as brabas Loren Margonar, Maria Eduarda Ososki, Giulia Ulbrich, Rafaela Pontes, Luma Ramos, Lana Evangelista e Gabriela Castro), que me ensinaram uma nova forma de ver rochas. Aos amigos que fiz aprendendo novas formas de movimentar meu corpo para acompanhar a minha mente – a yoga, a bicicleta, a escalada, o circo-, em especial Gabriela Cleto, Roberto (Lagarto), Rafaela Schaefer, Gustavo C(r)osta, Matias Maranhão, Isabel Witt Lunardi, Milena Beckert, Naiane Crisóstomo e Viviane Torzetto.

Em terceiro, de forma nada convencional, à cidade que me tornou quem sou. À Curitiba. Às incontáveis vezes que reclamei do clima. Ao caos hierárquico do Centro. Aos chiques triângulos do Juvevê. À ciclovia do Belém. Aos interparques. À feirinha do Largo. Aos pedais de quarta. Aos borrachudos dos parques. Aos dogões de fim de role. Às canaletas e viradas de cabeça estratégicas na contramão. Às arvores, impedidas de subir aos fios de luz e que lutam para cobrir as ruas com seus galhos e destruir calçadas com suas raízes. Aos cachorros do MON. Às corridas pela Avenida das Torres. Aos parques que sempre sei chegar e nunca lembro os nomes. Ao Curitiba/São José. Ao 905, onde sai de casa, e ao 72, onde me senti em casa. Ao nascer do sol das minhas janelas. Às idas ao Cataia, ao Frigideira Torta, ao Baba, a Trajano, a Itupava, a Vicente Machado, à Farmacinha. Aos morros que circundam a cidade, visíveis em dias limpos e de sol. À Serra do Mar, Morretes e o litoral. Até mesmo aos dias cinzas – que em raras vezes foram incrivelmente desfrutáveis. E, claro, a São Francisco do Sul, porque Curitiba não seria suportável sem as fugas até Ubatuba.

E, por fim, alguém que raramente ousamos pronunciar ou levar em conta na hora de agradecer. Alguém que levei anos para consolidar em pensamentos, e agora -com muita audácia- externalizarei de forma escrita. A mim. À jornada que me propus a intensificar nesses últimos dois anos. Me tornei mestre em Geologia, mas uma mera aprendiz em mim mesma. À bela inconstância do meu incoerente e complexo ser. Às minhas metamorfoses. À fluidez dos meus gostos e desgostos. Às minhas formas de expressão. Ao meu coração, que mesmo quebrado, já tendo deixado várias partes para trás e nitidamente remendado da melhor forma que pude ainda pulsa constantemente e dita a marcha que sigo. À liberdade que provei de forma tão breve tantas vezes, e que corro atrás todos os dias. Às memórias que nem lembro, e às sensações que sinto sem saber a origem. A tudo que eu falei, pensei, e ainda nem descobri. Aos machucados, visíveis ou não, abertos ou fechados, cicatrizados ou eternamente no processo. Aos momentos que abusei do meu corpo para fugir da

minha mente, e aos momentos que entrei na minha mente buscando ignorar meu corpo. À introspectiva e à expansiva, que hora precisa estar fora e hora não quer sair de casa. A todos os momentos que só consegui conversar sozinha, e às vezes que só entendi depois de falar em voz alta. À noite que escutou minhas suplicias e sonhos, e ao dia que recarregou minhas energias. A toda a água que coloquei para fora, as lágrimas, o sangue, o suor, a saliva. Às vezes que eu lutei, dando tudo sem ter nada. Quando não correspondi às minhas expectativas, me neguei um sim, roí minhas próprias garras. A todos que eu amei e não ficaram ou sequer souberam, e aos que ficaram até que virasse amor. À todas as vezes que o mínimo pareceu extraordinário - e vice-versa. Às vezes que a alegria irradiou do corpo, meus olhos expandiram para além do olhar, o canto não pode ser segurado, o toque não foi contido, a dança veio de dentro. A todas as trilhas que caminhei, os livros que devorei, as músicas que decorei, as vias que não terminei, os momentos que não estive lá. E ao lindo processo de conhecer a Terra e o mundo que existe dentro de si mesmo.

FIGURES

Chapter 3. Methodology

Chapter 4. Results & Discussion

TABLES

SUMMARY

1 INTRODUCTION

Evaporite sequences (referred to as salt) are common, yet unique and remarkable features in many sedimentary basins. Salt behaves as a viscous fluid when affected by gravity (i.e., gliding or spreading) or regional stresses, producing three-dimensionally complex structures and significantly influencing the tectonostratigraphic architecture of sedimentary basins. Understanding salt tectonics is crucial to constrain the evolution, stratigraphy, and kinematics of deformation in any salt basin, including passive margins (e.g. Jackson & Talbot 1986, Jackson & Talbot 1991, Vendeville & Jackson 1992, Warren 2006, Hudec & Jackson 2007, Fossen 2010, Jackson & Hudec 2017).

Minibasins (defined by Worrall & Snelson 1989, reviewed by Hudec et al. 2009) describe basins formed by salt tectonics. They are syn-kinematic basins in the order of tens of kilometers in diameter, surrounded by (i.e., lateral edges) and subsiding into relatively thick allochthonous or autochthonous evaporites, with relatively short lifespans but fast subsidence compared to crustal basins (Jackson & Talbot 1991, Hudec et al. 2009, Ingersoll 2012, Jackson & Hudec 2017, Hudec & Jackson 2022). These depocenters can originate from various settings (Hudec et al. 2009) and their evolution is closely linked to the processes that occur during their infiling.

Among wordwide passive continental margin basins influenced by salt tectonics (Jackson & Hudec 2017) the Santos Basin is located offshore southeastern Brazil (Fig. 1.1a) and was formed during the Gondwana rupture in the Cretaceous (Assine et al. 2008, Chang et al. 2008, Kukla et al. 2018). It is currently the most significant petroleum basin in the country, characterized by prominent salt deposition in the Aptian (Moreira et al. 2007, Chang et al. 2008). The evaporitic Ariri Formation was deposited during the latest stages of rifting, prior to continental breakup, when most tectonic activity had ceased, with increasing thermal subsidence (Moreira et al. 2007, Quirk et al. 2012, Rowan 2014).

The Ariri Formation significantly influenced the subsequent post-salt sequence. While extensive knowledge exists regarding the tectonosedimentary and halokinetic evolution of Santos Basin, most studies are either regional (Kumar & Gamboa 1979, Demercian et al. 1993, Cobbold et al. 1995, Mohriak et al. 1995, Szatmari et al. 1996, Cobbold et al. 2001, Meisling et al. 2001, Modica & Brush 2004, de Mio et al. 2005, Davison 2007, Karner & Gamboa 2007, Moreira et al. 2007, Gamboa et al. 2008; Assine et al. 2008, Chang et al. 2008, Souza 2008, Correa 2009, Lentini et al. 2010, Mohriak et al. 2010, Davison et al. 2012, Guerra & Underhill 2012, Quirk et al. 2012, Rigoti 2015, Szatmari & Milani 2016, Kukla et al. 2018, Rodriguez et al. 2018, Pichel et al. 2021, Pichel et al. 2022) or focused on Central or Southern Santos Basin (Caldas & Zalán, 2009; Garcia et al. 2012, Fiduk & Rowan 2012, Jackson et al. 2014; Jackson et al. 2015a, Jackson et al. 2015b, Alves et al. 2017, Pichel et al. 2018, Pichel et al. 2019, Magee et al. 2021, Rowan et al 2022, Bose & Sullivan, 2022). Nevertheless, major Brazilian oil and gas (O&G) fields and clusters are in Northern Santos Basin, making this an area of high economic significance. Since those petroleum accumulations are pre-salt plays, most studies there are focused on the pre-salt section (e.g. Leite et al. 2020, Santos & Gordon 2021, Araujo et al. 2022, Freitas et al. 2022, Vital et al. 2023, Antunes et al. 2024), lacking research in the salt and post-salt section and consequent insights on salt tectonics.

Therefore, the main question that guided this research was: "*how was the nucleation and evolution of minibasins in the mid-slope hallokinetic domain of Northern Santos Basin?*". Hence, the primary task was to map a 3D seismic block in the northern

part of the basin (Fig. 1.1b), nearby O&G fields and clusters (Fig. 1.1c) that collectively produce up to 1.582 Mboe/d from pre-salt carbonates (ANP 2023), with the aim of understanding the evolution of adjacent minibasins over time. The main working hypothesis was that trends observed across all minibasins may reflect major regional events, while characteristics found in only one of them may indicate local triggers.

As a result, I identified: (I) various types of three-dimensional minibasins, and their key geometric characteristics both in plan-view and cross-section; (II) deep-water sedimentary systems, most importantly Mass Transport Deposits (MTDs); and (III) salt bodies' geometry and intra-salt structures. With such mapping, it was possible to contribute to the current understanding of the halokinetic evolution in this area.

This dissertation aims to present these findings. It includes this Introduction, a Literature Review (focused on basic concepts regarding salt-bearing basins and Santos Basin), the used Methodology, a Results & Discussions section (on which abstracts, and an article draft are presented), and Conclusions.
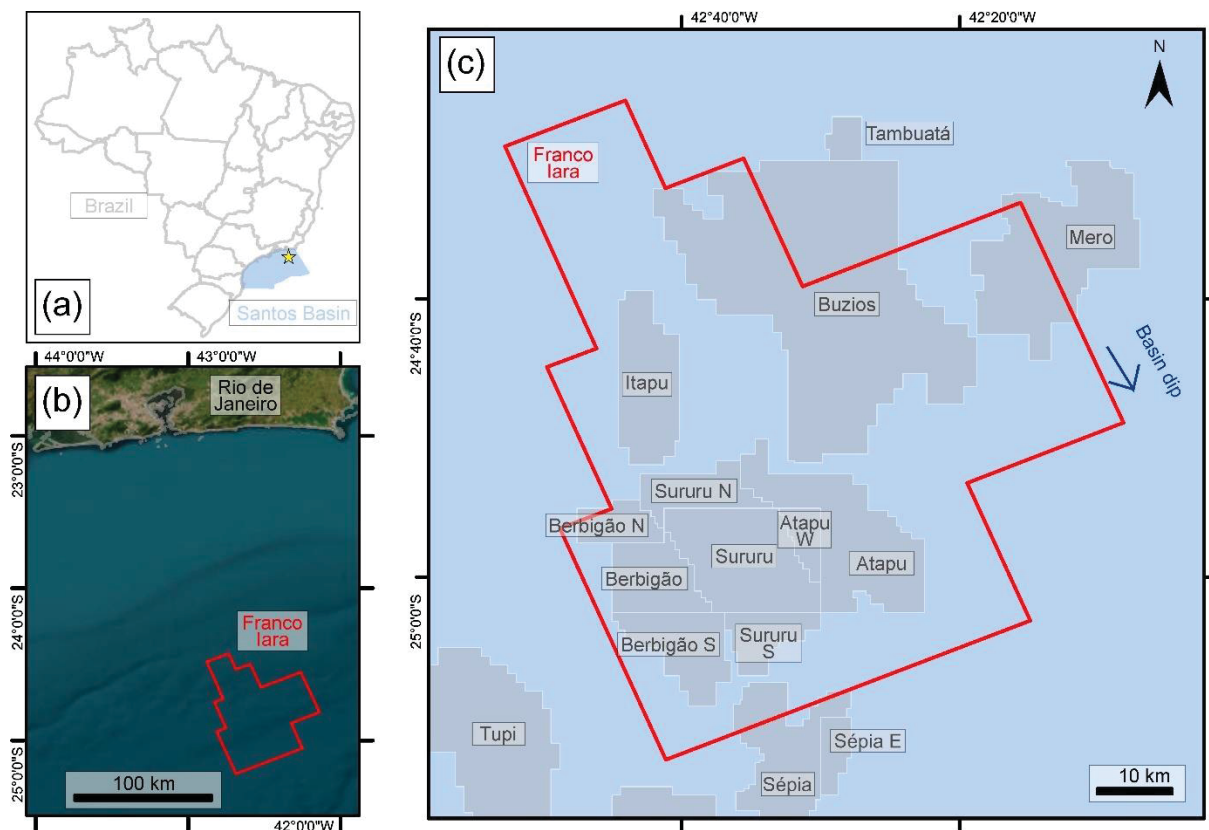
Figure 1.1: Study site. (a) Location (yellow star) in the northern Santos Basin (highlighted in blue), offshore Brazil. (b) Franco Iara's area, approximately 200 km from Rio de Janeiro, in a deep-water setting. (c) Major pre-salt oil fields (highlighted in grey) within Franco Iara.

2 LITERATURE REVIEW

2.1 SALT-BEARING BASINS

Multiple analysis can be conducted in salt-bearing basins. Firstly, salt deposition requires specific environmental conditions (e.g. Hardie 1991, Mohriak et al. 2008, Hudec & Jackson 2012, Warren 2016). Secondly, due to evaporites unique rheology (e.g., low density maintained when buried, mechanical weakness, fluid-like behavior in geological timescales, capacity to absorb and transmit stresses, see Jackson & Talbot 1986, Warren 2006, Hudec & Jackson 2007, Fossen 2010), they are responsible for salt tectonics, which involves deformation due to salt movement. Understanding the development of salt structures, their three-dimensional geometries, and their interaction with regional stresses are key aspects of such research (Hudec & Jackson 2007, Jackson & Hudec 2017). Lastly, evaporites are widely applied in the energy industry, both because of the common saying that "a salt basin is an oil basin" (Mohriak et al. 2008, Hudec & Jackson 2012), and as an option to store economic gases and liquids (Tarkowski et al. 2021, Duffy et al. 2023).

2.1.1 Salt deposition

Evaporites are salt rocks that form through the precipitation of a saturated surface or near-surface brine, typically as a result of solar heating and evaporation exceeding the inflow at sedimentary temperatures lower than 70°C (Warren 2016). This process occurs when seawater, with abundant dissolved ions such as Na^+, Cl^-, SO_4^{2-}, Mg^{2+}, Ca^{2+}, K^+, HCO^{3-} and Br^-, becomes restricted and isolated (Mohriak et al. 2008, Warren 2006). However, evaporites can also have non-marine origins, such as meteoric, hydrothermal or basinal, or a combination of these (Hardie 1991). After a new water input enters a restricted evaporative basin, evaporation leads to the formation of brines, resulting in the precipitation of various evaporitic minerals and the formation of Layered Evaporite Sequences (LES) (Table 2.1, Fig. 2.1). The most common minerals in LES are calcium sulfates and halite, while rarer occurrences include potassium or magnesium sulfates (bittern salts), and borates, which are typically non-marine in origin (Mohriak et al. 2008). In evaporitic basins, evaporite facies often exhibit lateral variations (Hudec & Jackson 2012), and lithological successions can provide insights into salinity variation over geological time, reflecting sequences of mineral precipitation (Mohriak et al. 2008).

Regarding the formation and preservation of evaporites, certain conditions are necessary (Hardie 1991, Mohriak et al. 2008, Hudec & Jackson 2012, Warren 2016): (I) Arid to semi-arid climatic settings; (II) Net evaporation that exceeds the inflow of solute-bearing waters, thereby maintaining substantial volumes of salt-saturated brine at or near surface; (III) Isolated basins with periodic water supply, allowing for the creation of a brine saline near or at the surface that progressively concentrates and deposits salts; (IV) Accommodation space within a sedimentary depression; and (V) Burial environment that prevents undersaturated porewater from dissolving buried salts. However, since tectonic cycles, climate, and eustasy vary often over geological time, salt deposits vary depending on the specific time and setting in which they were formed.
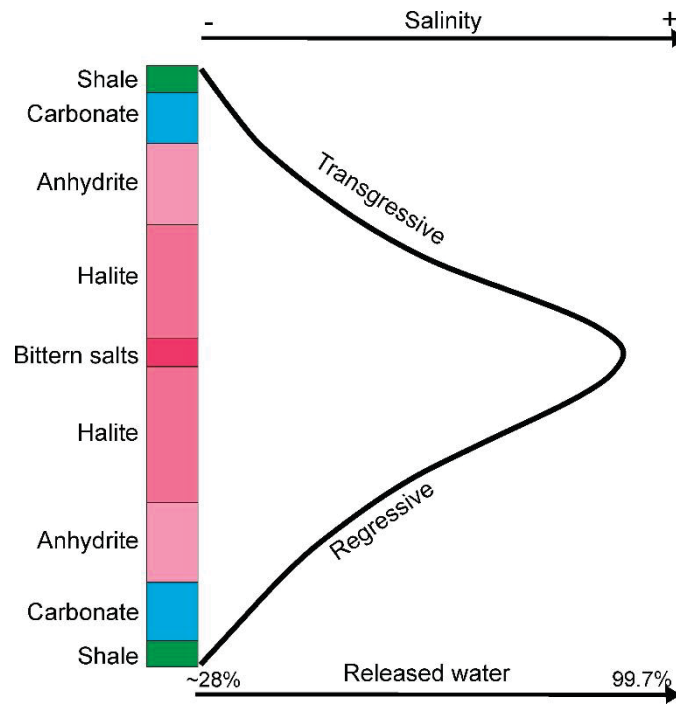
Figure 2.1: Schematic model illustrating an ideal evaporitic sequence cycle (after Hite 1972, Freitas 2006, Martins 2016).

Table 2.1: Main evaporitic sequences, common evaporitic minerals (chemical compositions and some densities in the table footer), gamma ray (API) responses, and their relationship to the initial seawater solution, without considering possible impurities (adapted from Mohriak et al. 2008, Warren 2016, Jackson & Hudec 2017, Museu Heinz Ebert 2023, Mindat.org 2023).

Precipitation order	Zone	Primary minerals*	Gamma Ray	Secondary minerals*	Gamma Ray	Inicial solution evaporation (%)
1	Gypsum - Anhydrite	Gypsum	0	Anhydrite	0	67.8%
2	Halite	Halite	0	Anhydrite	0	87.90%
		Gypsum	0	Polyhalite	18	
3	Bittern salts	Epsomite	0	Kieserita	0	97.10%
		Hexahydrite	-	Polyhalite	18	
		Polyhalite	18	Bloedite	-	
		Halite	0			
4	Sylvite	Sylvite	500	Kainite	225	97.54%
		Hexahydrite	-	Langbeinite	275	
		Epsomite	0	Kieserite	0	
		Polyhalite	18	Polyhalite	18	
		Halite	0	Leonite (?)	-	
5	Carnallite	Carnallite	200	Kieserite	0	98.82%
		Bittern salts	-	Langbeinite	275	
		Kainite	225	Kainite	225	
		Halite	0	Anhydrite	0	
6	Bischofite	Bischofite	0			99.07%
		Bittern salts	-	Boracite	-	
		Carnallite	200	Kieserite	0	
		Halite	0	Anhydrite	0	
		Gypsum	0			

* Anhydrite [CaSO$_4$], 2.82-2.93 g/cm^3; Bischofite [MgCl$_2$.6H$_2$O], 1.59-1.60 g/cm^3; Bloedite [Na$_2$SO$_4$.MgSO$_4$.4H$_2$O], 2.218-2.24 g/cm^3; Boracite [Mg$_3$B$_7$O$_{13}$.Cl], 2.91-3.1 g/cm^3; Calcite [CaCO$_3$], 2.71 g/cm^3; Carnallite [MgCl$_2$.KCl.6H$_2$O], 2.3 g/cm^3; Dolomite [Ca$_{(1+x)}$Mg$_{(1-x)}$(CO$_3$)$_2$], 2.86-3.36 g/cm^3; Epsomite [MgSO$_4$.7H$_2$O], 1.675-1.679 g/cm^3; Gypsum [CaSO$_4$.2H$_2$O], 1.3-1.7 g/cm^3; Halite [NaCl], 2.1-2.2 g/cm^3; Hexahydrite [MgSO$_4$.6H$_2$O], 1.757 g/cm^3; Kainite [4MgSO$_4$.4KCl.11H$_2$O], 2.15 g/cm^3; Kieserite [MgSO$_4$.H$_2$O], 2.571 g/cm^3; Langbeinite [2MgSO$_4$.K$_2$SO$_4$], 2.83 g/cm^3; Leonite [MgSO$_4$.K$_2$SO$_4$.4H$_2$O], 2.20 g/cm^3; Magnesite [MgCO$_3$], 2.98-3.02 g/cm^3;

Polyhalite [$2CaSO_4.MgSO_4.K_2SO_4.H_2O$]; Sylvite [$KCl$], 1.9-2.0 g/cm^3; Tachyhydrite [$CaCl_2.2MgCl_2.12H_2O$], 1.667 g/cm^3; Trona [$NaHCO_3.Na_2CO_3$], 2.11 g/cm^3.

Furthermore, characterizing salt deposits has numerous applications: (I) They can indicate global climate belts; (II) They can provide information about ancient seawater compositions; and (III) They aid in paleogeographic global reconstructions, particularly as indicators of arid climates at 30° latitudes (associated with Hadley circulation cells) or as orographic deserts behind tectonically uplifted mountain ranges in latitudes up to 55° (Hardie 1991, Hudec & Jackson 2012). As a result, salt deposits are found in various tectonic settings such as cratonic basins, syn-rift basins, late syn-rift or post-rift passive margins, continental collision zones and foreland basins (Hudec & Jackson 2012), mostly Phanerozoic in age. These deposits exhibit diverse depositional models, including basin-wide deposits, lacustrine settings, platforms, sea-edges, sabkhas, salt flats and saline lakes (Warren 2006, Warren 2016). However, it is challenging to find modern analogues to the thick extensive marine evaporites found in ancient deposits. This is primarily due to the current icehouse period and our current tectonic setting, which does not typically allow the formation of hydrographically isolated oceanic sump basins (Warren 2006, Warren 2016).

2.1.2 Salt tectonics

Salt tectonics, a term that appears to have been coined in 1925, impacts more than 130 sedimentary basins (Jackson & Hudec 2017). It is characterized by a distinct and unique deformation style (Hudec & Jackson 2007), as evaporites tend to accommodate the majority of stress (Hudec & Jackson 2007, Jackson & Hudec 2017). These rocks exhibit ductile behavior similar to that of a viscous fluid under typical geological strain rates, acting as a "geological lubricant" (Hudec & Jackson 2007, Mohriak et al. 2008, Fossen 2010). The sequence of increasing creep mobility (i.e., "*gradual flow of a crystalline material under a deviatoric load, leading to permanent distortion*"; Jackson & Hudec 2017) mobility typically follows the order of anhydrite, gypsum, halite, and bittern salts (Hudec & Jackson 2012).

Various factors can trigger salt tectonics. The primary driving process behind salt flow is believed to be differential loading (including gravitational, displacement, and thermal[1]), followed by buoyancy, and structures resulting from salt tectonics are primarily formed by regional tectonic forces or gravity-induced processes (Waltham 1997, Jackson & Hudec 2017).

When salt is buried, it tends to become gravitationally unstable and rises deforming the overlying rocks in a process known as halokinesis (Hudec & Jackson 2007). The characteristics and styles of deformation can vary depending on factors such as salt supply, rheological variability, post-salt sedimentation and regional settings.

_____

[1] According to Jackson & Hudec (2017), in gravitational or "vertical" loading "*differential loading is produced by gravitational body forces acting within the overburden and salt, typically caused by lateral variations in thickness (sedimentation, erosion, or structural features) or the overburden density or by relief on the salt top, a factor that may initiate halokinesis*". Displacement or "tectonic" loading results "*from forced displacement of one boundary of a rock body relative to another, that occurs when the flanks of a salt body move towards or away from one another during regional shortening or extension*". In thermal loading the "*differential loading results from expansion or shrinking of salt caused by temperature changes, and hot salt expands and becomes more buoyant*".

2.1.2.1   Salt tectonics in passive margins

Salt tectonics can significantly impact the tectonosedimentary evolution of passive continental margins (Jackson & Vendeville 1994), particularly through the combined effects of gravity spreading and gravity gliding[2] (Fig. 2.2, Jackson & Hudec 2017). Pure spreading can be driven by differential sedimentary loading, while dominant gliding is primarily influenced by margin tilt and slope instability, which are usually combined in natural settings (Vendeville 2005, Hudec & Jackson 2007, Brun & Fort 2011). Consequently, different phases and domains of salt tectonics can be formed (Rowan et al. 1999, Vendeville 2005, Brun & Fort 2011).
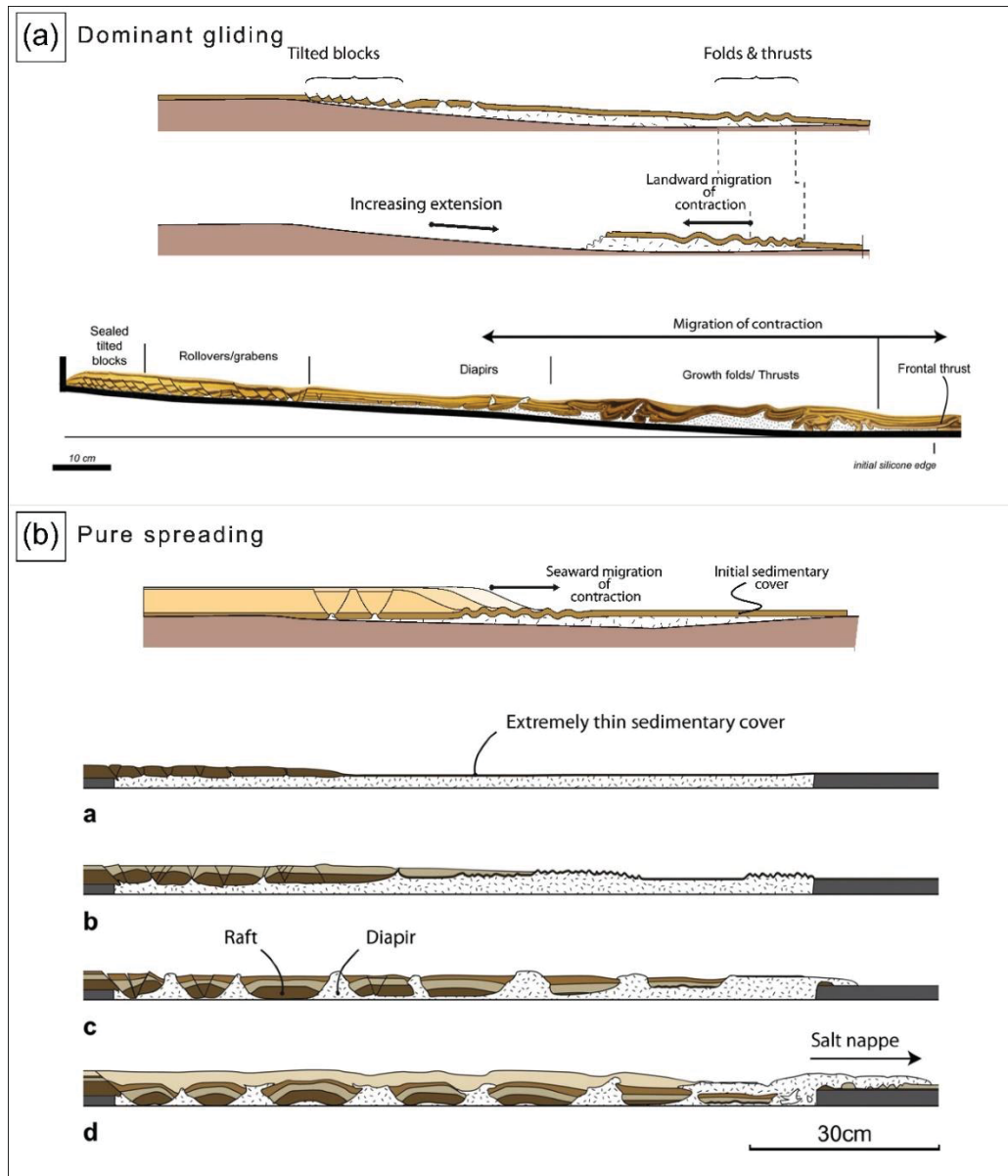
Figure 2.2: Tectonic styles and main features of salt-bearing passive continental margins affected by (a) dominant gliding, and (b) pure spreading. It is noticeable that in both cases an extensional proximal domain and a distal compressional domain are formed. Adapted from Brun & Fort (2011).

_____

[2] According to Jackson & Hudec (2017), gravity gliding is "*gravitationally induced downslope sliding of an overburden sheet or rigid block over a weak, ductile décollement layer or fault*". Gravity spreading is the "*vertical collapse and lateral spreading of a rock mass under its own weight, that typically operates on the salt and its overburden.*"

In general, salt tends to flow from an upslope extensional domain to a downslope contractional one due to basinwards tilting and/or prograding sedimentation, with secondary effects of salt flow over rift-related base-salt relief and ongoing rifting (e.g., Cobbold et al. 1991, Cobbold et al. 1995, Quirk et al. 2012, Davison et al. 2012, Alves et al. 2017, Pichel et al. 2019, Pichel et al. 2022), leading to the formation of distinct features in each setting (Cobbold et al. 1989, Jackson & Vendeville 1994, Brun & Fort 2011). As an example, Pichel et al. (2022) identified in Santos Basin basinward-dipping faults related to an earlier gliding-related phase, and later landwards-dipping faults form when spreading became more dominant. Nonetheless, a mid-slope transient translational zone lies between them, and it may present characteristics that reflect both (Jackson & Hudec, 2005). This translational domain has been sometimes depicted as being broadly simpler and less-deformed, but salt flow can undergo complex kinematics as it is highly variable depending on the geometry of the salt basin, base-salt relief, and supra-salt coverage (Cobbold et al. 1991, Dooley et al. 2007, Dooley et al. 2007, Dooley et al. 2017, Pichel et al. 2019, Ge et al. 2019, Pichel et al. 2021, Bose & Sullivan 2022). In natural systems, this domain is an area commonly with diapirs and minibasins, where stacking of depocenters controlled by salt tectonics and separated by rising diapirs.

Diapirs are salt body that move gravitationally, intruding overlapping layers in a discordant manner (Fossen 2010). Although the original configuration of salt deposits may vary (e.g., Hudec & Jackson 2022), numerous 3D geometries (Fig. 2.3) are observed in such salt bodies. Salt can migrate from linear or punctual sources and give rise to diverse structures, depending on the maturity of the system. The degree of maturity is linked to allochthonous salt, which refers to salt that has been transported from its original stratigraphic position (Hudec & Jackson 2007, Fossen 2010). When considering autochthonous salt geometries, four main types (anticlines, walls, pillows, and stocks) are distinguished in Table 2.2.
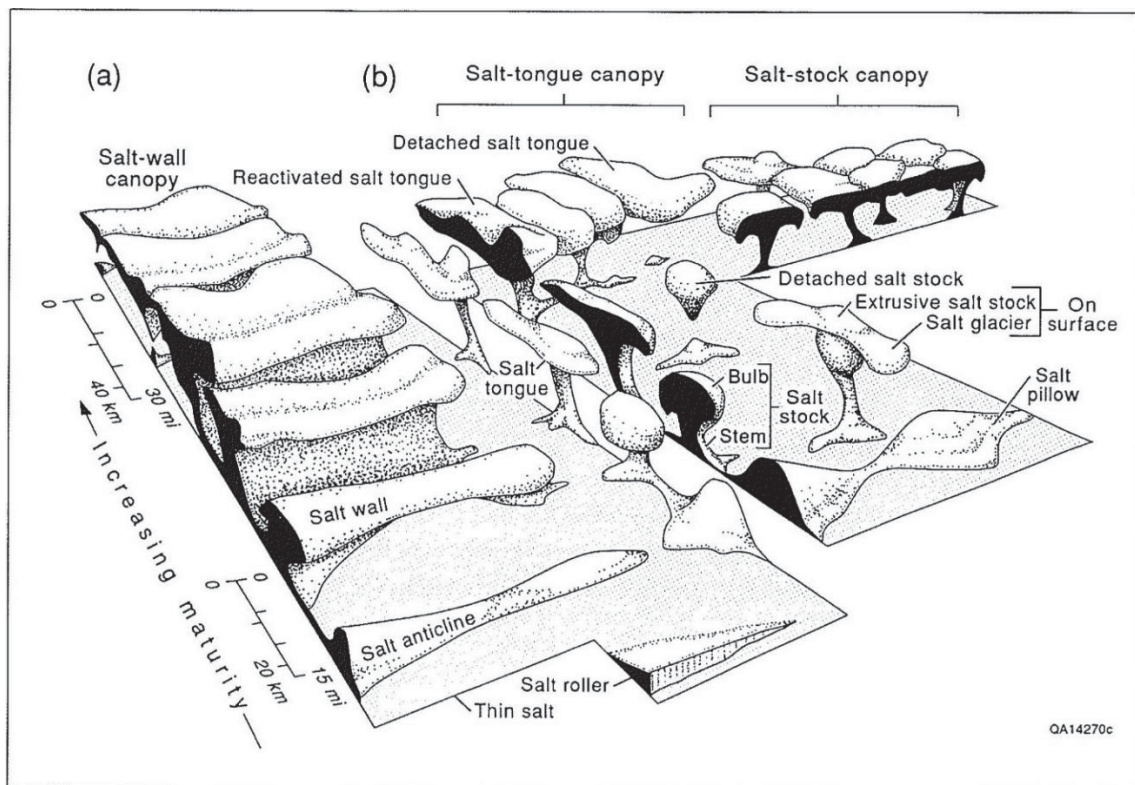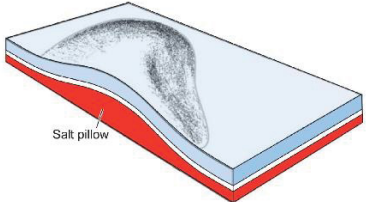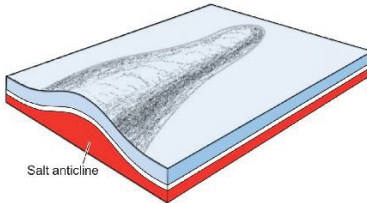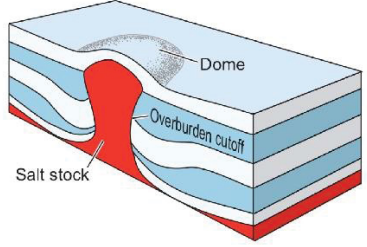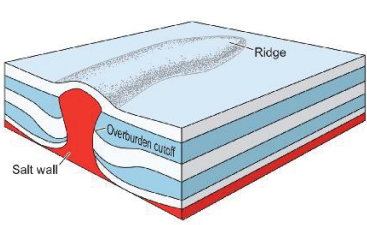
Figure 2.3: Names and geometries of salt structures, highlighting (a) linear and (b) punctual sources. From Jackson & Talbot (1991).

Table 2.2: Main characteristic of most important autochthonous salt bodies (after Trusheim 1960, Jackson & Talbot 1991, Jackson & Hudec 2017).

Geometry	Relation to overburden rocks	Plan view		Example
Salt pillow	Concordant (strata parallel to the upper salt contact)	equant		
Salt anticline		elongated		
Salt stock	Discordant (upper contacts cut across bedding)	anomalous, in discordant contact with strata that are younger than the units directly overlying them in the stratigraphic sequence	pluglike bodies; equant subcircular planform	
Salt wall			elongate; sinuous, parallel rows	

From a structural perspective, stress is primarily accommodated in salt due to its rheological contrast with the adjacent rocks (Rowan et al. 2020). Recognizing the geometry of salt and associated faults allows for the inference of past deformations related to diapiric rise in different stages (Hudec & Jackson 2007) and domains (Demercian et al. 1993, Vendeville 2005). In this context, there are three main mechanisms though which a diapir[3] can grow (Fig. 2.4): reactive diapirism, active diapirism and passive diapirism (Jackson et al. 1994, Jackson & Hudec 2017):

- Reactive diapirism (Fig. 2.4a): occurs during regional extension, such as in rifting grabens and half-grabens or gravity spreading. The overburden is

_____

[3] According to Jackson & Hudec (2017), true diapirs must pierce overburden rocks. There are three models for true piercement: (I) stretching by regional extension followed by reactive diapirism; (I) tilting of overburden by active diapirism; and (III) salt piercement in the hanging wall of a thrust fault. However, there are three other models that exhibit apparent piercement: (I) erosion of a roof, exposing and spreading the salt discordantly to the unconformity; (II) diapirs thinning their weak overburden; and (III) passive diapirism or downbuilding. Although these models do not strictly meet the criteria for true diapirism, Fossen (2010) suggest that they can still be referred to as diapirs because they represent initial stages that may eventually develop into true diapir.

thinned and weakened by fracturing and faults. Changes in pressure on buried evaporites caused by the overburden load led to the piercing and filling of the created space by salt diapirs. As a result, salt upwells in response to extension;

–	Active diapirism (Fig. 2.4b): involves the active rise of salt diapirs through arching, uplifting, or shouldering aside their roofs. There are two main mechanisms for this: (I) halokinetic diapirism driven by the overburden load (that can be buoyancy alone), which creates upwards pressure pushing relatively tall diapirs against relatively thin roofs; and (II) compressional diapirism driven by regional shortening, where the diapir is squeezed and forced to uplift, arch, or intrude into thicker roofs;

–	Passive (or downbuilding, Fig. 2.4c): refers to the growth of a diapir as sediments accumulate around its margin in a syndepositional manner. The competition for space between the rising salt and the surrounding sediment accumulating is the main controlling factor, as the roof presents less resistance to salt rise. As sedimentation can occur episodically, exposed diapiric crests rise as sediments accumulate around them, and the diapir is periodically buried during rapid sedimentation. Burial can trigger brief episodes of active diapirism, where the diapir breaks through the thin ephemeral roof and continues to grow by downbuilding. The salt base subsides among the surrounding strata as the basin fills with sediment.
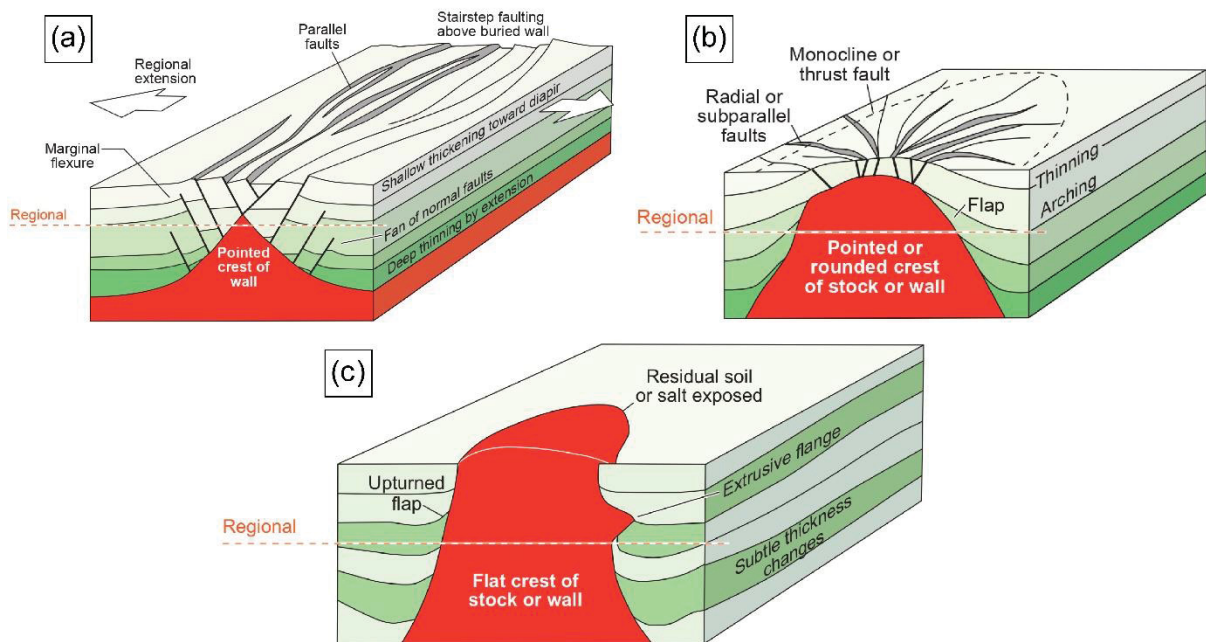
Figure 2.4: Main and distinguishable characteristics of different mechanisms of diapiric growth. (a) Reactive diapirism. This mechanism is associated with regional extension. Steep faults parallel to the buried wall and marginal flexure are inherited from the extensional system. (b) Active diapirism. Diapirs that rise actively exhibit features such as monoclines, radial thrust faults resulting from diapiric rise, as well as roof flaps and arching. The roofs of actively rising diapirs are arched, subjected to slumping and erosion, and often show an angular unconformity around the diapir. (c) Passive diapirism. Passive diapirism shows various types of interaction with adjacent layers. From: Jackson & Hudec (2017).

Time plays a central role in understanding salt tectonics (Jackson & Hudec 2017), as complex histories of salt tectonics can go through multiple stages (Vendeville & Jackson 1992). Passive diapirism can occur in any tectonic setting where salt is exposed at the surface. However, diapirs often reach the surface through active

diapirism, particularly if following a phase of reactive diapirism, during which extension creates a load gradient and weakens the roof (Jackson & Hudec 2017).

The rise of salt can give rise to various types of structures in passive margins (Fig. 2.5). The most common structures include bending-related normal (Fig. 2.5a-c) and thrust faults (Fig. 2.5d-f) in salt anticlines, faults that radiate outwards from diapirs, and crestal grabens (refer to Fig. 2.4b), as well as conjugated planar normal faults that root into the crest of a diapir (Fig. 2.5g-j; Jackson & Hudec 2017).
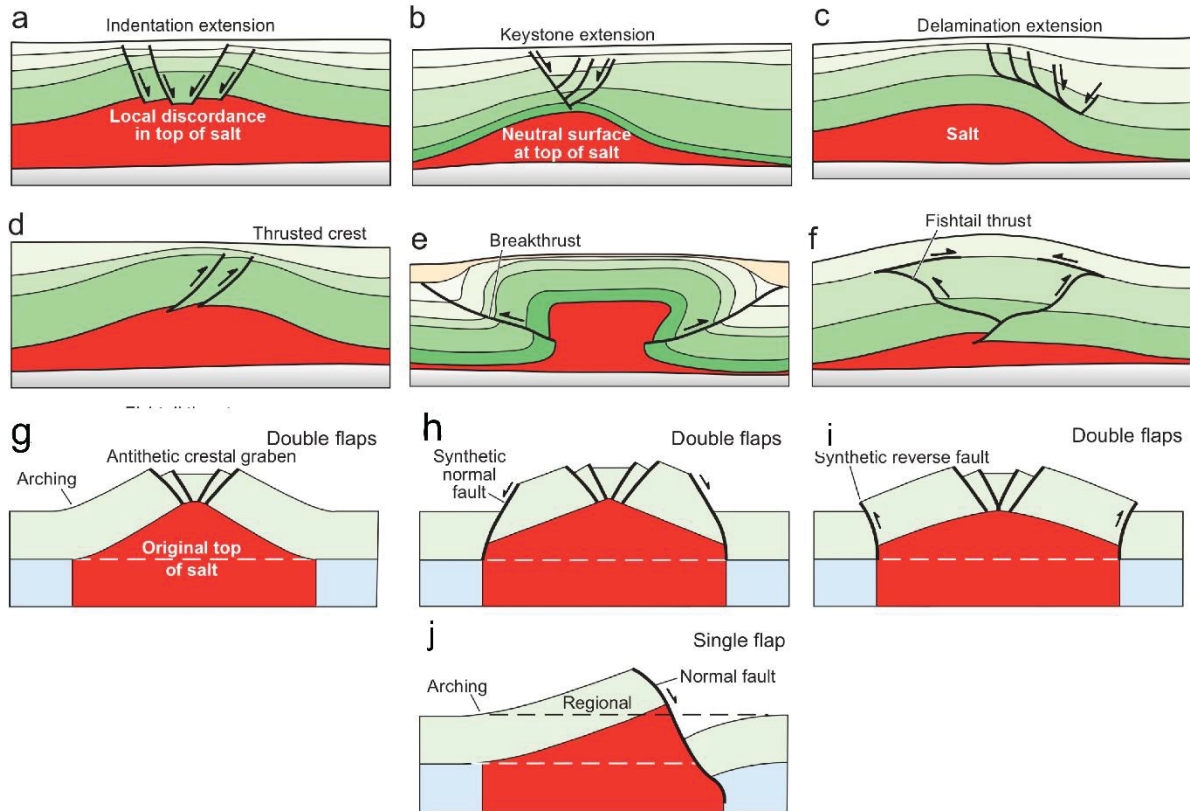
Figure 2.5: Fault styles related to (a-f) salt anticlines and (g-h) crests. From Jackson & Hudec (2017).

The sedimentary record of salt tectonics can be classified into three main types (Jackson & Talbot 1991). The prekinematic sequence represents the strata that record sedimentation before salt tectonics began, commonly with a constant stratigraphic thickness. The synkinematic sequence records sedimentation during salt tectonics, where thickness varies, with thickening occurring above salt-withdrawal structures and thinning above salt-rising structures. This package is also characterized by onlaps and truncations. Finally, the postkinematic sequence refers to strata intervals that record sedimentation after salt tectonics has ceased.

In relation to sequences deposited prekinematically, there is a particular type of deformation structure known as raft tectonics (Burollet 1975, Duval et al. 1992). In extensional settings, syndepositional grabens widen, and fault blocks separate the previously deposited overburden into rafts that slide downslope. In these systems, rafts are displaced from their original footwall position by faults and rest on a characteristic thin salt décollement and are separated by younger synkinematic strata (Duval et al. 1992, Jackson & Hudec 2017).

In synkinematic layers, the rise of salt creates structural highs and lows, which can lead to the divergence or accumulation of sediments (e.g., Seni & Jackson 1983, Rowan et al. 1999, Castro & Holz 2005, Caldas & Zalán 2009, Callot et al. 2016, Hudec et al. 2020). This active topographic relief can significantly influence the deposition of chrono-correlated units. In this context, minibasins play a crucial role as depocenters

controlled by salt tectonics, and their significance will be further discussed in the following section.

A particular type of synkinematic deposition is commonly observed during passive diapirism, as identified by Giles & Lawton (2002) and further detailed by Giles & Rowan (2012) in the El Papalote diapir in northeastern Mexico. During cycles of salt rise and burial, distinct sequences of sedimentary records separated by angular unconformities are formed. These sequences differ in scale and formation mechanism from other sedimentary sequences, representing a characteristic growth strata response to the near-diapiric (<1 km) activity. They are known as halokinetic sequences (Fig. 2.6), which document the processes of burial, breakout, and downbuilding. Two end-members are identified: hook (Fig. 2.6a) and wedge (Fig. 2.6b). These sequences are stacked together to form composite halokinetic sequences, such as tabular (Fig. 2.6c), which represents a stack of hook sequences during slow aggradation, and tapered (Fig. 2.6d), which represents a stack of wedge sequences during fast aggradation.
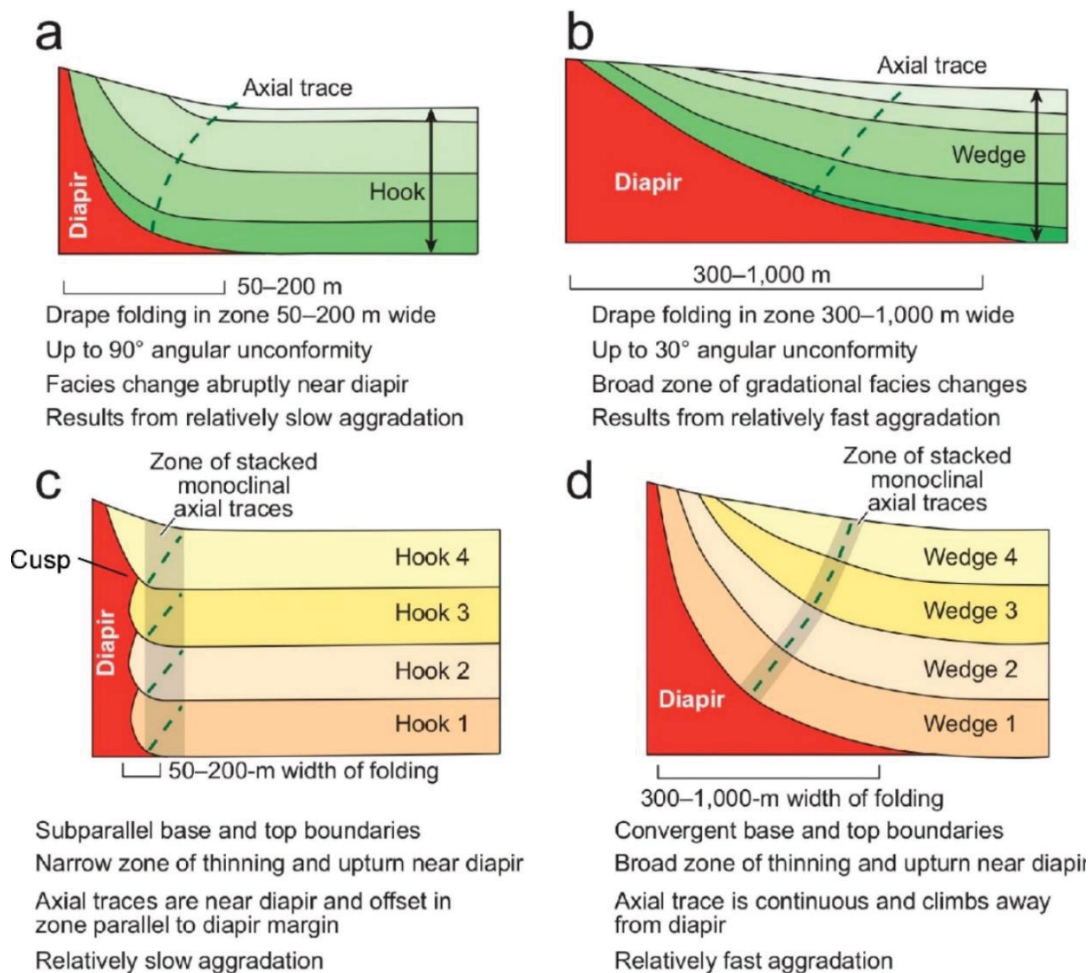
Figure 2.6: Principles of halokinetic squences can be observed through various characteristics. (a) Hook halokinetic sequences exhibit narrow deformation zones, high degrees of angular discordance, and abrupt facies changes. (b) Wedge halokinetic sequences are characterized by broad zones of folding, low-angle truncation, and gradual facies changes. When these sequences are stacked together, they form composite halokinetic sequences. (c) Tabular composite halokinetic sequence have subparallel boundaries, thin roofs, and localized deformation. (d) Tapered composite halokinetic sequence show folded, convergent boundaries, thicker roofs, and broad zones of deformation. From Jackson & Hudec (2017).

In certain cases, salt diapirs can reach a state of stagnation due to salt depletion or resistance from the weight and strength of the diapir roof (Jackson & Hudec 2017). Alternatively, diapirs may collapse as their crests subside due to salt depletion or when salt flows into another rising salt body, or through dissolution processes (Vendeville & Jackson 1991, Caldas & Zalán 2009, Jackson & Hudec 2017). Two characteristic structures associated with these mechanisms are turtle-structure anticlines, which have a flat base and rounded crest that tend to have the thickest sedimentary sequence compared to their surroundings, and mock-turtle anticlines, which lack a significant portion of the stratigraphic section in their core (Fig. 2.7, Trusheim 1960, Vendeville & Jackson 1991, Jackson & Hudec 2017).
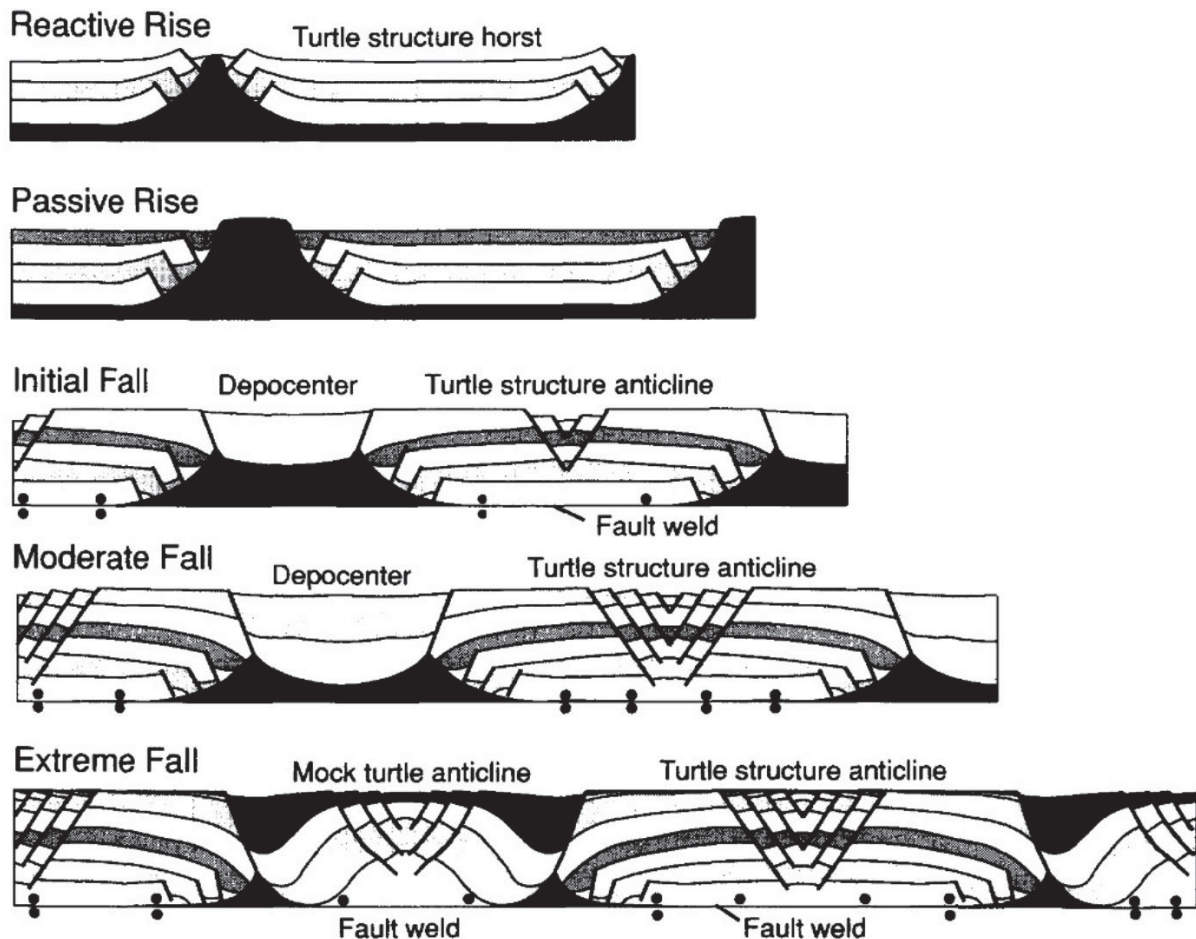
Figure 2.7: Examples of turtle-structure anticlines can be observed in situations where diapirs are surrounded by flanks that subside due to regional extension or salt structures with withdrawal basins that migrate and widen. Mock-turtle anticlines, on the other hand, are formed by salt depletion (i.e., salt weld) at the base of the structures, process that leads to the collapse of the diapir. From Vendeville & Jackson (1991).

2.1.2.2   Minibasins

Terms such as "minibasins" (reviewed by Hudec et al. 2009), "withdrawal basins", "intrasalt basins" (Jackson & Talbot 1991) and "halokinetic basins" (Ingersoll 2012) have been introduced to describe basins that form as a result of salt tectonics, i.e., directly related to salt deformation and halokinetic processes (Fig. 2.8). As typical salt-evacuation geometries formed above relatively thick salt, they typically occur in deepwater regions where late syn-rift salt is present, as the salt thickens downdip due to its original depositional thickness and subsequent salt flow processes (Hudec & Jackson 2022).

Minibasins are syn-kinematic basins or depressions with sizes in the order of tens of kilometers in diameter. They are surrounded (i.e., lateral edges) by relatively thick allochthonous or autochthonous evaporites and subside into these salt units. As they sink into the thick salt, they become filled with sediments. Minibasins have relatively short lifespans and low post-sedimentation preservation potential compared to crustal basins (Jackson & Talbot 1991, Hudec et al. 2009, Ingersoll 2012, Jackson & Hudec 2017, Hudec & Jackson 2022).

Minibasins can be classified as either primary, which form above autochthonous salt, or secondary, which form above allochthonous salt canopies with a high relief base and a complex salt geometry (Hudec & Jackson 2022). In the formation of minibasins, salt is expelled from beneath the basin and migrates to the surrounding margin, resulting in the development of a network of diapirs around the minibasin (Jackson & Hudec 2017, Hudec & Jackson 2022). For instance, the lateral boundaries of the minibasin may be comprised of salt stocks interconnected by a polygonal network of salt anticlines. In cases where salt thickness is greater, minibasins can be encompassed by a network of salt walls (Rowan et al. 1999, Hudec & Jackson 2022).

There is a wide range of possible geometries for minibasins (Fig. 2.8), and over time, they can merge to form larger composite basins (Jackson & Hudec 2017). Primary minibasins tend to have simpler conFiguretions, as their structural style can be controlled by salt thickness[4] (Pilcher et al. 2011), subsidence mechanism (Hudec et al. 2009), and structural controls (e.g., Nalpas & Brun 1993, Rowan & Vendeville 2006). Secondary minibasins can exhibit more complex geometries, which often include feeders and basal structures, and may present unique characteristics, such as: (I) be more likely to be transported and sink rapidly into salt feeders, displacing salt into interfeeder areas, and (II) they may have unusual shapes, sometimes undergoing rotation (Hudec & Jackson 2022). Additionally, encased, or encapsulated minibasins refer to minibasins that are entirely covered by a higher allochthonous salt sheet or equivalent salt weld (Hudec & Jackson 2022, Pilcher et al. 2011).

The subsidence mechanisms of minibasins resemble models of crustal basins and can be distinguished based on specific criteria (see Fig. 2.9, Hudec et al. 2009). Although the main formation mechanism is sedimentary loading (Ingersoll 2012), it commonly involves other local factors such as density contrasts (Fig. 2.9a), diapir shortening (Fig. 2.9b), extensional diapir fall (Fig. 2.9c), decay of salt topography (Fig. 2.9d) and sedimentary topographic loading (Fig. 2.9e), and/or subsalt deformation (Fig. 2.9f; Hudec et al. 2009), which result in different features in minibasins.

---

[4] According to Pilcher et al. (2011), when the original salt layer is thin, isolated salt stocks are common and tend to become buried. In case of intermediate salt thickness, isolated salt stocks and walls develop and gradually grow to form extensive salt canopies. However, when the salt layer is thick, salt stocks and ridges form a polygonal network that fragments primary minibasins.
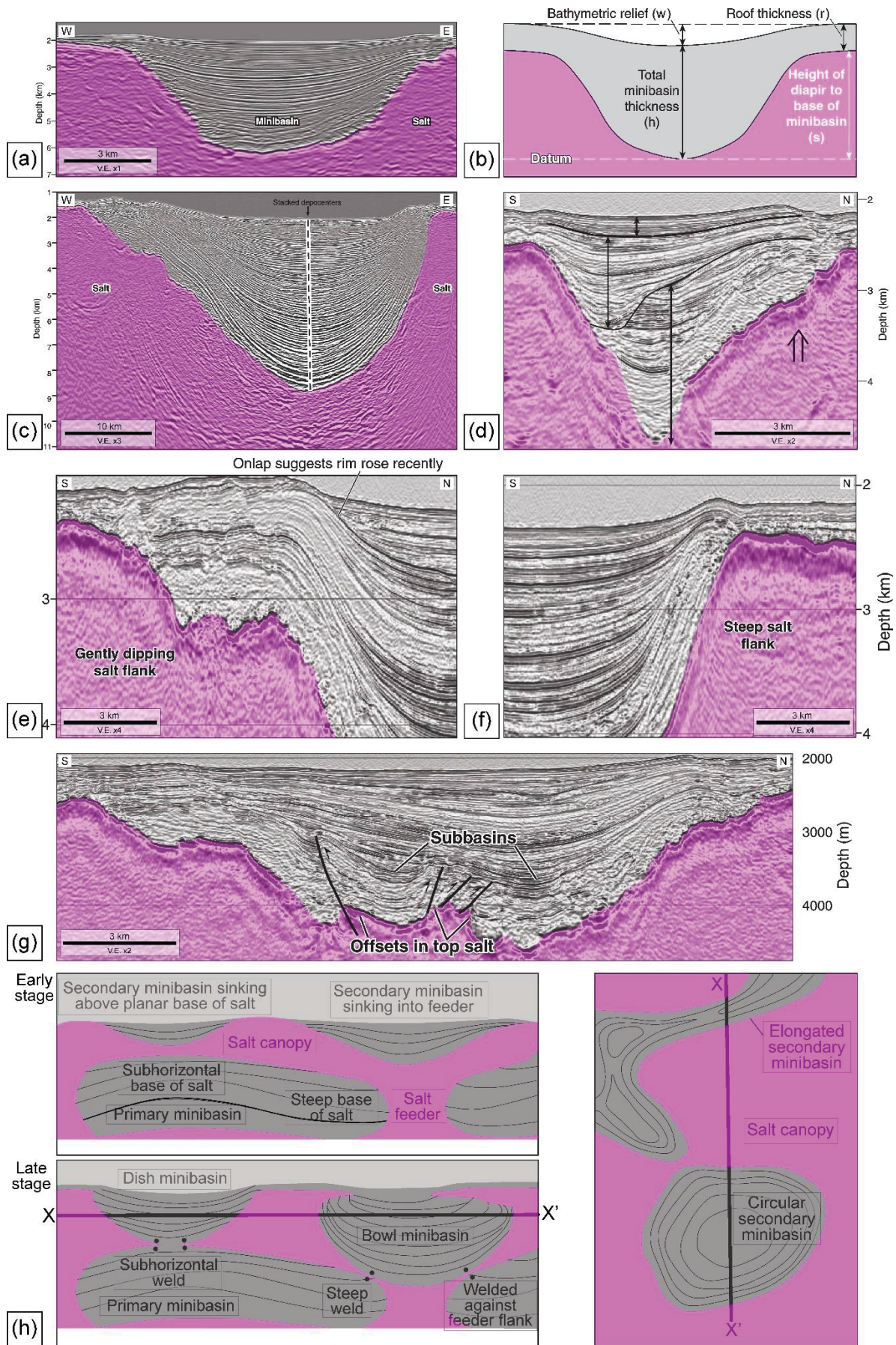
Figure 2.8: Main characteristics and features of minibasins (V.E.—vertical exaggeration). (a) A depiction of a minibasin sinking into an allochthonous salt sheet (Hudec et al. 2009). (b) Idealized cross sections showing buried diapirs and bathymetric relief within a minibasin (Hudec et al. 2009). (c) Examples of fill

patterns in minibasins, with a trace connecting the depocenters where the sedimentary packages are thickest (Hudec et al. 2009). (d) An example demonstrating abrupt shifts in minibasin depocenters (Hudec et al. 2009). (e) and (f) Examples of minibasins with uplifted rims, exhibiting either a gentle tapering outwards where the rim rose relatively recently or a narrow shape where the minibasin tapers abruptly (Hudec et al. 2009). (g) Asymmetric anticlines and thrusts within minibasins, dividing them into subbasins (Hudec et al. 2009), deformation which can later be interrupted by continued sedimentation. (h) Evolution of secondary minibasins sinking into allochthonous salt, connected to primary minibasins through salt welds. The possible shapes of minibasins can be generalized as subcircular in plan view, but they can also be elongated or dish-shaped or bowl-shaped in cross section (Jackson & Hudec 2017, Hudec & Jackson 2022).

Density-driven subsidence — Raised rim

Salt — $\rho_{sed} > \rho_{salt}$

(a)

1. Vertically stacked depocenters
2. Raised bathymetric rims
3. Maximum thickness >2300 m in siliciclastic settings

Diapir shortening

(b)

1. Synclinal bathymetry above tapered minibasin flanks
2. Thrust faults within minibasin
3. Abrupt lateral shifts in depocenters (double arrows)
4. Compressional tectonic setting

Extensional diapir fall

Horn of salt — Structural low in base of salt

(c)

1. Minibasin overlies structural low in base of salt
2. Extensional faults extend along strike from ends of salt structure
3. Horns of salt up along minibasin flanks
4. Extensional tectonic setting

Decay of salt topography — Depocenter trace

Structural low in base of salt

(d)

1. Absence of contractional structures
2. Minibasin overlies structural low in base of salt
3. Syncline has stacked depocenters, maybe tilted by later deformation
4. Location on bathymetric slope

Sedimentary topographic loading — Depocenter trace — Seaward

(e)

1. Location on bathymetric slope
2. Seaward-migrating depocenters

Subsalt deformation

(f)

1. Minibasin overlies downthrown base of salt
2. Minibasin overlies synclinally folded base of salt

Figure 2.9: Main minibasin-subsidence models and a summary of the criteria used to distinguish them: (a) density-driven subsidence, (b) diapir shortening, (c) extensional diapir fall, (d) decay of salt topography, (e) sedimentary topographic loading, and (f) subsalt deformation. Modified from Hudec et al. (2009).

As salt moves, minibasins can also be transported downslope. Once again, the salt base has a significant influence on the translation of the system. If there is a structural highs in the salt base, minibasins can become pinned in place, causing distortion in the movement of nearby units. The velocity of tridimensional downdip translation may vary within diapirs depending on the salt thickness, which can result in minibasins moving apart or colliding with each other (Hudec & Jackson 2022). Additionally, asymmetric synclinal depocentres, known as ramp syncline basins, can form when basinwards or landwards-dipping ramps exist within the salt base, causing units to translate above salt layers as the movement generates a downwarp of the overburden, thereby creating accommodation space (Jackson & Hudec 2005, Pichel et al. 2018).

Finally, as salt flow causes subsidence above areas of salt expulsion and uplift where salt rises, surface reliefs are commonly created, varying from 100 to 400 m

(Jackson & Hudec 2017). Minibasins play a role in capturing sediments as they act as dams, hindering sediment moving downslope (Jackson & Talbot 1991). The local relief generated by salt diapirs (Jackson & Hudec 2017) can influence paleotopography differently depending on the stage of diapir development (e.g., Seni & Jackson 1983). In depositional environments, sedimentary systems often develop on active topography, exhibiting complex characteristics such as spoke circulation or random patterns of differential loading (Jackson & Talbot 1991). These systems can be confined or partially confined (e.g., Cumberpatch et al. 2021), or even occur in ponded accommodation spaces (Jackson & Talbot 1991, Booth et al. 2003, Ingersoll 2012, Jackson & Hudec 2017). The topography of diapirs influences facies distribution and geometries in these environments, considering factors such as the degree of confinement, distance from diapir crests, and creation of local slopes (e.g., Booth et al. 2003, Giles et al. 2008, Jackson & Hudec 2017, Cumberpatch et al. 2021). For instance, deepwater channels respond differently depending on erosion rates and their timing with respect to active salt tectonics (Fig. 2.10, Mayall et al. 2010). Compensatory stacking and debrites can be associated with diapir growth (e.g., Hudec et al. 2009, Ge et al. 2020, Cumberpatch et al. 2021) and fill and spills systems are common on slopes with flow perpendicular to strike, where sediments bypass minibasins or progressive fill their bathymetry (e.g., Booth et al. 2003).
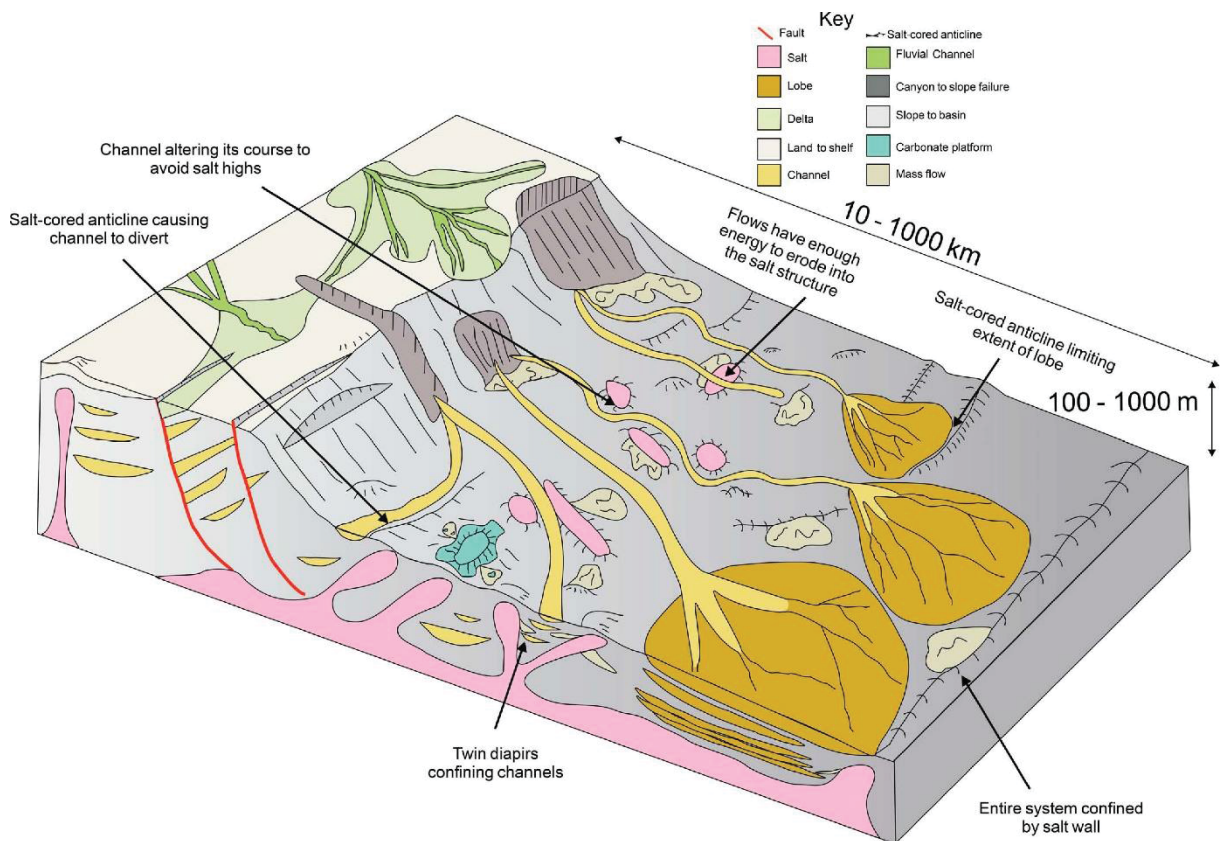
Figure 2.10: Summary of salt structural controls in deep-water (i.e., shelf, slope, and base-of-slope) gravity-driven processes. In the slope environment, salt structures play a significant role, influencing the formation of complex channel paths that diverge from these structures. From Cumberpatch et al. (2021), after Mayall et al. (2010).

2.1.3 Applications in the energy industry

Evaporites are not only important when understanding the tectonostratigraphic evolution of a basin, but their study also has wide applications in the energy industry.

It is estimated that approximately 50% of the world's largest oil fields are associated with evaporitic rocks (Grunau 1987; Warren, 2006). According to Magoon & Dow (1994), a petroleum system:

> Encompasses a pod of active source rock and all related oil and gas and includes all the essential elements and processes needed for oil and gas accumulations to exist. The essential elements are the source rock, reservoir rock, seal rock, and overburden rock, and the processes include trap formation and the generation-migration-accumulation of petroleum. All essential elements must be placed in time and space such that the processes required to form a petroleum accumulation can occur. (Magoon & Dow 1994).

Therefore, synchronicity is required among the four elements (source, reservoir, sealing and overburden rocks) and processes (traps and generation-migration-accumulation) for the formation of O&G accumulations. This synchronicity involves stratigraphy, geography, and temporal extent allow generation (i.e., overburden gradually increasing temperature) and facilitate migration (i.e., movement of hydrocarbons, primarily driven by buoyancy, from their source through permeable formations into reservoirs) and maturation processes (Magoon & Dow 1994, Milani et al. 2000, Jackson & Hudec 2017). In this context, the genetic evaporite-petroleum association was first recognized by Carl Ochsenius in 1888 and subsequently became more evident in the 1950s and 1960s (see Hite & Anders 1991, Jackson & Hudec 2017), and it is now well-established that salt can significantly influence essential elements and processes involved in hydrocarbon accumulation (Fig. 2.11).
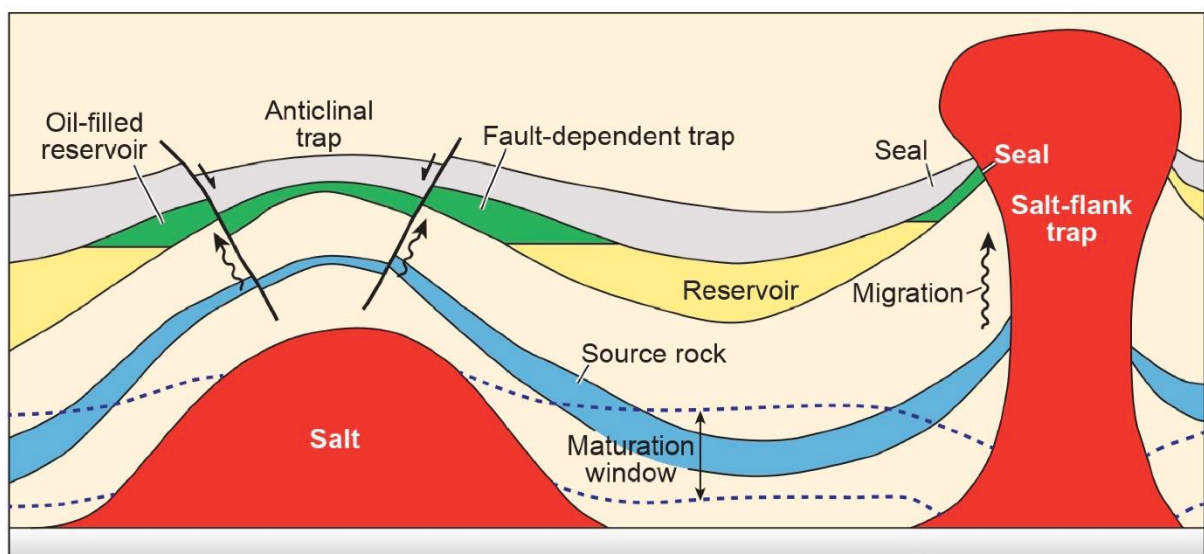
Figure 2.11: How large salt structures can influence petroleum systems (from Jackson & Hudec 2017).

Firstly, salt exerts a significant influence on elements of petroleum systems. While salt itself does not contain sufficient organic matter to act as an effective source rock, it is often genetically associated with source rocks and may play a role in their formation (Hite & Anders 1991, Warren 2006, Jackson & Hudec 2017). They are crucial and effective sealing rocks in giant oilfields worldwide (Grunau 1987), including Santos Basin (Chang et al. 2008), due to properties such as low porosity and permeability, and its plastic behavior (Warren 2006).

The influence of salt tectonics on adjacent and overlying units (Fig. 2.12) has been recognized for a long time (e.g., Trusheim 1960, Seni & Jackson 1983, Jackson & Hudec 2017). In terms of reservoirs, salt has an impact on deposition, diagenesis, and fracturing, and in some cases acts as a reservoir itself (Jackson & Hudec 2017). During deposition (Fig. 2.12a), salt-induced topography influences facies distribution

in continental, shallow-marine, and deep-marine systems (Trusheim 1960, Seni & Jackson 1983, Jackson & Hudec 2017). Regarding minibasins, some best-known accumulation cases are found in the Gulf of Mexico (Fig. 2.12b), where salt-related relief reduction in intraslope minibasins leads to fill-and-spill systems and facies variations in neighboring oil fields (Booth et al. 2003) and primary encased minibasins can contain complete petroleum systems within themselves (Pilcher et al. 2011). While less common, intrasalt reservoirs can also be found in cap rocks (such as bioalteration of anhydrite to secondary limestone, which was common in the first oil discoveries in Texas), as well as in the presence of intrasalt hydrocarbon source rocks (Jackson & Hudec 2017).

Salt tectonics also influences processes in petroleum systems and plays a fundamental role affecting the special relation among various processes and elements. One of the key contributions of salt tectonics is the formation of large structures that can serve as traps, such as anticlinal closures, fault-block traps, erosional truncations, stratigraphic pinch-outs, salt-face truncations, crestal reefs, and cap-rock traps (Chang et al. 2008, Jackson & Hudec 2017). In terms of generation and maturation, if salt is thick and laterally continuous, its high thermal conductivity can result in a complex temperature distribution around diapirs, typically heating the rocks above and cooling rocks below, thereby preserving trapped hydrocarbons (Mello et al. 1995, Mohriak et al. 2008, Jackson & Hudec 2017). Importantly, it can influence migration, by altering porosity and permeability framework, having its sealing capability ruptured due to internal discontinuities (i.e., welds, sutures, or impure evaporites), folding and faulting adjacent layers during salt rise, influencing cementation and diagenesis through changes in fluid chemistry, influencing pressure distribution, causing erosion, generating unconformities, serving as conduits during emplacement, and developing of time-varying fluid-escape structures (e.g. Chang et al. 2008, Mohriak et al. 2008, Andersen et al. 2011, Jackson & Hudec 2017).

Last, although it is already known that characterising internal deformation patterns reduces risks in extracting any resource from within salt and drilling through salt (Rowan et al. 2019), nowadays studies have been exploring salt as a safe option for storing waste and various economic gases (hydrogen, carbon dioxide and natural gas) and liquids (Tarkowski et al. 2021, Duffy et al. 2023). Indeed, large-scale underground hydrogen storage in salt caverns is considered a cheap and safe option and salt formations are already considered viable options in countries such as Australia (Bradshaw et al. 2023).

(a)

Debris derived from diapir or its roof interfingers with fluvial sands

Fluvial channels diverted around diapir

Emergent crest is a sediment source

Shelf

Slope

Diapir overlain by condensed shales

Shelf edge

Rise

Shoreface sands above diapir

Reef above diapir crest

Sediment-transport systems diverted away from diapirs on graded slope

Minibasin sands

Sands pinch out onto structural high in toe-of-slope fans

(b)

A: Schematic salt geometries

B: Top primary basin interpretation

Base of Canopy | Base of Canopy | Bucket Minibasin and Bucket Weld | Keel | Encased Minibasin and Bowl weld | Keel Suture | Ridge | Open Primary Basin

Minibasin Weld

Welded canopy

Minibasin Weld

Base of Canopy

C: Primary basin trap style

T   B   F   F   T   R   S   C

primary basin trap types: turtle structure (T), bucket weld (B), salt feeder (F), salt ridge (R), base-of-salt truncation (S), and salt cored fold (C).

Figure 2.12: Salt tectonics has significant impact on the units that overlie it. (a) It influences facies distribution in all depositional environments (from Jackson & Hudec 2017). (b) Salt-related geometries within minibasins in the Gulf of Mexico have implications for petroleum systems. This includes differences between primary and secondary basins, the classification of the primary basin surface, and the types of traps found in primary minibasins (from Pilcher et al. 2011).

2.2 SANTOS BASIN

The Santos Basin is a passive margin sedimentary basin located on the southeastern Brazilian coast (see Fig. 1.1). It is bounded to the north by the Cabo Frio High, which separates it from the Campos Basin, and to the south by the Florianopolis high, which separates it from the Pelotas Basin (Moreira et al. 2007). The basin covers an area of approximately 350,000 km^2, extending from the coastline to a depth of around 3,000 m (Santos & Gordon 2021).

As well as a series of nine genetically related marginal basins (Williams & Hubbard 1983), the formation of the Santos Basin can be attributed to the breakup of Gondwana and the subsequent opening of the Atlantic Ocean, which began in the Early Cretaceous (de Mio et al. 2005, Chang et al. 2008). There is a remarkable evaporitic phase during the Aptian, followed by extensive widespread salt tectonics that affected the deposition of subsequent Drift Sequence (e.g., Pereira & Feijó 1994, de Mio et al. 2005, Moreira et al. 2007, Assine et al. 2008, Guerra & Underhill 2012).

The tectonostratigraphic evolution of the Santos Basin is divided into syn-rift, post-rift, and drift sequences, based on sequence stratigraphy (Fig. 2.13), which focused on identifying depositional sequences (Moreira et al. 2007). Pereira & Feijó (1994) noted that the basin does not have outcrops, and its stratigraphic knowledge relies on correlations between indirect (seismic) and direct (drill core) data. Assine et al. (2008), following the identification of "well-marked seismic horizons" by Pereira et al. (1986), defined seismic horizons majorly associated with regional unconformities that are recognizable in seismic lines.

Currently, Santos Basin is the largest producer of oil and natural gas in Brazil (PETROBRAS 2023) and is considered one of the most productive petroleum provinces in the deep-water offshore region (Santos & Gordon 2021). Exploration activities began in the 1970s, and the first oil discovery by Petrobras took place in the 1980s on turbidites of the drift sequence, and pre-salt production started in 2009 (ANP 2021, Pré-sal Petróleo 2023, PETROBRAS 2023). Since then, more than 240 wells have been drilled, leading to the discovery of one of the world's largest oil provinces, known as the pre-salt play (Mello et al. 2021).The pre-salt play represents a vast but complexly compartmentalized oil province associated with source rocks and carbonate reservoirs within the pre-salt lacustrine rift system (Santos & Gordon 2021, Vital et al. 2023), sealed by salt layers (ANP 2021, Chang et al. 2008). Many of the major pre-salt oil and gas fields, such as Tupi and Buzios (see Fig. 1.1), are located offshore, ca. 300 km from the coastline, at depths of ca. 5,000 m (PETROBRAS 2023). As of February 2023, pre-salt production from 136 wells amounted to 2,566 Mbbl/d and 111,55 Mm^3/d, accounting for 78.1% of the total oil and gas produced in Brazil (ANP 2023).
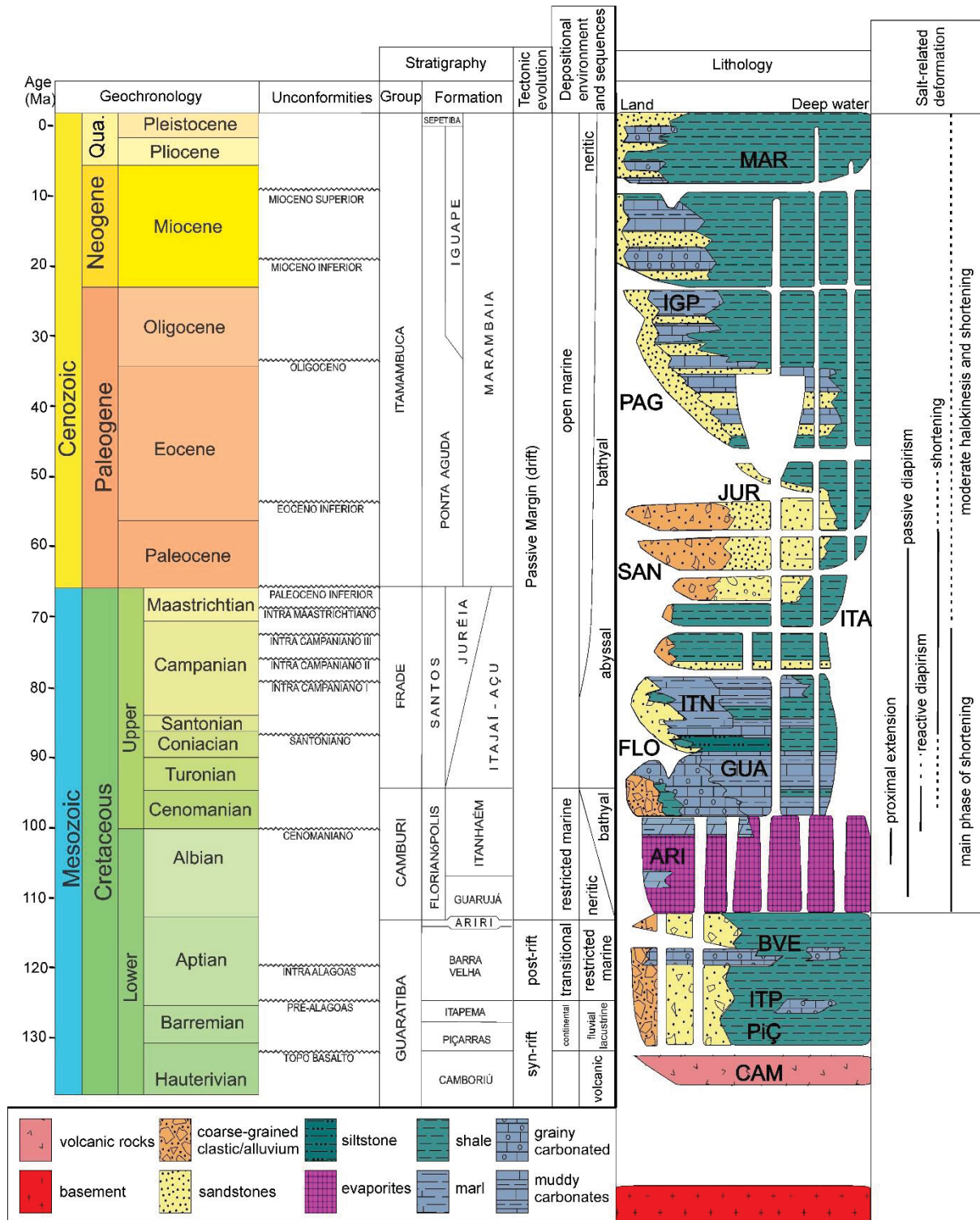
Figure 2.13: Santos Basin chronostratigraphic chart, highlighting unconformities, chronostratigraphy, tectonic evolution, depositional environments and sequences, lithology and main salt-related deformation events. From: Modica & Brush (2004), Moreira et al. (2007), Guerra & Underhill (2012), Cohen et al. (2013), Jackson et al. (2015a), and Alves et al. (2017).

2.2.1 Syn-rift sequence

With the Gondwana breakup and the opening of the Atlantic Ocean (Fig. 2.14) (e.g., Kukla et al. 2018), the syn-rift sequence in Santos Basin is characterized by a diachronous and progressive basin-wide rifting process (Zalán et al. 2009). The thickest and most continuous rift sequence is found in the northern part of the basin (Chang 2023). Initially, the rifting developed along regional crustal weakness zones

inherited from the onshore Proterozoic Ribeira Belt, which exhibited fault trends oriented in the NE-SW and ENE-WSW directions (Meisling et al. 2001, Garcia 2012, Dehler et al. 2016). Consequently, the basin experienced a general oblique extension and rifting, characterized by a regional anastomosing structural framework. This framework is marked asymmetric en échelon NE-SW normal faults, which are influenced by E-W strike-slip transfer zones exhibiting an "S" geometry (Fig. 2.14, Meisling et al. 2001, Zalán & Oliveira 2005, Souza 2008, Pereira et al. 2021, Freitas et al. 2022). The overall tectonic regime in the region is characterized by sinistral strike-slip motion, leading to the compartmentalization of syn-rift depocenters in an NNE-SSW trend (Meisling et al. 2001, Kukla et al. 2018).

The syn-rift sequence comprises three formations filling series of grabens and half-grabens: the Camboriú Formation basalts, followed by the continental Piçarras Formation and the non-marine Itapema Formations (Moreira et al. 2007). The basement rocks underlying these units consist of granites and gneisses from the Coastal Complex and metasedimentary rocks from the Ribeira Belt (Moreira et al. 2007). The oldest Camboriú Formation consists of Hauterivian (ca. 136.4 and 130 Ma) tholeiitic basalts, that represent syn-rift continental volcanic flows, which are in discordance with the underlying Precambrian rocks and are considered the economic basement of Santos Basin (Pereira & Feijó 1994, Szatmari 2000, Moreira et al. 2007). Besides these basalts, most dating in Santos Basin comes from magmatic events that are intercalated with Piçaras and Itapema Formations dated at 121 and 130 Ma (Moreira et al. 2007, Vital et al. 2023). Discordantly overlaying the basalts, the Barremian siliciclastic Piçarras Formation consists of sandstones and polymictic conglomerates in proximal regions (alluvial fans and fluvial deposits), and sandstones, siltstones, and organic-rich shales in more distal regions (lacustrine environment) (Moreira et al. 2007). The lacustrine Neobarremian to Eoaptian Itapema Formation, which lies over an unconformity, consists of coquinas (bivalve rudstone, grainstone, wackestone, and packstone) and calcirudites in structural highs, intercalated with black shales and organic-rich mudstones in distal portions (restricted fluvio-lacustrine environment), and conglomerates and alluvial fans in proximal portions (Moreira et al. 2007, Leite et al. 2020, Santos & Gordon 2021). The upper boundary of this sequence is the regional Pre-Alagoas Unconformity, after which there is less tectonic activity and increasing thermal subsidence (Moreira et al. 2007, Santos & Gordon 2021).

Figure 2.14: Syn-rift setting. (a) Current setting of basins formed during the Gondwana breakup (Kukla et al. 2018). (b) Paleomap from the Barremian (Paleomap Project 2003). (c) Interpreted South Atlantic geodynamic evolution during the syn-rift phase (Kukla et al. 2018). (d) Regional basement map of Santos Basin, highlighting 'S' shaped fault systems (Vital et al. 2023).
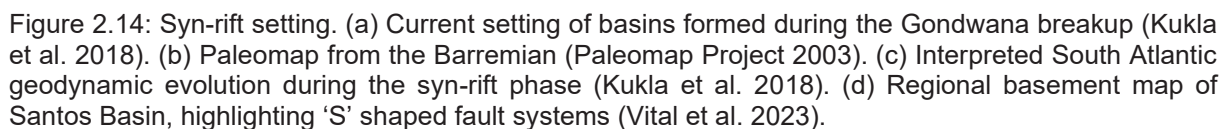
2.2.2 Post-rift sequence

The post-rift sequence in Santos Basin consists of the Barra Velha Formation, which comprises complex carbonates, and the Ariri Formation, an evaporitic unit (Moreira et al. 2007). This sequence represents the transition to a proto-oceanic stage and the beginning of phase of thermal subsidence phase (Quirk et al 2012).

The basal Barra Velha Formation is a series of lacustrine and restricted carbonate environments marked by in situ and reworked facies, subdivided into two sequences (Lower and Upper) separated by the Intra-Alagoas Unconformity dated at 117Ma (see Moreira et al. 2007, Vital et al. 2023). Carbonate deposition was particularly enhanced in structural highs and currently are reservoir rock in important pre-salt fields (Moreira et al. 2007, Gomes et al. 2013).

The subsequent unit is the evaporitic Ariri Formation, composed of halite and anhydrite, along with bittern salts like tachydrite, carnallite, and sylvinite (Freitas 2006, Moreira et al. 2007, Gamboa et al. 2008, Rodriguez et al. 2018), comprising almost exclusively evaporitic LES. Deposition occurred in a restricted environment, primarily to the north of the FH, with variable thickness and partially controlled by pre-existing non-uniform salt base relief (Demercian 1996, Davison 2007, Lentini et al. 2010, Davison et al. 2012, Alves et al. 2017, Rodriguez et al. 2018, Pichel et al. 2019). This led to multiples cycles of flooding and evaporation registered in Ariri Fm., resulting in the presence of 4-6 major seismically distinguishable intra-salt units (Gamboa et al. 2008, Fiduk & Rowan 2012, Rodriguez et al. 2018). On average, salt deposition is estimated to range from 2-2.5 km (Davison et al. 2012, Rodriguez et al. 2018), occurring in a relatively short geological timespan (<530 k.y. according to Rodriguez et al. 2018).

2.2.3 Drift sequence

The still-active drift phase initiated in the Albian and is divided into Camburi, Frade, and Itamambuca Groups (Moreira et al. 2007). During this phase, the gradual opening of the volcanic barrier (São Paulo and Walvis ridges) led to the establishment of open marine conditions (Quirk et al. 2012, Garcia 2012, Jackson et al. 2015a, Santos & Gordon 2021). Despite occurring during a phase of thermal subsidence phase (Quirk et al. 2012), where most tectonic stresses are over, the deposition of the Drift Sequence was heterogeneous. Its deposition was controlled by variations in eustatic sea level, the Serra do Mar uplift, reorganization of the ancestral Paraiba do Sul drainage system, sedimentary input, and salt tectonics, as the Ariri Formation began moving, with its major displacement occurring in the Upper Cretaceous (e.g. Meisling et al. 2001, Cobbold et al. 2001, Modica & Brush 2004, Assine et al. 2008, Caldas & Zalán 2009, Quirk et al. 2012, Guerra & Underhill 2012, Garcia et al. 2012, Jackson et al. 2015a, Pichel et al. 2019).

As accommodation space started to increase, the basal Camburi Group records a marine transgression, culminating in an anoxic environment (Arai 1988, Pereira & Feijó 1994, Moreira et al. 2007, Assine et al. 2008). It comprises the Florianópolis, Guarujá, and Itanhaém Formations (Moreira et al. 2007). The Florianopolis Formation represents the proximal facies and consists of conglomerates, sandstones, and shales deposited by alluvial fans and deltas (Moreira et al. 2007). The subsequent Guarujá Formation represents an Albian carbonate platform, characterized by shales and carbonate rocks (Pereira & Feijó 1994, Moreira et al. 2007). The upper part of this formation is marked by radioactive shales (Beta Mark), indicating the termination of the marine transgression (Arai 1988, Moreira et al. 2007). On the other hand, the Itanhaém Formation primarily consists of pelites (shales, siltstones and marls), with some sand

deposits from gravitational processes (Tombo Member), typically occurring in structural lows created by salt tectonics (Pereira & Feijó 1994, Moreira et al. 2007).

After the Turonian maximum flood surface, the Frade Group documents increasing terrigenous sediment supply in the basin and strong lateral variations in sedimentary content, influenced by the Serra do Mar uplift (Pereira & Feijó 1994, Milani et al. 2000, Moreira et al. 2007, Assine et al. 2008). It comprises the laterally correlated Santos, Juréia, and Itajaí-Açu Formations (Moreira et al. 2007). Overlying the previous group with an unconformity, the proximal Santos Formation consists of reddish conglomeratic continental sediments associated with alluvial fans (Pereira & Feijó 1994, Moreira et al. 2007). The intermediate Juréia Formation comprises clastic sediments (sandstones, shales and siltstones) extending from the continent to the slope (Moreira et al. 2007). The distal Itajaí-Açu Formation consists of pelites (shales, claystones, diamictites and marls), with some sections containing sandy turbidites (Ilha Bela Member) (Pereira & Feijó 1994, Moreira et al. 2007).

After a major global sea level fall and forced regression, siliciclastic-carbonate depositions on the marine Itamambuca Group were affected by changes in the basin depocenter due to tectonic reactivations, sea level fluctuations and consequent shifts in the coastline, and records variations in coastal to deep-water environments (Pereira & Feijó 1994, Moreira et al. 2007, Duarte & Viana 2007, Assine et al. 2008). It encompasses the Ponta Aguda, Iguape, Marambaia, and Sepetiba Formations, representing a marine environment ranging from proximal alluvial deposits to bathyal pelites (Moreira et al. 2007) highly influenced by the reorganization of the ancestral Paraiba do Sul drainage system (Modica & Brush 2004). The proximal Ponta Aguda Formation consists of siliciclastic sediments (conglomerates, sandstones, and pelites) deposited in alluvial fans, the marine coastline, and shallow platforms (Moreira et al. 2007). The formation transitions to a more restricted environment with the intermediate Iguape Formation, characterized by carbonates and pelites deposited as banks in a shallow environment near the slope, attributed to an Oligocene regressive trend (Pereira & Feijó 1994, Moreira et al. 2007). Being extensive in area and covering the sea floor, the distal Marambaia Formation consists of pelites (shales, siltstones, diamictites, and marls) and exhibits influences from deep-water systems, including sandy turbidites (Maresias Member) near the slope or as low-confined fans, besides ocean currents, and mass-transport deposits associated with listric faults on the slope or within minibasins (Pereira & Feijó 1994, Moreira et al. 2007, Duarte & Viana 2007, Diório 2021). Lastly, the proximal Pleistocene Sepetiba Fomation is related to alluvial fans and is predominantly composed of sandstones with fossil content (Pereira & Feijó 1994, Moreira et al. 2007).

In this geological setting, salt tectonics has produced complex and highly variable salt-related structures across Santos Basin as a product of seawards salt flow and overburden translation driven by differential sediment loading (i.e., spreading) and the seawards slope caused by margin tilting (i.e., gliding), with a main ESE to SE direction (e.g. Cobbold et al. 1995, Guerra & Underhill 2012, Davison et al. 2012, Garcia et al. 2012, Quirk et al. 2012, Jackson et al. 2015a, Alves et al. 2017, Pichel et al. 2018, Pichel et al. 2019, Pichel et al. 2022). This resulted in kinematically-linked domains of deformation defined by up dip extension and downdip shortening connected by an intermediate translational domain where deformation is highly variable depending on the geometry of the salt basin, base-salt relief, and supra-salt coverage, as well as the migration of the extensional domain basinwards (Cobbold & Szatamari 1991, Dooley et al. 2007, Dooley et al. 2017, Pichel et al. 2019, Ge et al. 2019, Pichel et al. 2021, Zwaan et al. 2021, Pichel et al. 2022).

In the Santos Basin, salt withdrawal created different types of passive and reactive salt structures related to updip extension of the overburden and creation of accommodation spaces. Those include salt rollers in the footwalls of NE-trending landwards-dipping listric normal faults, basinwards-dipping normal faults, salt domes and walls sometimes along synthetic and antithetic faults, basinwards-thickening wedges, extensional turtle anticlines, expulsion rollovers, raft tectonics, overburden erosion, and salt welds (Cobbold et al. 1995, Assine et al. 2008, Guerra & Underhill 2012, Pichel & Jackson 2020, Pichel et al. 2022). This extension and lateral salt expulsion has contributed to the formation Albian Gap, roughly parallel to the coastline and bounded seawards by the Cabo Frio Fault (CFF) and post-Albian rollover (Mohriak et al. 1995, Modica & Brush 2004, Guerra & Underhill 2012, Pichel et al. 2019). The compressive domain presents high variation in salt deformation styles and salt thickness as it translated and inflated downslope forming fold-and-thrust belts. In these, multiple-directed, symmetric and asymmetric, reactive and passive salt-cored structures (predominantly linear salt anticlines and walls) present contractional growth folds (e.g., angular and concentric, sometimes tight), thrusts (which may thicken or repeat LES), eroded upper parts, minibasins, and overburden buckle-folding (Cobbold & Szatmari 1991, Cobbold et al. 1995, Guerra & Underhill 2012, Alves et al. 2017, Pichel et al. 2022).

3 METHODOLOGY

The chosen methods were: (I) seismostratigraphic mapping to delimitate tectono-stratigraphic framework and understand the geological evolution; and (II) bibliographic reviews to enhance understanding of Santos Basin, salt tectonics, and minibasins.

Geological mapping is fundamental in defining the tectono-stratigraphic framework of a region and understanding its geological evolution. Therefore, it serves as a primary methodology for this research, involving the mapping of seismostratigraphic reflectors that represent chronostratigraphic contacts between formal units of Santos Basin and the main existing faults in the region.

During this stage, three main data sources were utilized (Fig. 3.1): (I) 3D PSTM (Pre Stack Time Migration) seismic survey R0302 Franco Iara, conducted in 2012, covering an area of ca. 3,700 km^2 in the northern Santos Basin, depth measured in meters and georeferenced using the SAD69 UTM 23S coordinate system; (II) 2D post stack seismic survey R0258_2D_SPEC_PSDM_BM_S, encompassing the entire basin, with depth measured in meters and georeferenced using the SIRGAS2000 UTM 23S coordinate system; (III) information from 19 wells located within Franco Iara area, with all locations converted to the SAD69 UTM 23S coordinate system. These materias were made available by the *Agência Nacional do Petróleo, Gás Natural e Biocombustíveis* (ANP; National Petroleum, Natural Gas and Bifuels Agency), through requests 10982 and 9880. Seismostratigraphic mapping was conducted in the OpendTect PRO software, with an academic license provided to LABAP by dGB Earth Science.
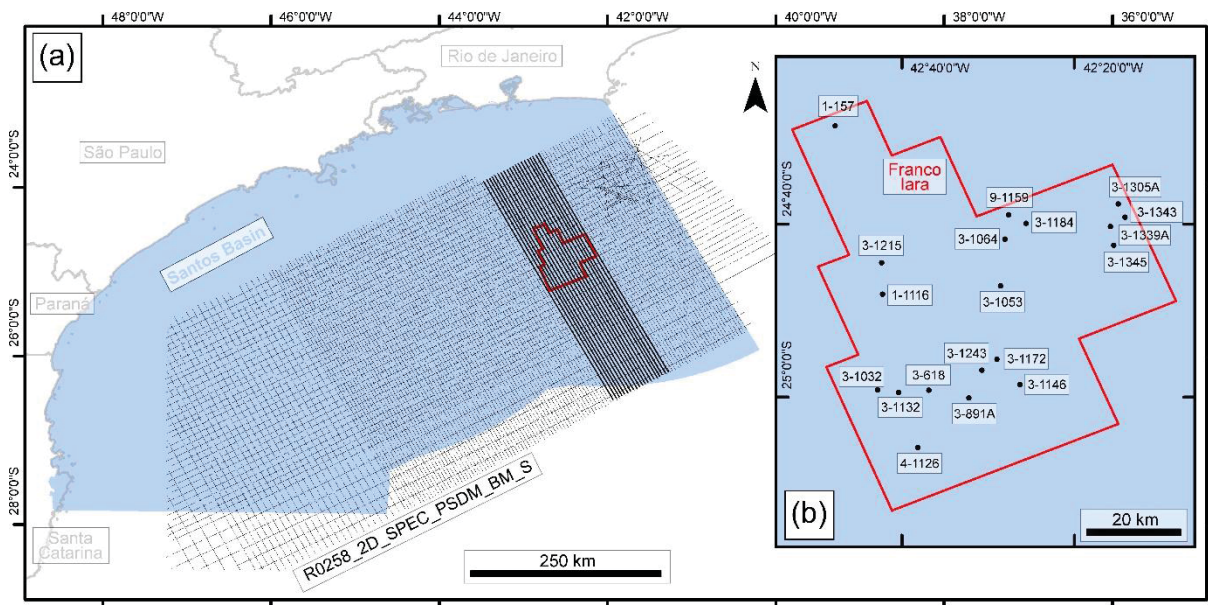
Figure 3.1: Materials used for seismostratigraphic mapping. (a) Regional 2D seismic survey, with thicker lines representing the interpretated ones covering Franco Iara survey (highlighted in red). (b) Franco Iara 3D seismic survey, showing the location of the 19 selected wells. As well code is PURPOSE OF WELL - WELL OPERATOR - DRILLING ORDER -GEOGRAPHIC REFERENCE, but the format used for this study simplifies it to PURPOSE OF WELL – DRILLING ORDER, as wells belong to the same operator (Petrobras - BRSA) and were drilled in Rio de Janeiro state (RJS). The purposes of wells include 1-pioneer well, 3-extension well, 4- adjacent pioneer well, and 9-special well (PETROBRAS 2015, ANP 2017). Data from ANP (2020), georeferenced in SIRGAS 2000.

The 2D seismic data was used to locate the study area within the salt domains of Santos Basin. For this purpose, 20 2D dip-oriented, with a dip length of ca. 330 (in-

lines), were selected (Fig. 3.1a). The salt top, sea floor, and main fault planes in the post-salt area were mapped within these sections.

The main material analyzed was the 3D PSTM seismic survey. A regular grid with a 50-step interval in both in-lines and crosslines (spaced at ca. 620 m) was employed, resulting in over 200 lines per mapped horizon. Initially, continuous seismostratigraphic reflectors were mapped on each depocenter (i.e., areas unaffected by rising diapirs). These reflectors mainly include onlap, truncations, top lap, and downlap terminations (Fig. 3.2). Markers from 14 wells (Fig. 3.1b) were added to establish correlations between different minibasins by representing the depth of contacts between formal units in each well. Subsequently, the tracked horizons were compared with well data and existing seismic profiles in the area (e.g., Assine et al. 2008, Caldas & Zalán 2009, Guerra & Underhill 2012). The selected horizons for analysis across the entire area included the Ariri Fm. (salt) base and top, Itanhaém Fm. top, Itajaí-Açu Fm. top, and the sea floor. The horizons were interpolated using the triangulation method, followed by median and average filtering. Isopach maps were generated to illustrate changes in depocenters over different time intervals. Main fault planes, particularly above salt structures, were also mapped for subsequent kinematic restoration.
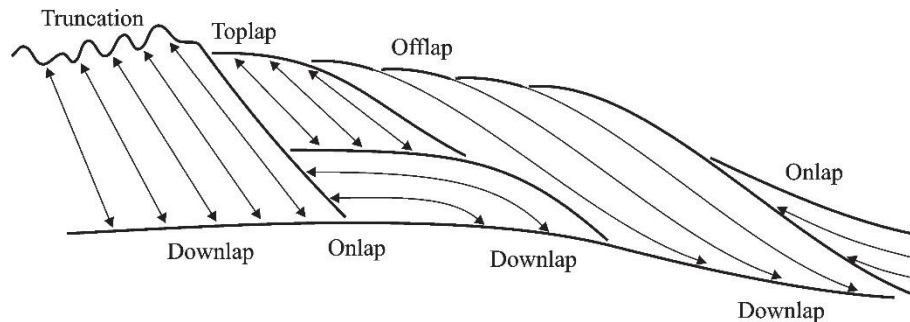
Figure 3.2: Types of stratal terminations (Catuneanu 2002).

To determinate the dip angle of the salt base, the deep steering filter was applied, followed by the dip attribute and the dip angle attribute.

In certain areas, a finer grid interval of 20 steps (~250 m) was used for in-line and crossline sections to identify and characterize specific depositional features and deep-water systems. The focus was Mass-Transport Deposits (MTDs), important features formed by sediment failure in response to gravitation that present characteristic patterns of internal deformation (Sobiesiak et al. 2018). The displaced mass tends to flow down the regional slope towards basin's depocenter, however in basins characterized by complex bathymetries due to active salt tectonics, mass failure may affect local slopes and trigger MTDs within minibasins (e.g., Biancardi et al. 2020; Poprawski et al. 2021). In these settings, each minibasin has its individual setting and evolution, including halokinetically induced MTDs that may diverge from trends found in the basin itself and can help elucidate minibasins' structural evolution once they are related to the uplifting of bounding slopes. Therefore, the base and top of MTDs were traced and interpolated using the inverse distance method, followed by median and average filtering. The similarity attribute was employed to highlight internal features, and isopach maps were created to evaluate thickness.

4 RESULTS & DISCUSSION

This section presents the findings, interpretations, and relevant observations from this study. The main findings, on minibasins and halokinetic evolution, are presented in the form of an article, which will later be submitted to the *Marine and Petroleum Geology* journal. Two other secondary results, regarding MTD and collapsing features in salt walls, were written in the form of abstracts, submitted, presented as posters (see Supplementary Materials 1 and 2) and published (see Diório et al. 2023a, Diório et al. 2023b) in national and international events.

USING MINIBASINS' GEOMETRY AND INTRA-SALT STRUCTURES TO EVALUATE SALT TECTONICS IN OFFSHORE NORTHERN SANTOS BASIN, BRAZIL

Abstract

Aptian evaporites underwent salt tectonics influencing post-salt deposition in Santos Basin. Its northern region is a pre-salt hydrocarbon producer, lacking research on intra-salt and post-salt sections. Seismostratigraphic mapping was conducted in a 3D seismic block, emphasizing five key-surfaces and four chronostratigraphic units, and identifying intra-salt structures (faults, folds, and eroded tops), and minibasins' main characteristics in plan-view (shape and thickness) and cross-sections (depocenters stacking patterns) for each time-interval. Base-salt is non-plane, and ramps (>5o) present two main trends (NW/SE and NE/SW). The evaporitic Ariri Fm. is heterogenous, and diapirs' maturity decreases basinwards. In the north E/W-directed salt walls and stocks exhibit intra upright folds, whereas in the south NNE/SSW-directed salt anticlines with intra-salt fold-and-thrust prevail. In the thinnest (max. ca. 800 m) Camburi Gr. depocenters are near-circular or E/W-elongated in plan-view, and there is a predominance of vertically stacked depocenters, followed by subbasins near the E/W Itapu-Búzios salt wall (IBSW). It records an Albian-Cenomanian phase of salt movement towards the south leading to the rise of the IBSW, and formation of density-driven minibasins above base-salt lows. The thickest (max. ca. 2.2 km) Frade Gr. exhibit constant changes in depocenters' geometries in plan-view (rounded to N/S elongated) and cross- section (most changing depocenters, followed by stacked but dipping). It records the Turonian-Maastrichtian apex of two salt tectonics trends. The first prevails northern and is related to sedimentary input and salt spreading towards the south, indicated by reactive diapirism and piled but dipping depocenters. In the south, the second one indicates salt E-directed translation, forming N/S elongated minibasins, ramp syncline basins and contractive features within N/S salt bodies. Depocenters of the Cenozoic Itamambuca Gr. are rounded-shaped, predominating changing depocenters, followed by vertically stacked ones. It records decreasing salt tectonics, as mature salt walls collapse and salt bodies above base-salt highs continue rising.

4.1.1. Introduction

Evaporites (often referred to as salt) are common in many sedimentary basins. Salt is, however, a unique sedimentary rock as it behaves as a viscous fluid when affected by differential load, basin slope or regional stresses producing three-dimensionally complex structures, significantly influencing the tectonostratigraphic architecture of sedimentary basins. Understanding salt tectonics and the development and three-dimensional geometries is crucial to constrain the evolution, stratigraphy, and kinematics of deformation in any salt basin (e.g. Jackson & Talbot 1986, Jackson & Talbot 1991, Vendeville & Jackson 1992, Warren 2006, Hudec & Jackson 2007, Fossen 2010, Jackson & Hudec 2017).

Salt tectonics has strongly impacted the tectonosedimentary evolution of passive continental margins (Rowan 2014) particularly through the combined effects of gravity spreading and gravity gliding (Vendeville 2005, Hudec & Jackson 2007, Brun & Fort 2011). When gravity-driven, salt rises in a process known as halokinesis (Hudec & Jackson 2007), and different phases and domains of salt tectonics can be formed (Rowan et al. 1999, Vendeville 2005, Brun & Fort 2011). In general, salt tends to migrate from an upslope extensional domain to a downslope contractional one due to

basinwards tilting or prograding sedimentation, leading to the formation of distinct features in each setting (Cobbold et al. 1989, Vendeville 2005 Brun & Fort 2011). Nonetheless, a mid-slope transient translational zone lies between them, and it may present characteristics that reflect both (Jackson & Hudec 2005). This translational domain has been sometimes depicted as being broadly simpler and less-deformed, but salt flow can undergo complex kinematics as it is highly influenced both by supra-salt and sub-salt features (Dooley et al. 2007, Dooley et al. 2017, Pichel et al. 2019, Ge et al. 2019, Pichel et al. 2021, Bose & Sullivan 2022, Santos et al. 2023). In natural systems, this is an area commonly with diapirs and minibasins (i.e., stacking of depocenters controlled by salt tectonics and separated by rising diapirs).

Terms such as "minibasins" (defined by Worrall & Snelson 1989, reviewed by Hudec et al. 2009), "withdrawal basins", "intrasalt basins" (Jackson & Talbot 1991) and "halokinetic basins" (Ingersoll 2012) have been introduced to describe basins formed by salt tectonics. Minibasins are syn-kinematic basins in the order of tens of kilometers in diameter, surrounded by (i.e., lateral edges) and subsiding into relatively thick allochthonous or autochthonous evaporites, with relatively short lifespans but fast subsidence compared to crustal basins (Jackson & Talbot 1991, Hudec et al. 2009, Ingersoll 2012, Jackson & Hudec 2017, Hudec & Jackson 2022). Multiple subsidence mechanisms can be described, distinguishable by specific criteria (Hudec et al. 2009). Most importantly, they hinder sediments moving downslope (Jackson & Talbot 1991), as local relief generated by salt diapirs can influence paleotopography differently depending on the stage of diapir development (e.g., Seni & Jackson 1983). This active topography, which creates structural highs and lows, impacts depositional environments of chrono-correlated units, influencing sediment divergence or accumulation and facies distribution and geometries, considering factors such as the degree of confinement, erosion rates, distance from diapir crests, and creation of local slopes (e.g., Seni & Jackson 1983, Jackson & Talbot 1991, Booth et al. 2003, Giles et al. 2008, Mayall et al. 2010, Ingersoll 2012, Jackson & Hudec 2017; Cumberpatch et al. 2021).

The Santos Basin, situated offshore southeastern Brazil and formed during the Cretaceous Gondwana rupture (Assine et al. 2008, Chang et al. 2008, Kukla et al. 2018), is one of the largest (area of approximately 350,000 km2, to a depth of around 3,000 m and extending ca. 700 km into the Atlantic Ocean, Moreira et al. 2007) and most notorious passive margin salt basin worldwide, being influenced by complex and spatially variable salt tectonics. It is also Brazil's most significant petroleum basin, in which the salt exerts a key role by guiding migration paths, forming traps, acting as a highly efficient seal for pre-salt hydrocarbon reservoirs and serving as a thermal blanket inhibiting pre-salt hydrocarbon source rock maturity in excess (Chang et al. 2008, Souza & Sgarbi 2019, Zuo et al. 2023).

The evaporitic Ariri Formation also significantly influenced the subsequent post-salt Drift Sequence. While extensive knowledge exists regarding the tectonosedimentary and halokinetic evolution of Santos Basin, most studies are either regional (Kumar & Gamboa 1979, Demercian et al. 1993, Cobbold et al. 1995, Mohriak et al. 1995, Szatmari et al. 1996, Cobbold et al. 2001, Meisling et al. 2001, Modica & Brush 2004, de Mio et al. 2005, Davison 2007, Karner & Gamboa 2007, Moreira et al. 2007, Assine et al. 2008, Chang et al. 2008, Souza 2008, Correa 2009, Lentini et al. 2010, Mohriak et al. 2010, Davison et al. 2012, Guerra & Underhill 2012, Quirk et al. 2012, Rigoti 2015, Szatmari & Milani 2016, Kukla et al. 2018, Pichel et al. 2021, Pichel et al. 2022) or focused on Central or Southern Santos Basin (Garcia et al. 2012,

Jackson et al. 2015b, Alves et al. 2017, Pichel et al. 2019, Magee et al. 2021, Rowan et al 2022). In this scenario, some attention has been paid to minibasins (e.g. Caldas & Zalán 2009, Jackson et al. 2014, Pichel et al. 2018) and to the well-marked Layered Evaporitic Sequences (LES, e.g. Gamboa et al. 2008, Fiduk & Rowan 2012, Jackson et al. 2015a, Dooley et al. 2015, Rodriguez et al. 2018, Pontes et al. 2021, Bose & Sullivan 2022), and their insights into diapiric rise within the Santos Basin and its salt domains. However, since major oil and gas (O&G) fields and clusters are in Northern Santos Basin, most studies there are focused on the pre-salt section (e.g. Leite et al. 2020, Santos & Gordon 2021, Araujo et al. 2022, Freitas et al. 2022, Vital et al. 2023, Antunes et al. 2024), lacking research in the salt and post-salt section and consequent insights on salt tectonics.

To address this gap, we conducted seismostratigraphic mapping in the Franco Iara 3D seismic block in the northern Santos Basins' mid-slope salt domain, situated within the São Paulo Plateau. Our objectives were to (1) characterize the geometry and distribution of the Aptian salt and subsequent post-salt, focusing on the LES and minibasins in plan-view and cross-sections; and (2) analyze the implication of these features on interpreting salt tectonics evolution in this area, particularly in comparison to previous analyses on Santos Basin and other existing models (e.g., the influence of base salt relief and sedimentation in halokinesis). By distinguishing various types of depocenters and diapirs and identifying key geometric characteristics in different time intervals, we aim to enhance the understanding of the intrinsic relationship between primary minibasins and salt flow, investigating whether there is a clear association during the nucleation and evolution of these depocenters and associated diapirs.

4.1.2. Geological context

The Santos Basin is a passive rifted margin sedimentary basin located on the southeastern offshore Brazil (Fig. 4.1). It is bounded to the north by the Cabo Frio High (CFH), separating it from Campos Basin, and to the south by the Florianópolis High (FH), separating it from Pelotas Basin (Moreira et al. 2007). Its formation and tectonostratighraphic evolution (Fig. 4.2) are attributed to the breakup of Gondwana and the subsequent opening of the Atlantic Ocean in the Early Cretaceous (e.g. de Mio et al. 2005, Moreira et al. 2007, Chang et al. 2008).
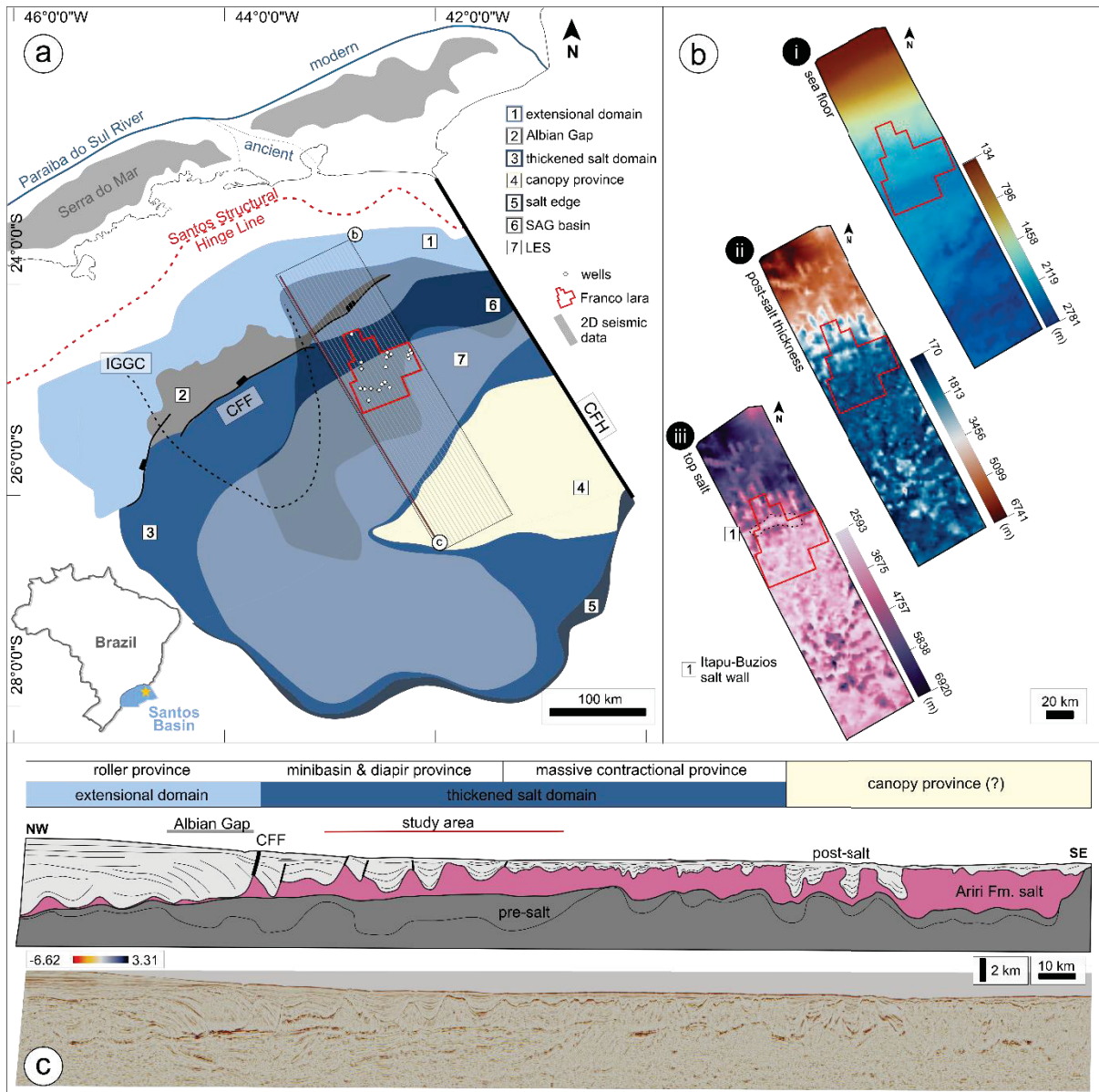
Figure 4.1: Geological setting of the studied area. (a) The studied area is in northern Santos Basin (yellow star in the regional map), near where it is separated from Campos Basin by the Cabo Frio High (CFH). Different salt domains were recognized in offshore Santos Basin (after Davison et al. 2012, Jackson et al. 2015a), such as an extensional domain separated from the thickened salt domain by the Cabo Frio Fault (CFF), a canopy province and the salt edge area. The Ilha Grande Gravitational Cell (IGGC) is western of the studied area, where the CFF influence and the Albian Gap are most present. The studied area is the 3D Franco Iara seismic block (in red), but part of the regional 2D seismic data R0258_2D_SPEC_PSDM_BM_S (gray lines) was used to locate the study area in these different domains, as well as well data (white circles) to correlate tracked horizons. Onshore, the Serra do Mar uplift (in gray) re-organized the Paraíba do Sul River course, as it used to input into Santos Basin (dotted blue line) (see Modica & Brush 2004). (b) Interpolated surfaces and sequences (color schemes after Crameri 2018) which highlight the general setting of the Franco Iara seismic block within Santos Basin 2D cross-sections. (i) Sea floor depth, where the current slope of the basin can be seen northern of Franco Iara. (ii) Thickness of the post-salt section, decreasing in the basin-dip direction. (iii) Depth of the top salt layer, significantly decreasing in the Franco Iara area after the Itapu-Búzios salt wall (dotted lines). (c) Seismic data and interpreted cross-section (see location in (a)) highlighting the post salt, salt, and pre-salt sections, as well as salt domains (see Davison et al. 2012, Jackson et al. 2015a, Bose & Sullivan 2022) and the setting of the study area.
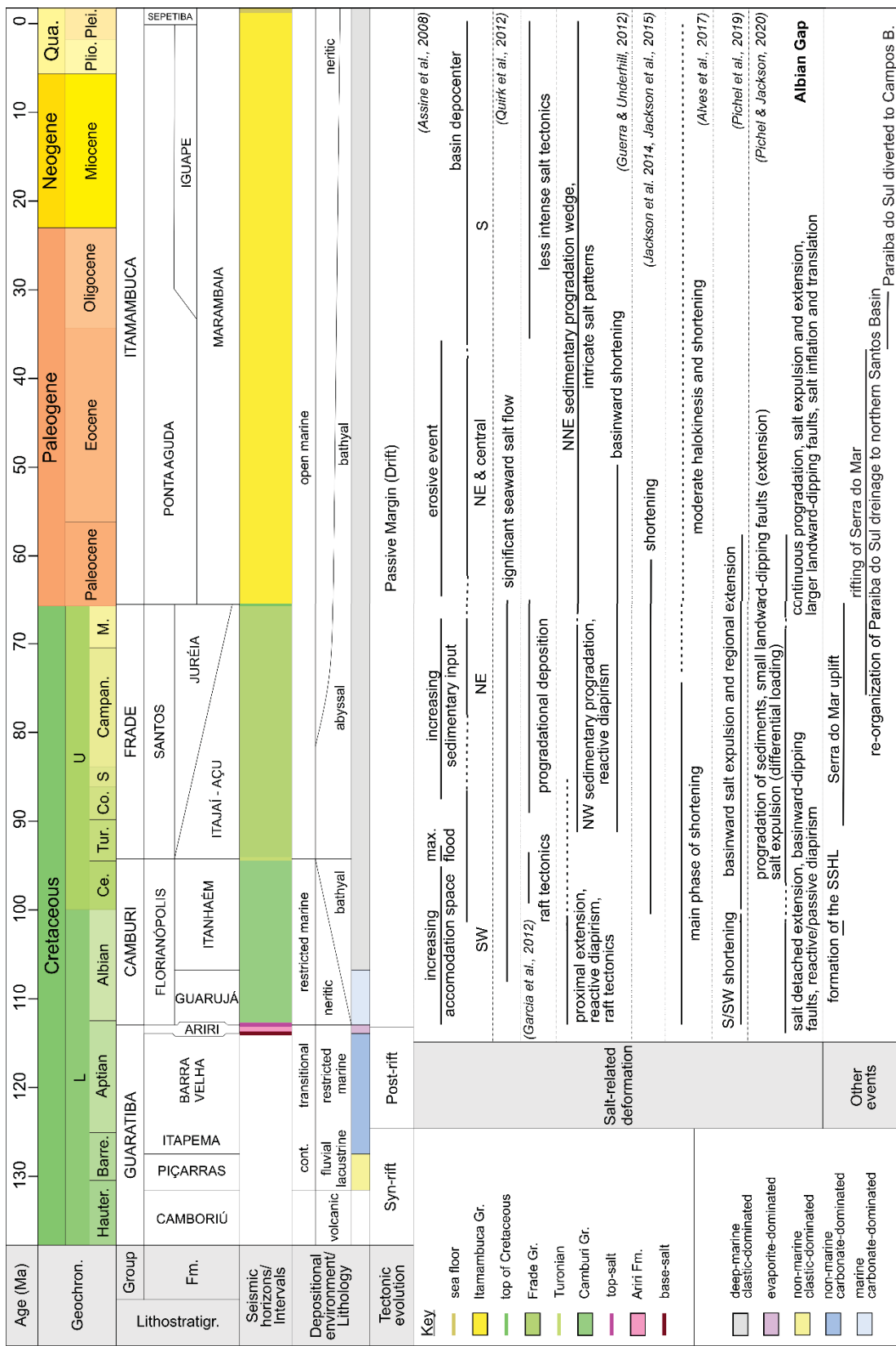
Figure 4.2: Chronostratigraphic chart, highlighting the tectonic phases, stratigraphy, tracked horizons and sequences, depositional settings, salt-related deformation, and other important events in the basin. After Modica & Brush (2004), Moreira et al. (2007), Davison et al. (2012), Quirk et al. (2012), Guerra & Underhill (2012), Cohen et al. (2013), Jackson et al. (2014), Jackson et al. (2015), Alves et al. (2017), Bose & Sullivan (2022).

Deposition initiated along regional inherited crustal weakness zones from the Proterozoic Ribeira Belt (Meisling et al. 2001, Garcia 2012, Rigoti 2015, Dehler et al. 2016,), resulting in the compartmentalization of syn-rift depocenters in an NNE/SSW trend grabens and hemi-grabens (Meisling et al. 2001, Guerra & Underhill 2012, Kukla et al. 2018). Hauterivian tholeiitic basalts from the Camboriú Formation constitute the economic basement (Szatmari 2000, Pereira & Feijó 1994, Moreira et al. 2007), overlaid by Barremian continental siliciclastic sediments from the Piçarras Formation (Moreira et al. 2007). The passage to a transitional environment, influenced by waves and currents, is represented by the carbonate-dominated Itapema Formation (Moreira et al. 2007, Leite et al. 2020, Santos & Gordon 2021, Antunes et al. 2024).

The post-rift sequence (i.e., less tectonic activity and transition to a proto-oceanic stage with increasing thermal subsidence) consists of complex carbonates from the Barra Velha Formation and the evaporitic Ariri Formation (Moreira et al. 2007, Quirk et al. 2012, Santos & Gordon 2021, Vital et al. 2023). The evaporitic Ariri Formation is composed of halite, anhydrite, and bittern salts (Freitas 2006, Moreira et al. 2007, Gamboa et al. 2008, Rodriguez et al. 2018), comprising almost exclusively evaporitic LES, as bittern salts not-so-common worldwide and all non-evaporite interbeds are rare and confined (Rowan et al. 2019). Deposition occurred in a restricted environment, primarily to the north of the FH, with variable thickness and partially controlled by pre-existing non-uniform salt base relief (Demercian 1996, Davison 2007, Lentini et al. 2010, Davison et al. 2012, Alves et al. 2017, Rodriguez et al. 2018, Pichel et al. 2019). This led to multiples cycles of flooding and evaporation registered in Ariri Fm., resulting in the presence of 4-6 major seismically distinguishable intra-salt units (Gamboa et al. 2008, Fiduk & Rowan 2012, Rodriguez et al. 2018). On average, salt deposition is estimated to range from 2-2.5 km (Davison et al. 2012, Rodriguez et al. 2018), occurring in a relatively short geological timespan (<530 k.y. according to Rodriguez et al. 2018).

During the drift phase, the gradual opening of the southern volcanic barrier led to the establishment of open marine conditions and onset of thermally induced subsidence (Quirk et al. 2012, Garcia 2012, Jackson et al. 2015a, Santos & Gordon 2021). Despite most tectonic stresses nearly ceased, the deposition of the Drift Sequence was heterogeneous, controlled by variations in eustatic sea level, the Serra do Mar uplift, reorganization of the ancestral Paraiba do Sul drainage system, sedimentary input, and salt tectonics (e.g. Meisling et al. 2001, Cobbold et al. 2001, Modica & Brush 2004, Assine et al. 2008, Caldas & Zalán 2009, Quirk et al. 2012, Guerra & Underhill 2012, Garcia et al. 2012, Jackson et al. 2015a, Pichel et al. 2019).

The drift phase, initiated in the Albian and still active, and is divided into Camburi, Frade, and Itamambuca Groups (Moreira et al. 2007). As accommodation space started to increase, the basal Camburi Group recorded a marine transgression, culminating in an anoxic environment ceased at radioactive shales (Arai 1988, Pereira & Feijó 1994, Moreira et al. 2007, Assine et al. 2008). After the Turonian maximum flood surface, the Frade Group documents increasing terrigenous sediment supply in the basin and strong lateral variations in sedimentary content from mostly clastic proximal to mostly pelitic distal deposits (Pereira & Feijó 1994, Milani et al. 2000, Moreira et al. 2007, Assine et al. 2008). After a major global sea level fall and forced regression, siliciclastic-carbonate depositions on the marine Itamambuca Group were affected by changes in the basin depocenter due to tectonic reactivations, sea level fluctuations and consequent shifts in the coastline, and records variations in coastal to deep-water environments (Pereira & Feijó 1994, Moreira et al. 2007, Duarte & Viana 2007, Assine et al. 2008).

Salt tectonics has produced complex and highly variable salt-related structures across Santos Basin as salt moved basinwards, with a main ESE to SE direction (e.g.

Guerra & Underhill 2012, Davison et al. 2012, Garcia et al. 2012, Quirk et al. 2012, Jackson et al. 2015a, Pichel et al. 2018, Pichel et al. 2022). Most authors agree that salt began moving during or shortly after its deposition (e.g., Davison et al. 2012, Guerra & Underhill 2012, Pichel et al. 2019, Pichel et al. 2022, Bose & Sullivan 2022). However, since the basin tilted in the late Albian, some authors believe salt tectonics was triggered in this period (Demercian et al. 1993, Assine et al. 2008, Garcia et al. 2012, Quirk et al. 2012).Anyhow, existing salt-related structures were a product of seawards salt flow and overburden translation driven by differential sediment loading (i.e., spreading) and the seawards slope caused by margin tilting (i.e., gliding), with secondary effects of salt flow over rift-related base-salt relief and, in places, ongoing rifting (Cobbold & Szatmari 1991, Cobbold et al. 1995, Quirk et al. 2012, Davison et al. 2012, Alves et al. 2017, Pichel et al. 2019, Pichel et al. 2022, Santos et al. 2022, Santos et al. 2023).

These processes resulted in kinematically-linked domains of deformation defined by updip extension and downdip shortening connected by an intermediate translational domain where deformation is highly variable depending on the geometry of the salt basin, base-salt relief, and supra-salt coverage, as well as the migration of the extensional domain basinwards (Cobbold & Szatmari 1991, Dooley et al. 2007, Dooley et al. 2017, Pichel et al. 2019, Ge et al. 2019, Pichel et al. 2021, Zwaan et al. 2021, Pichel et al. 2022). In the Santos Basin, salt withdrawal created different types of passive and reactive salt structures related to updip extension of the overburden and creation of accommodation spaces. Those include salt rollers in the footwalls of NE-trending landward-dipping listric normal faults, basinwards-dipping normal faults, salt domes and walls sometimes along synthetic and antithetic faults, basinwards-thickening wedges, extensional turtle anticlines, expulsion rollovers, raft tectonics, overburden erosion, and salt welds (Cobbold et al. 1995, Assine et al. 2008, Guerra & Underhill 2012, Pichel & Jackson 2020, Pichel et al. 2022). This extension and lateral salt expulsion has contributed to the formation of the enormous (>450 km long, up to 60 km wide) Albian Gap, roughly parallel to the coastline and bounded seaward by the Cabo Frio Fault (CFF) and post-Albian rollover (see Fig. 4.1). The Albian Gap coincides roughly with the limit between the updip extensional and intermediate translational domain which is located approximately over a large rift-related base-salt plateau (Mohriak et al. 1995, Modica & Brush 2004, Guerra & Underhill 2012, Pichel et al. 2019). This complex feature, which varies along-strike and is highly affected by basement features, records contrasting kinematic and growth strata geometries, indicating that post-Albian salt-detached 25-30 km extension and Albian salt expulsion by differential loading played a significant role in its evolution, which also involved basinwards translation of the overburden (Pichel & Jackson 2020, Pichel et al. 2022). The compressive domain presents high variation in salt deformation styles and salt thickness as it translated and inflated downslope forming fold-and-thrust belts. In these, multiple-directed, symmetric and asymmetric, reactive and passive salt-cored structures (predominantly linear salt anticlines and walls) present contractional growth folds (e.g., angular and concentric, sometimes tight), thrusts (which may thicken or repeat LES), eroded upper parts, minibasins, and overburden buckle-folding (Cobbold & Szatmari 1991, Cobbold et al. 1995, Guerra & Underhill 2012, Alves et al. 2017, Pichel et al. 2022).

4.1.3. Methodology

As salt tectonics is intrinsically a spatially and temporally complex 3D process, we undertook multiple steps integrating regional and local observations, aiming for a

multiscale seismostratigraphic approach, from 2D regional analysis to detailed 3D seismic interpretation of a key area in the basin.

We first analyzed regional 2D depth-migrated seismic lines to understand the regional salt tectonic context of Franco Iara's block within the Santos Basin. Twenty 2D dip-oriented lines, with a dip length of ca. 330 km (Fig. 4.1), were selected from the post stack seismic survey R0258_2D_SPEC_PSDM_BM_S, which crosses the entire basin. For this, we mapped 2 key horizons (top salt and seafloor), and main supra-salt fault planes. These horizons were then used to produce structural and regional maps (see Fig. 4.1b).

We then focused our analysis on a selected area that was key for diapirism, minibasin development and structural compartmentalization within the basin, the Franco Iara's block. For this, we used the post-stack depth-migrated (PSDM) 3D seismic survey R0302 Franco Iara (Fig. 4.1), covering an area of ca. 3,700 km^2 in northern Santos Basin. Inline (northwest-southeast) and crossline (northeast-southwest) spacing is ca. 12 and 11 m, respectively.

As the study area contains multiple unconnected minibasins, the initial approach consisted in mapping broadly continuous and well-marked reflectors that defined important internal unconformities within each minibasin (Fig. 4.3a). Picking of key seismic reflectors was performed using a regular grid with a 50-step interval in both in-lines and crosslines (spaced at ca. 620 m). We then added markers representing the depth of contacts between formal chronostratigraphic units from 14 wells (see Fig. 4.1a) to establish chronostratigraphic correlations between different minibasins that helped understanding their relative timing of formation. We also compared the 72 mapped seismic reflectors (i.e., in total, including internal unconformities in all minibasins) with well data and previous published interpretations (Assine et al. 2008, Caldas & Zalán 2009, Guerra & Underhill 2012). In this approach, the horizons that were analyzed throughout the entire studied area (Fig. 4.2a) were base- and top-salt (Aptian Ariri Fm.), Itanhaém Fm. top (Turonian), Itajaí-Açu Fm. top (top of Cretaceous), and the seafloor (Fig. 4.2 and Fig. 4.3a). These were interpolated to produce 3D surfaces, which were then used to generate interpolated isopach maps individualizing 4 sequences (refer to Fig. 4.2): Ariri Fm. (Aptian), Camburi Group (Albian-Cenomanian), Frade Group (Turonian-Maastrichtian), and Itamambuca Group (Cenozoic). Colour schemes from Crameri (2018) were used in both surfaces and isopach maps.

At first, isopach maps done between key-horizons helped identifying main minibasins, and their geometry and thickness through time. Geometry in plan-view analyses may help separate the absence of structural control which forms subrounded or polygonal shapes (Rowan & Vendeville 2006) from regional tectonics interference or slope-related developed forming more linear shapes (Nalpas & Brun 1993).

Further geometric analyses in cross-section were done on minibasins in the post-salt sequence, based features and mechanisms proposed by Jackson & Hudec (2005), Hudec et al. (2009), Giles & Rowan (2012), Rowan et al. (2016) and Ge et al. (2020). Geometric patterns in cross-section of minibasins in each analyzed time interval were also described, focused stacking patterns of depocenters (Fig. 4.3b) and following the same interval as for horizon picking. These stacking patterns have an intrinsic relation to salt movement: vertically stacked depocenters with raised rims are related to density-driven subsidence; changing depocenters and subbasins to diapir shortening; merging depocenters to merging of multiple minibasins or to salt welding; and stacked but dipping depocenters to sedimentary topographic loading (higher dipping angle) or salt translation (lower dipping angle). Terminations of minibasins adjacent to diapirs were separated as wedge (pilled forming tapered composite

halokinetic sequences), hook (piled forming tabular composite halokinetic sequences, with associated cusps) or megaflaps.

However, some challenges were faced when defining features in cross-sections. Even though geometries tend to be as in Figure 4.3b, they can be hard to settle because they can change in adjacent minibasins (e.g. Ge et al. 2021) and are not continuous throughout a single minibasin. Firstly, it can be challenging to separate vertically stacked depocenters from slightly changing depocenters and stacked but gently dipping depocenters, a situation eased by vertical exaggerations and decreasing spacing between analyzed sections. Secondly, depocenters may change either from (i) the first to the last deposited sequence (i.e., depositional evolution), (ii) border to center of a minibasin and/or (iii) in different perspectives (e.g., crossline or in-line). Even sometimes subtle, these changes are important as they may indicate different settings, such as unidirectional salt movement (e.g., vertically stacked depocenters in crosslines and slightly changing depocenters in in-lines). Thirdly, the interpretation of depocenters and especially rims can be difficult in diapiric settings, once they can obliviated by faulting or erosion, common during salt tectonics (Hudec & Jackson 2012). Places with no raised rims may indicate either not-density driven subsidence or salt rise faster than sedimentary accretion (Hudec et al. 2009). For the latest, the description of halokinetic sequences (Giles & Rowan 2012) is of much aid. Lastly, there are difficulties in choosing the most representative depocenter style for each interval. When more than one pattern occurred at the same time-interval, we chose to represent either the most pervasive or the one with the most important genetic implication, as relying on a single section to define the whole setting of a minibasin can be misleading.

For the salt horizons, as the top- and base-salt are commonly the better imaged reflectors, relative to intra-salt ones (van Gent et al. 2010), they are the only ones that were confidently mapped throughout the entire study-area. Intra-salt reflectors are thus only described in cross-sections. We use these, in particular 3D top-salt geometries to classify the salt structures in terms of kinematics and maturity using the terminology established by Jackson & Talbot (1991) and Jackson & Hudec (2017). We therefore consider if the top-salt is concordant or discordant to overlying units, if its plan view geometry is equant or elongated, and if it autochthonous or allochthonous. Intra-salt structures, such as faults and folds, were described and interpreted using LES, based mostly on Jackson et al. (2015a) and Bose & Sullivan (2022). The main characteristics defined were eroded tops, anticlinal folds, and faults or shear-zones (Fig. 4.3c), defined using a regular grid with a 100-step interval (ca. 1,250 m) in both in-lines and crosslines.

As a complement, dip angles were calculated using the deep steering filter, followed by the dip attribute (dGB 2024a) and the dip angle attribute (dGB 2024b). Some sedimentary settings, such as Mass Transport Deposits (MTDs) and contourites, were described when seen and sometimes mapped using a regular grid with a 20-step interval in both in-lines and crosslines (spaced at ca. 250 m). Finally, the main fault planes above salt structures were mapped and classified, following the same 50-step interval method.
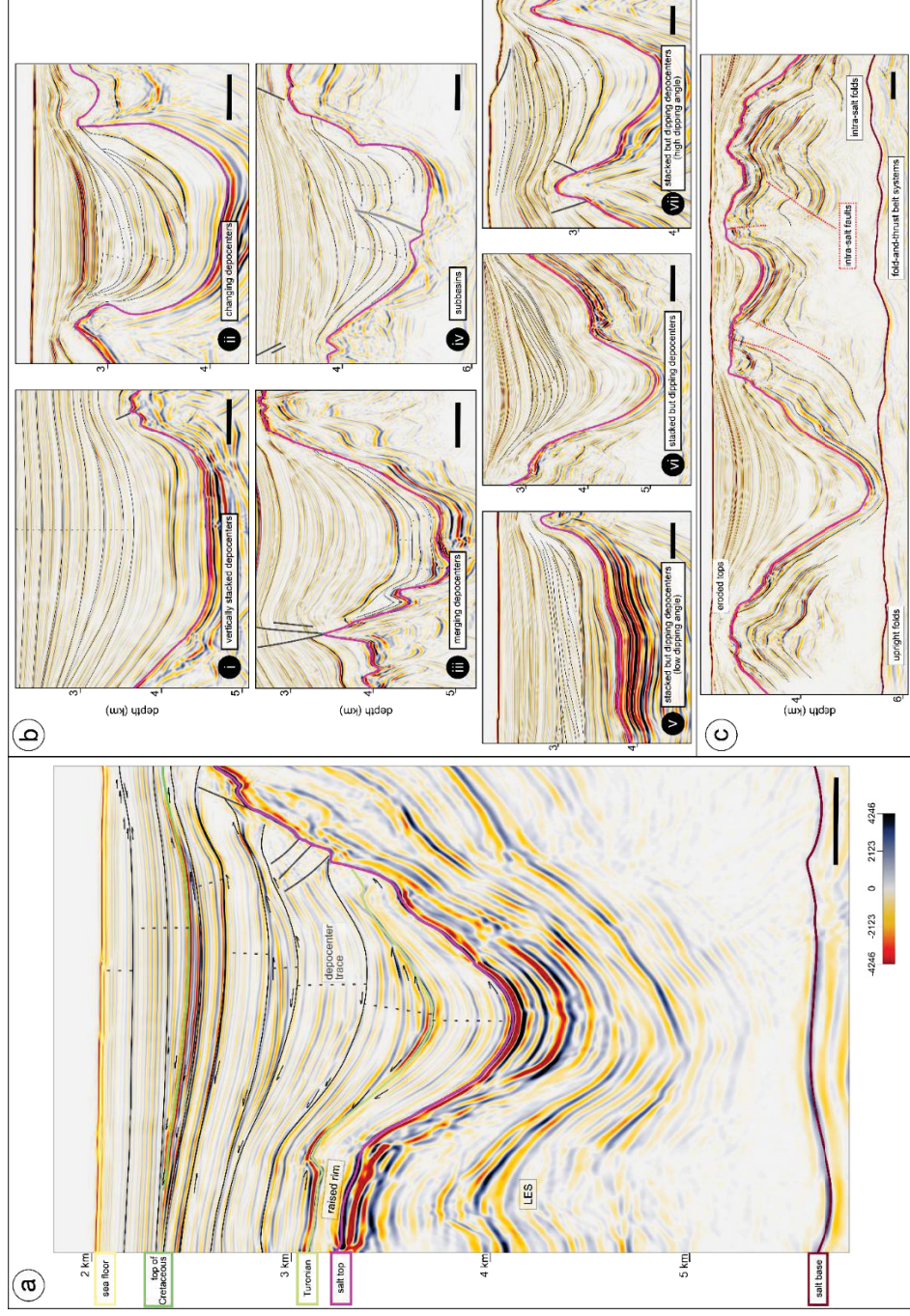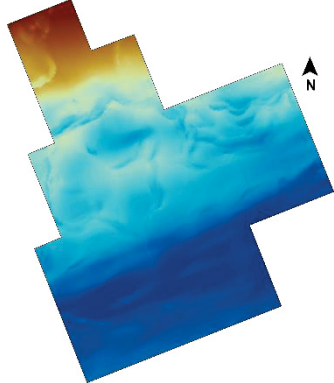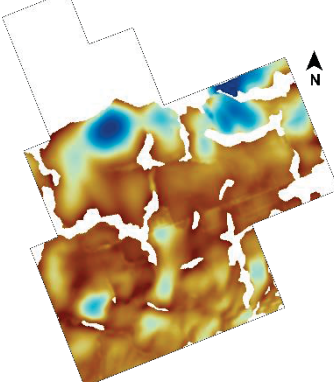
Figure 4.3: Summary of used methodology. a) An example of a minibasin, made of stacking depocenters (dashed gray lines) which are delimited by stratal terminations (black arrows, mostly on-lap and down-lap), and may have been raised or not on salt rims. Based on well data, some of these reflectors were correlated to chronostratigraphic units. b) Main cross-view geometries of minibasins' depocenters, including (i) vertically stacked depocenters, (ii) changing depocenters (in this case associated with a megaflap), (iii) merging depocenters, (iv) subbasins, and (v, vi and vii) stacked but dipping depocenters, with different dipping angles. For all cases, notice how those patterns are not maintained throughout the hole minibasin depositional history. c) Mapped intrasalt patterns, visible due to LES, including eroded tops, intrasalt faults (dashed red lines) and anticlinal folds. All horizontal scales correspond to 1km.

4.1.4. Franco Iara intra-salt and post-salt framework

As shown in Figure 4.1, the studied area is at the translational salt domain. North-eastern of it, there is the present-day toe-of-slope (Fig. 4.1b-i) and bathymetry reaches ca. 1,500m. Also, there is a significant decrease in the post-salt section thickness, from ca. 5km to ca. 3.5km (Fig. 4.1b-ii), as well as an increase in salt depth from ca. 7 km to ca. 3 km (Fig. 4.1b-iii). This change in the seafloor and salt depths and post-salt thickness is related to the CFF (Fig. 4.1c), as sediments tend to become trapped within this structure. Alongside, major (> 20 km wide) NE/SW salt walls with prominent normal faults related to crestal grabens (offsets of ca. 350 m) are important markers of this transition between domains. Basinwards of the Itapu-Búzios salt wall (IBSW, Fig. 4.1b-iii), continuous faults (lengths exceeding 8 km) are no longer observed. However, the area is situated prior to the occurrence of salt canopies, indicating that the analysis focused on primary rather than secondary minibasins.

The general basic local setting was first defined based on tracked chronostratigraphic horizons, summarized in Table 4.1. Except for the salt top, all other surfaces exhibit distinct positive peaks. Northern in the studied area, the transition from the salt extensional to transitional domains is characterized by the prominent E/W-oriented IBSW, and the surfaces related to the drift sequence were not tracked in the northwestern area due to the increased difficulty and uncertainty of correlation.

Table 4.1: Main characteristics of tracked horizons.

Horizon	Geochron.	Depth (m) Max.	Depth (m) Min.	Figure	Observations
Sea floor	Present-day	2300	1480		-Non-plane, affected by salt tectonics and deep-water settings
	1487 1690 1892 2095 2297 (m)				
	Representative colour				
Itajaí-Açú Fm. top	Cretaceous / Cenozoic transition	3450	2320		-Intense deformation caused by salt tectonics and some parts are eroded
	2325 2603 2882 3160 3438 (m)				
	Representative colour				
Itanhaém Fm. top	Turonian	5320	2520		

	2524 3222 3920 4618 5316 (m)				-Not continuous -Lows in the northern area and above salt welds -Highs occurring after salt walls in the southern part
	Representative colour				
Salt top	Aptian / Albian transition	5900	2650		-Depths variation due to autochthonous salt tectonics -Northern characterized by the E/W-oriented IBSW (dotted lines, over 30 km wide and 2 km high), with prominent crestal grabens. -Lowest salt depths in salt welds, especially near the IBSW -Southwards, salt highs exhibit more complex orientations, although N/S and W/E trends can be discerned.
	2653 3464 4275 5086 5897 (m)				
	Representative colour				
Salt base	Upper Aptian	6590*	5250*		- Lineaments separating the structural highs from lows exhibit two main orientations: NW/SE and NE/SW. The transitions from highs to lows are less abrupt in the NW/SE lineaments compared to the NE/SW ones.
	5253 5586 5919 6251 6584 (m)				
	Representative colour				

*These values may slightly vary due to the layered nature of salt, exhibiting different compositions, and the velocity model used to convert the seismic data from time to depth assumes a homogeneous composition.

Franco Iara is located in important O&G fields and clusters (Fig. 4.4a) that collectively produce up to 1.582 Mboe/d from pre-salt carbonates (ANP 2023). In this area, the seafloor highlights current depositional settings (Fig. 4.4b), such as the end of the slope in the northern region where MTDs are found, and variations southern from it attributed to active minibasins, rising diapirs, crestal grabens or depression bottom-current related.
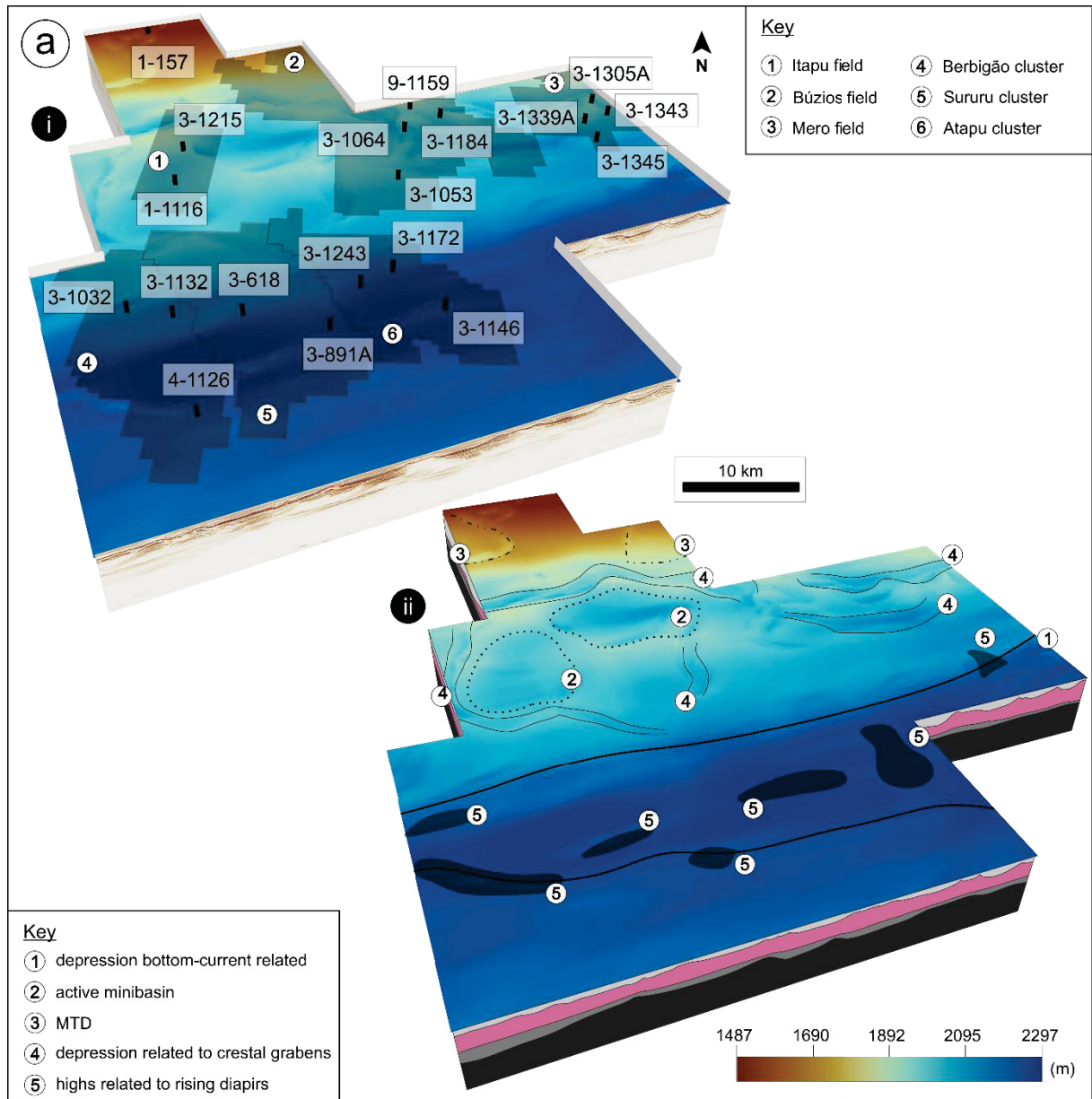
Figure 4.4: Seafloor setting. a) Sea floor, with wells used for correlation and main O&G fields and clusters, b) and interpreted present-day sedimentary settings.

4.1.4.1.   Ariri Formation (Aptian salt) and intra-salt patterns

Due to salt tectonics, the distribution of Ariri Formation is heterogeneous through the studied area (Fig. 4.5a), and diapirs' thickness vary from ca. 340 to 3,170 m (Table 4.1).

The area is mostly included in the zone of Layered Salt (see Davison et al. 2012, Fig. 4.1). Well data indicates this LES, with an intercalation of anhydrite, gypsum, halite, and bittern salts (sylvinite, tachydrite, and carnallite). There is an increase in bittern-salts content towards the top, and common intercalations of halite and anhydrite in the bottom (see Fig. 4.6 a-ii and b-ii). Carbonates and pelites are also present, either at the very beginning or very end of the successions.

There is a decrease in salt bodies' maturity basinward (Fig. 4.5a-ii), from NW to SE, although no allochthonous salt was found. Piercing features (i.e., salt walls and

stocks) prevail in the northwest, among salt welds, and eroded tops were described in these. IBSW (Fig. 4.6a-b) is an asymmetric feature (dip angles up to ca. 20° towards the north and ca. 50° towards the south). In its northern part there are features indicative of salt collapse such as mock-turtle anticlines. Also north, Cretaceous post-salt units are displayed in a rollover anticline, followed by thickening Cretaceous and Cenozoic units (see Fig. 4.6b), indicating its association to a normal-fault system. On the other hand, concordant structures (i.e. salt anticlines) are more common in the southeast, particularly within stratified salt layers, and the salt highs exhibit more complex orientations. Also, where there was a predominance of elongated in-plane

geometries, two main trends were seen: a NS direction trend in the southestern part of Franco Iara, and an EW trend in the northeast (Table 4.1 and Fig. 4.5a).
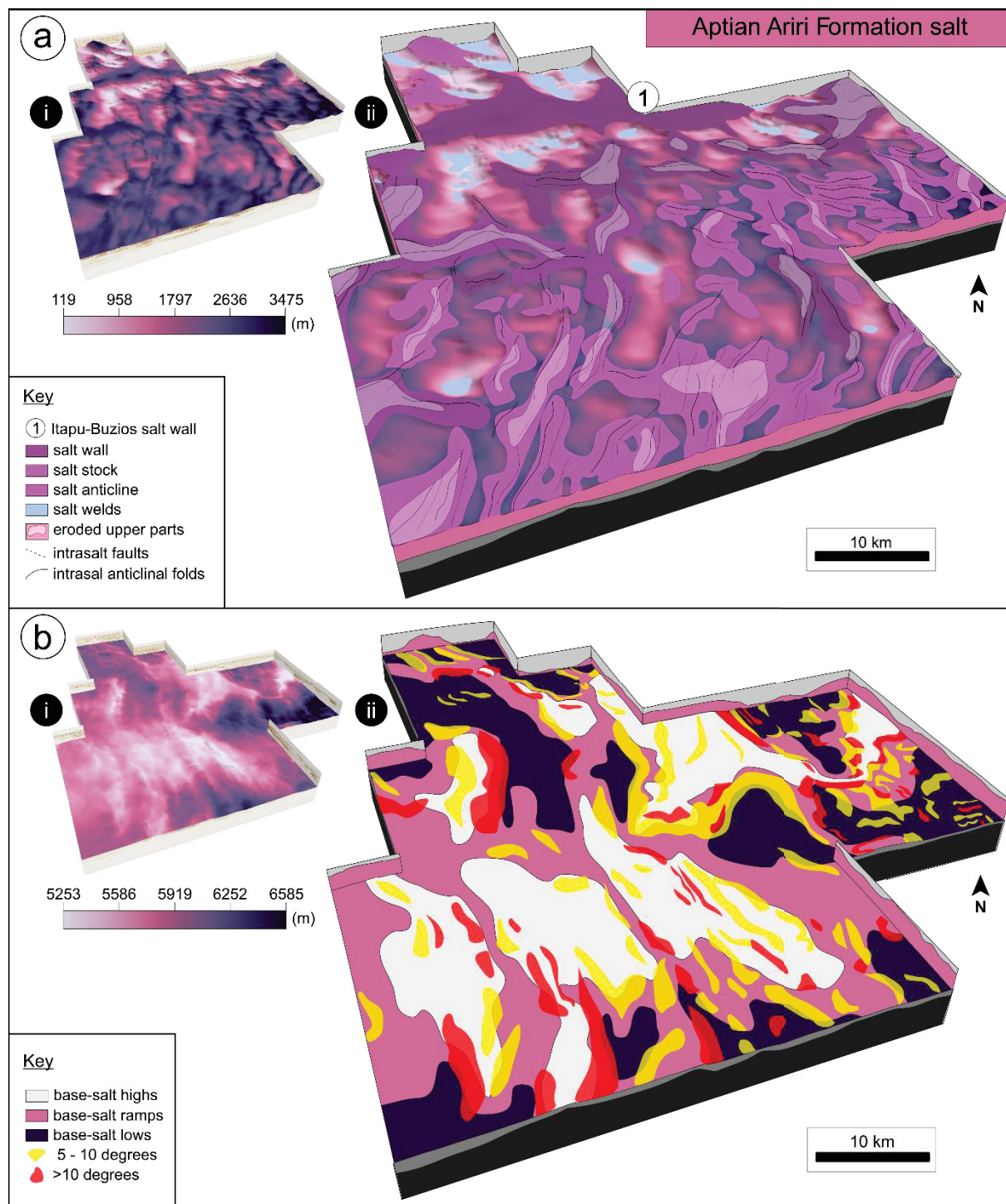
Figure 4.5: Aptian salt general setting. a) Aptian Ariri Fm. (i) thickness and (ii) interpreted types of salt bodies, with intra-salt faults, anticlinal folds and eroded upper parts. b) (i) Base-salt depth and (ii) base-salt highs and lows separated by ramps with dips up to 30o.
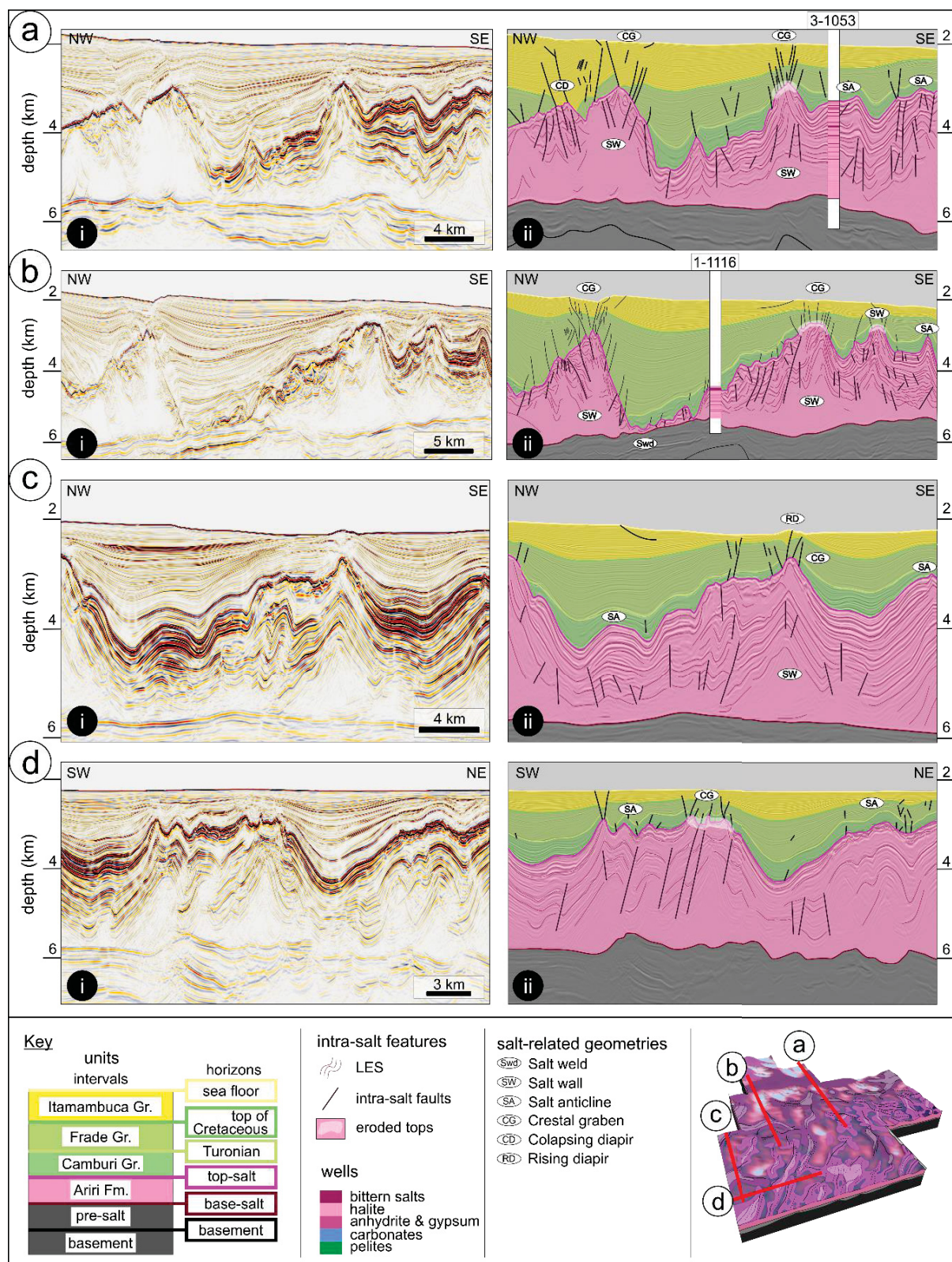
Figure 4.6: Key-sections illustrating interpreted intra-salt main features. a) Collapsing of the IBSW, and salt wall in the south are with eroded tops and crestal grabens. Well 3-1053 highlights LES, with a predominance of anhydrite and halite at the base of the section and bittern salts towards the top. b) Asymmetric IBSW with fault-related features, a salt weld, and salt wall in the south area with eroded tops, crestal grabens and a salt anticline. Well 1-1116 also highlights LES with the occurrence of carbonate and pelites either at the top or end of the succession. c) Salt anticlines and a salt wall with

intra-salt folds and faults, as well as current rising diapiric features in the salt wall. d) Salt anticlines with structures reassembling fold-and-thrust belt systems.

Intra-salt faults and anticlinal folds are common throughout the whole area (see Fig. 4.3c), usually associated and resembling either upright folds or fold-and-thrust belt systems. As IBSW presents collapsing features, these fault and fold systems were not defined there as in other salt bodies. Folds were recognized in salt walls and salt anticlines, and folds-and-thrust were seen on salt anticlines, in both cases following its plan-view direction. The presence of faults is recognized basinward from anticlinal folds, which gives it a sense of transport direction. In the northeastern part of the area (Búzios and Mero fields), there is a predominance of salt walls and anticlines with an E/W direction and upright folds (see Fig. 4.6a), but some fold-and-thrust with an E/W direction indicate that transport was from north to south (Fig. 4.6c). On the other hand, in the southern part (Berbigão, Sururu and Atapu clusters), fold-and-thrust have an N/S direction prevail, and transport was from west to east (Fig. 4.6d).

Analysis of dip angles done in the salt base proved a non-plane base, with dip angles varying in value (reaching up to ca. 30°) and direction (Fig. 4.5b-ii). Salt base highs and lows are separated by ramps with higher dipping angles, especially those located in the northeast and south parts of the studied area. Higher dipping angles (10°-20°) are most common in NW/SW orientations, most dipping to the east.

4.1.4.2. Post-salt minibasins

Primary minibasins filled by the post-salt drift sequence were initially identified through an isopach map created between the salt top and the sea floor (Fig. 4.7a-i). In the northern area, near the IBSW, there is a prevalence of near-circular minibasins with diameters up to 14 km and maximum thicknesses ranging from ca. 4 to 3 km. In the southern area (Berbigão, Sururu and Atapu clusters), minibasins exhibit a rounded to N/S elongated shape, with diameters of up to 10 km and maximum thicknesses varying between ca. 2.5 to 1.8 km, even though most minibasins are not over 2 km thick (Fig. 4.7a-ii). Some key minibasins were named after the fields and clusters of which they are near (Fig. 4.4a), chosen due to their different locations regarding diapirs, different in-plan shapes, different thickness, and different geometries.

The post-salt drift sequence is also influenced by multiple fault types (Fig. 4.7b-ii). The main type are normal faults related to crestal grabens (in black), which are pervasive through the whole area, following the direction of salt walls and anticlines and they are better developed in salt walls (salt bodies with higher maturity) in the western part of the studied area. Faults separating subbasins (in blue) are more common near the IBSW. Listric faults (in orange) are more common in the north (Búzios and Mero fields) displacing Cenozoic units (see Fig. 4.9d), and dip basinwards, towards the depocenter of minibasins or into crestal grabens.

Geometry of depocenters were analyzed in cross-section for three time-intervals (Fig. 4.8a, b, and c). Interval 1 corresponds to the Camburi Group (Albian-Cenomanian, Fig. 4.8c), Interval 2 to the Frade Group (Turonian-Maastrichtian, Fig. 4.8b), and Interval 3 to the Itamambuca Group (Cenozoic, Fig. 4.8a). As for end-member types in minibasins there is a major predominance of wedge end-member types, as well as tapered composite halokinetic sequences (CHS). As a matter of fact, hook end-members and megaflap structures were identified and therefore represented only in the Camburi Gr. (Fig. 4.8c-ii).
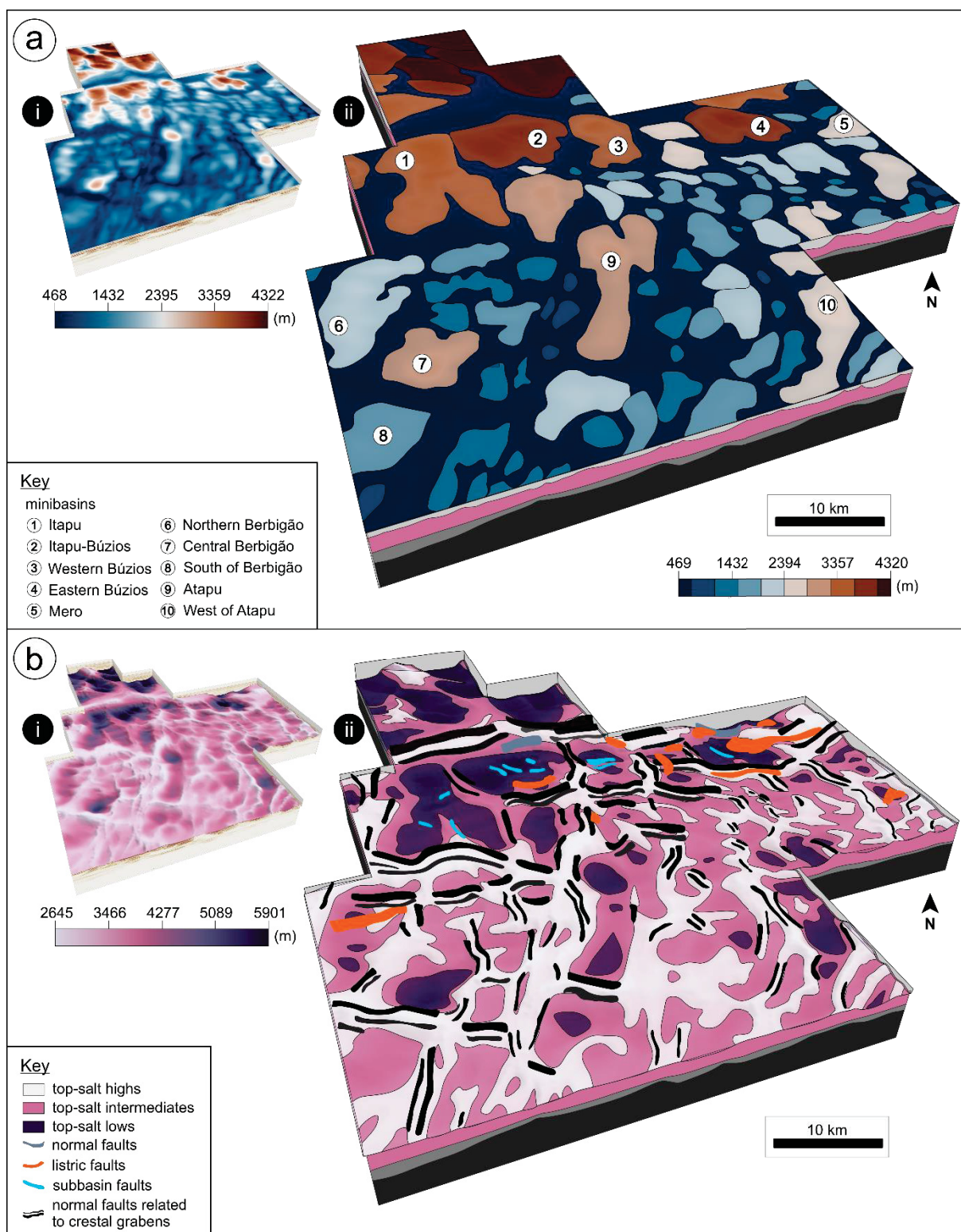
Figure 4.7: Post-salt sequence setting. a) (i) Post-salt thickness, and (ii) main minibasins, highlighting different thicknesses and in-plan shapes distribution. b) (i) Salt-top depth and (ii) sketch of main post-salt faults above salt structures, separated into normal faults (in dark blue), diapir crestal grabens (in black), listric faults (in orange) and subbasins (in blue).
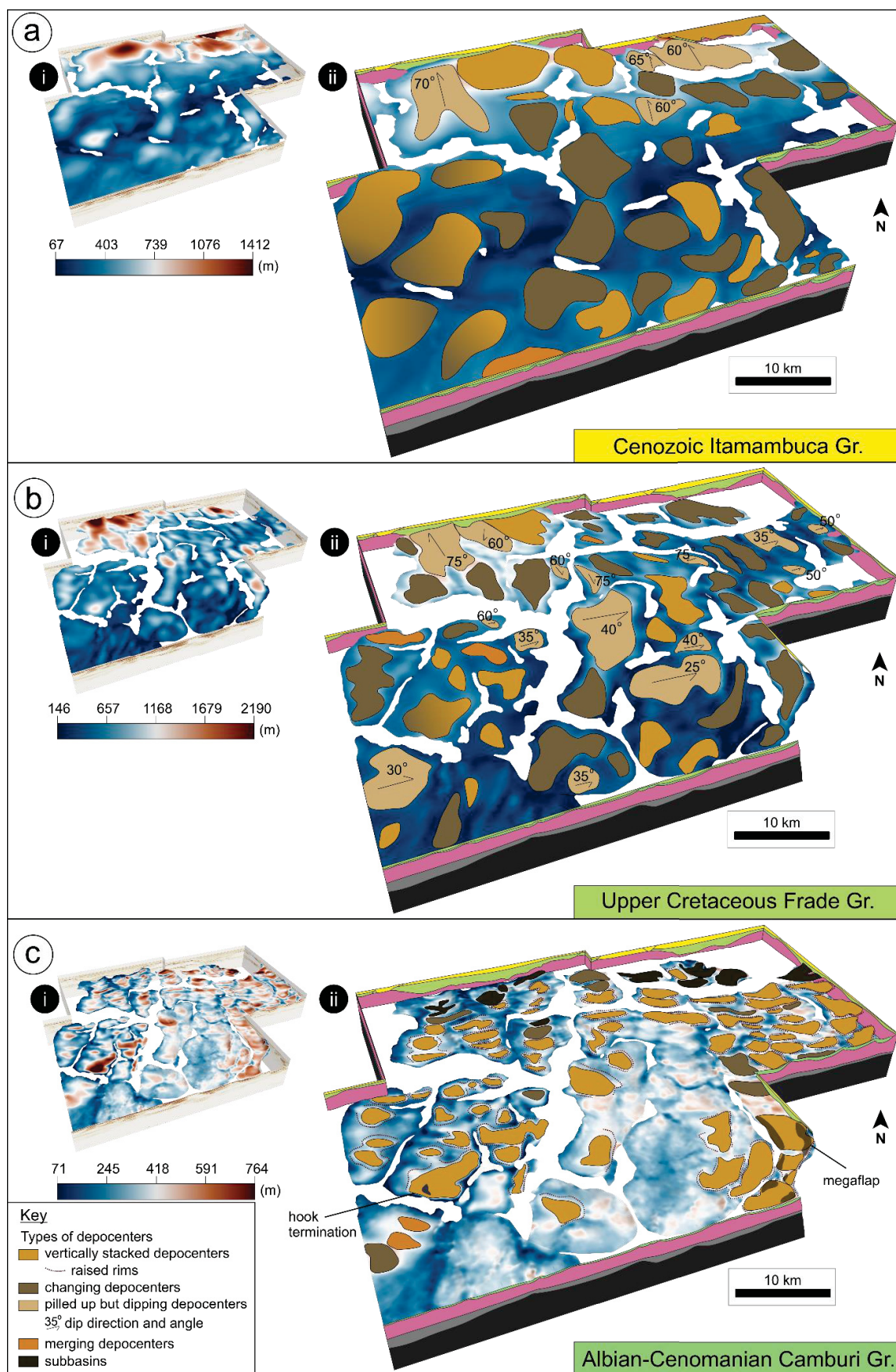
Figure 4.8: Minibasins results in each analyzed time-interval. a) Cenozoic Itamambuca Gr. (i) thickness and (ii) interpreted types of depocenters. b) Upper Cretaceous Frade Gr. (i) thickness and (ii) interpreted

types of depocenters. c) Albian to Cenomanian Camburi Gr. (i) thickness and (ii) interpreted types of depocenters.

The thickest depocenters from the Camburi Group (Fig. 4.8c) reach up to ca. 800 m and are spread though the Franco Iara area. Depocenters are either with a near-circular or an E/W elongated shape in plan-view, widths of ca. 3 km and located within O&G clusters, therefore less present in the southern part of Franco Iara. Except from the Berbigão field area, those minibasins are located above base-salt lows. There is a predominance of vertically stacked depocenters, followed by subbasins near the IBSW and changing depocenters mainly in the northern and eastern areas. Most depocenters near the IBSW and those in the western part of Franco Iara are not associated with raised rims, differently from the ones in western portion. Some different types of end-member terminations were also seen in this unit, including megaflaps (Fig. 4.10b) in the West of Atapu minibasin and hook terminations with associated cusps (Fig. 4.10c) in Central Berbigão minibasin.

The Frade Group presents more complex geometries (Fig. 4.8b), as some previously isolated depocenters merge into larger ones (see, e.g., Eastern Búzios, Itapu and Itapu-Búzios minibasins in Fig. 4.9a, b and d). Most depocenters in the Berbigão and Sururu fields are rounded-shaped with widths ca. 8 km, and in the rest of the area N/S elongated shape in plan-view with widths up to 10 km. Thickest depocenters, which are located near the IBSW, reach up to ca. 2.2 km. In general, there is a predominance of changing depocenters, followed by piled up but dipping depocenters with different dipping angles and directions (near the IBSW they dip south and are maintained throughout the whole time-interval, and in the rest of the area they dip mostly to the east and are present only in part of this Group's deposition), vertically stacked depocenters and, last, merging depocenters. Furthermore, in general there is a difficult to identify rims relation due to diapir-related faults, since most termination are wedge end-member types and influences of contourites (see Fig. 4.11c), and erosive features were found particularly southern from the Mero and Búzios fields and eastern of Atapu cluster.

In the Cenozoic Itamambuca Group (Fig. 4.8a), depocenters are larger (widths up to 15 km) as some depocenters continued merging (see e.g., Central Berbigão minibasin, Fig. 4.10c), resulting in predominantly rounded-shaped, with some NE/SW elongated ones. MTDs can be found at the base of this succession, dipping towards minibasins (Fig. 4.11a and b). The thickest depocenters continue to be located near the IBSW, reaching up to ca. 1.4 km. There is a predominance of changing depocenters, followed by vertically stacked depocenters (especially near the IBSW) and piled up but dipping depocenters.
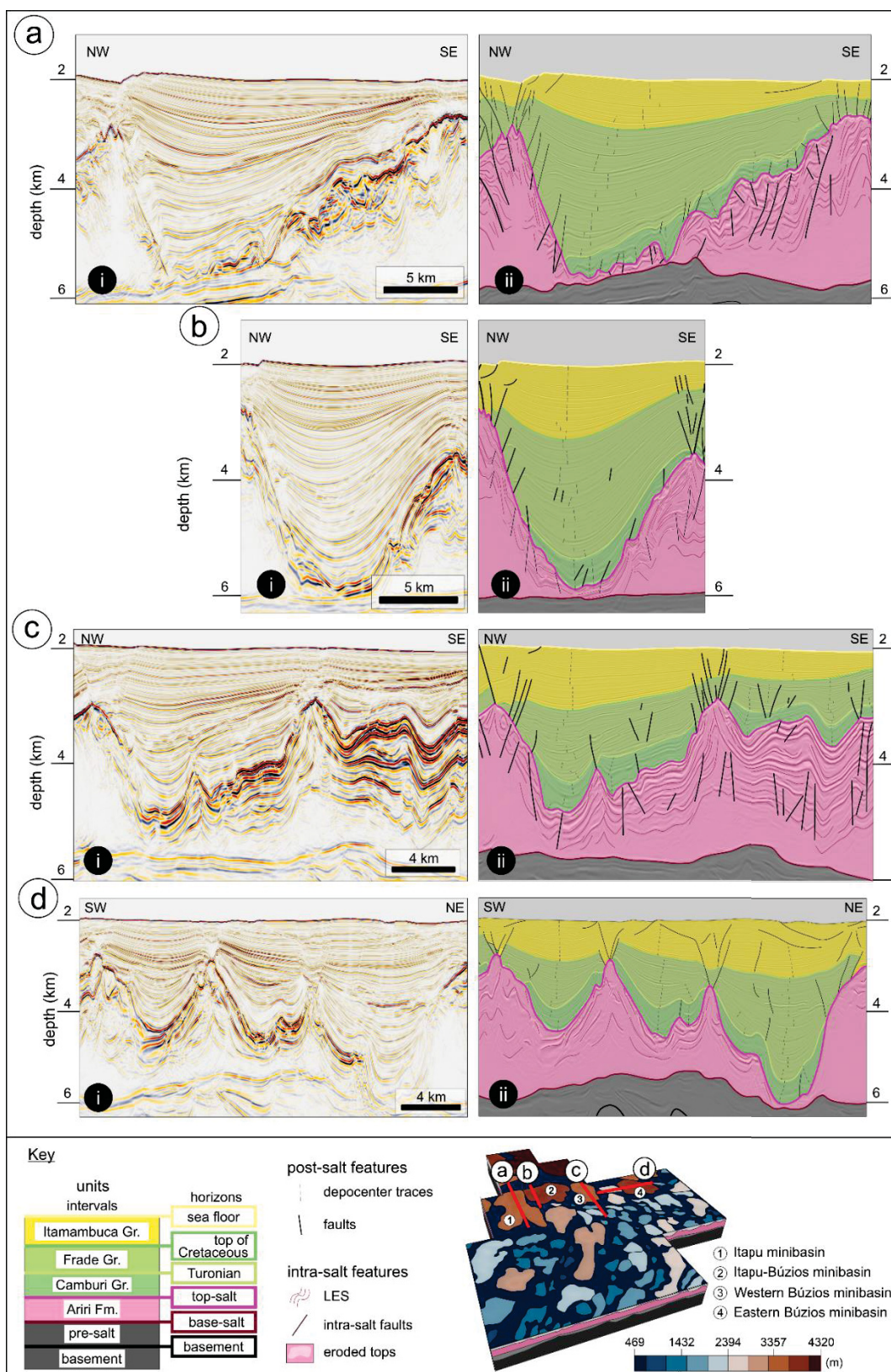
Figure 4.9: Key-sections illustrating the main features interpreted for minibasins near the IBSW. a) Itapu minibasin, which started as subbasins, which merged and changed and overall stacked but dipping depocenters towards the north. b) Itapu-Búzios minibasin, changed to stacked but dipping depocenters towards the south, which resulted in a main vertically stacked depocenters trend. c) Western Búzios minibasin, with predominant changing depocenters in the Cretaceous that only became vertically stacked depocenters in the Cenozoic. d) Eastern Búzios minibasin, with subbasins, moving to changing

depocenters and later stacked but dipping depocenters intensely faulted by listric Cenozoic faults and faults related to crestal grabens.
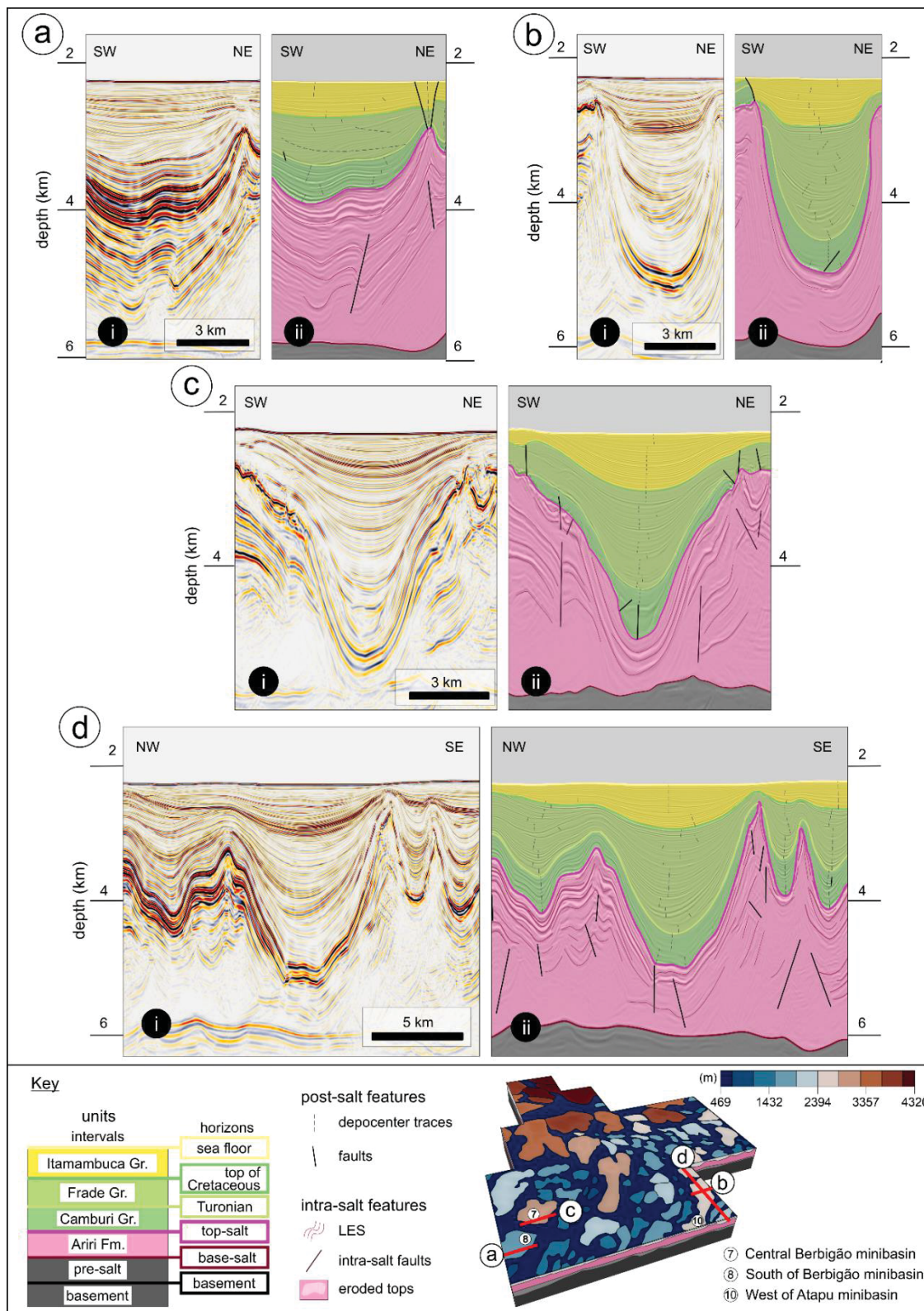
Figure 4.10: Key-sections illustrating main features interpreted for minibasins in the south of Franco Iara. a) South of Berbigão minibasin, where changing depocenters merged into stacked but dipping depocenters with a high dipping angle, with a predominance of vertically stacked depocenters in the Cenozoic. b and d) West of Atapu minibasin, with vertically stacked depocenters in the Camburi Gr.

turned into a megaflap, changing depocenters for the rest of the post-salt. c) Central Berbigão minibasin, predominantly vertically stacked depocenters with a hook termination in the Lower Cretaceous.
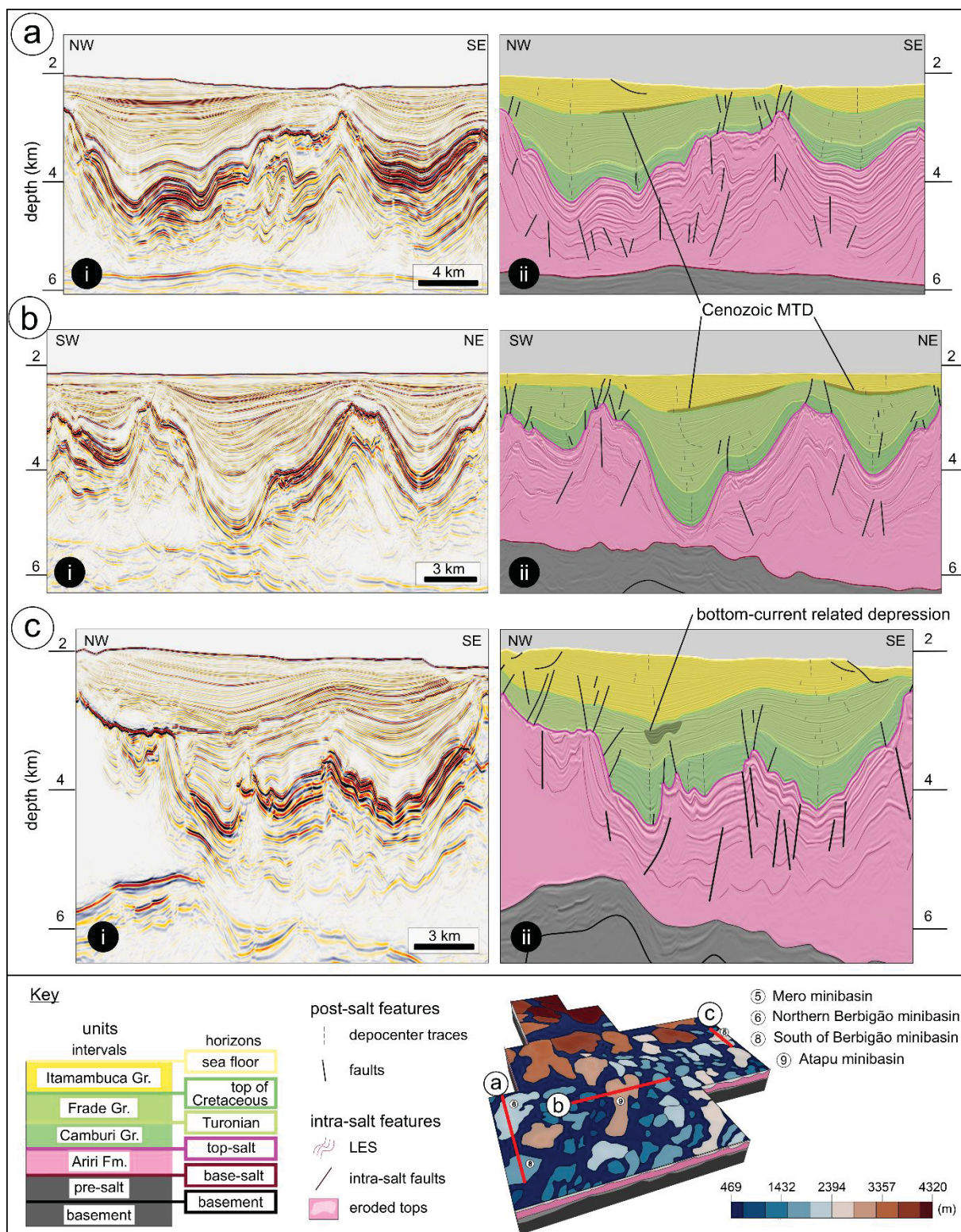
Figure 4.11: Key-sections illustrating main features interpreted for minibasins with identified deep-water systems. a) Northern Berbigão minibasin, with initially vertically stacked depocenters which merged into changing depocenters and since the Cenozoic there is a predominance of vertically stacked depocenters, even though changing depocenters can be found near currently rising diapirs. b) Atapu minibasin area, with a high base-salt dipping angle where vertically stacked depocenters changed to stacked but dipping with a low dipping angle depocenters and Cenozoic MTDs marking changing

depocenters. c) Mero minibasin, subbasins that merged to a predominance of changing depocenters, which in the Upper Cretaceous were eroded by contourites.

4.1.5. Discussion

The Franco Iara area in Northern Santos Basin records the evolution of diachronous adjacent primary minibasins within a period of ca. 110 Ma. These were developed above autochthonous linear salt bodies, that present two different faults and folds trends (EW and NS) recognizable due to LES. The different tracked horizons and interpreted time intervals help elucidate the tectono-sedimentary evolution of this part of the basin, as well as contribute to the general understanding of such salt tectonics settings.

4.1.5.1. Salt-base relief

The setting of the salt base (here considered the detachment surface) is an important feature in salt tectonic studies (e.g. Dooley et al. 2007, Dooley et al. 2017, Pichel et al. 2019, Zwaan et al. 2021), although there can be detachments within LES due to different rates of salt creep (Weijermars et al. 2014). Overburden failures are sensitive to basement hinges, as well as large-scale basin geometry, tilting and salt thickness (Cobbold & Szatmari 1991, Dooley et al. 2007, Zwaan et al. 2021). Santos Basin is no exception. In Central Santos Basin, land- and basinwards syn-rift NNE/SSW faults separate basement highs and lows (see Freitas et al. 2022), and towards the northern studied area it changes to an anastomosed "S"-shaped, as NE/SW normal faults are influenced by E/W strike-slip transfer zones (Meisling et al. 2001, Zalán & Oliveira 2005, Souza 2008, Freitas et al. 2022), and such structural elements bound deep-water structural provinces (Modica & Brush 2004). As well, the Cretaceous Santos Structural Hinge Line (Zalán et al. 2011) and Brazilian coastline change from a NE/SW to an E/W direction (see Fig. 4.1). In Central Santos Basin it is recognized how these inherited rift-related structures influence salt deposition (e.g., Davison et al. 2012, Rodriguez et al. 2018) and flow (e.g., Alves et al. 2017, Pichel et al. 2019, Pichel et al. 2021, Bose & Sullivan 2022).

Even though pre-salt successions and structures were not focused on this study, two main trends can be seen in the oldest tracked horizon, the salt base (see Fig. 4.5b and Table 4.1): a NW/SE and a NE/SW, on which higher (>5 degrees) dipping angles separate structural highs from lows. Indeed, in Franco Iara's area faults in the Santos Basin economic basement changes from a NE-trending to a "S-like" shape (Freitas et al. 2022), which can also be seen in the base-salt (Fig. 4.12), maybe due to the influence of transfer zones or strike-slip faults (Meisling et al. 2001, Souza 2008) such as the Itamambuca Transfer Zone (Rigoti 2015). These faults and structures might have strongly impacted salt flow as they did in Central Santos Basin.
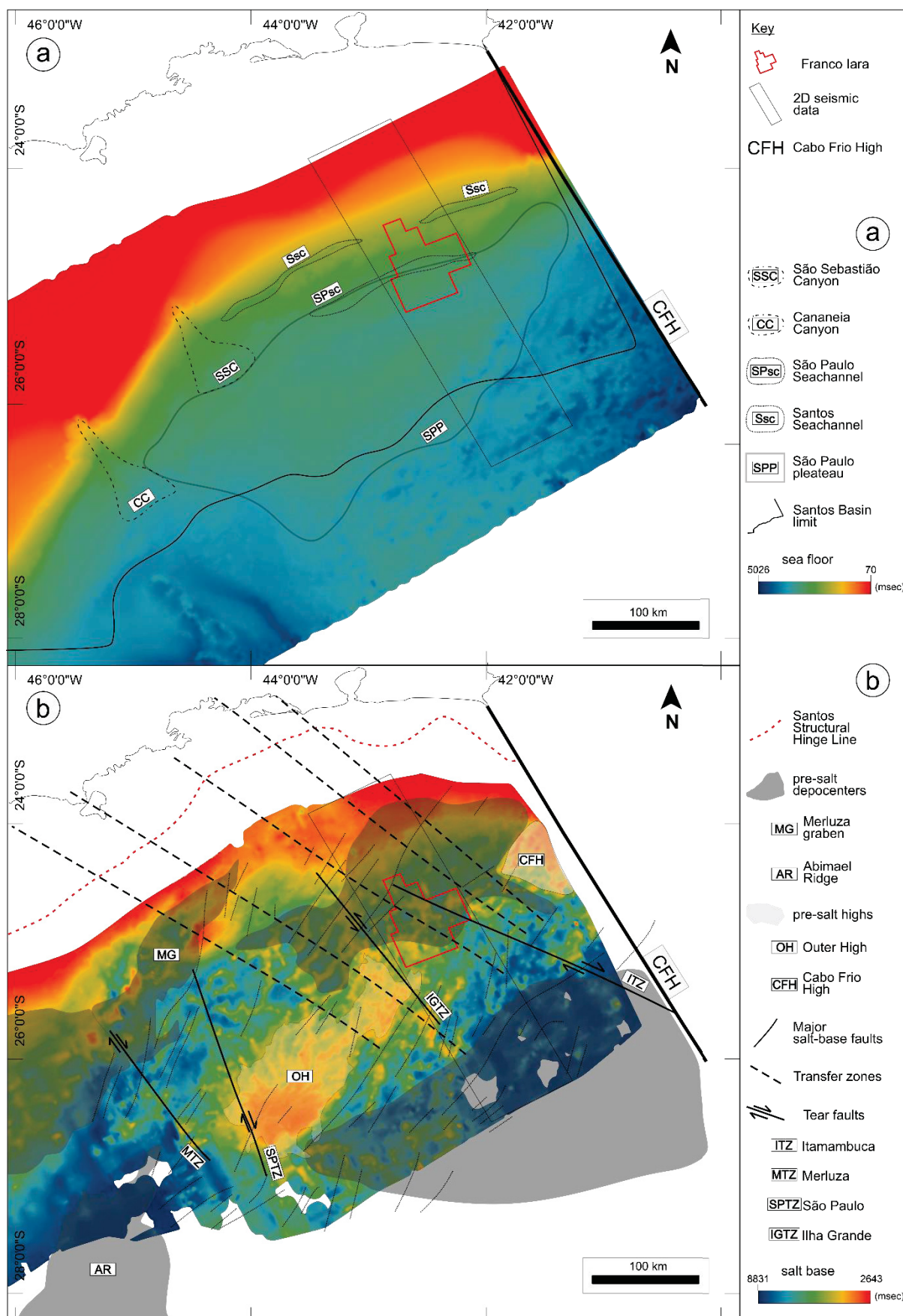
Figure 4.12: Key structures in Santos Basin. (a) Sea floor (Marinha do Brasill 2023), on which the São Paulo Plateau (Kumar & Gamboa 1979) and other deep-sea features (Marinha do Brasill 2023, Hercos

et al. 2023) are highlighted. (b) Pre-salt setting, regarding the base-salt time-depth surface (Freitas 2019) and main pre-salt depocenters (Mohriak 2003, Rigotti 2015, Pichel et al. 2021, Freitas et al. 2022), highs (Ysaccis et al. 2019, Freitas et al. 2022), base-salt faults with offsets over 1 km (Davison et al. 2012), and transfer and tear zones (Meisling et al. 2001, Modica & Brush 2004, Souza 2008, Rigoti 2015).

4.1.5.2. Insights on salt movement

By merging both cross section (i.e., changes in patterns of stacking depocenters) and cartographic (i.e., geometry and thickness) information from minibasins' filling patterns with salt geometries and internal deformation some inferences can be done for the evolution of each analyzed key-time interval.

4.1.5.2.1. Camburi Group (Albian-Cenomanian)

Salt movement in passive margins is triggered by spreading (driven by differential sedimentary loading) and gravity gliding (influenced by margin tilt and consequent slope instability), which are usually combined in natural settings (Vendeville 2005, Hudec & Jackson 2007, Brun & Fort 2011, Jackson & Hudec 2017). In this sense, the characteristics of the overburden deposited immediately after evaporites may help elucidate the beginning of salt tectonics.

In northern Santos Basin, even though Camburi Gr. is the least thick of all mapped units (max. ca. 800 m), there is a predominance of vertically stacked depocenters in base-salt low-relief areas, with relatively small widths (ca. 3 km), and an in-plane linear E/W shape. Although some changing depocenters were found in the southern part of Franco Iara near base-salt highs, the biggest anomalies from this vertically-stacked-depocenters trend were subbasins and changing depocenters near the IBSW.

Santos Basin has a different setting than other Atlantic margin basins. On the Kwanza, Campos and Espírito Santos basins, continental margins are roughly straight or convex and symmetric rift generated more linear structures that dip predominantly basinwards (e.g., Lentini et al. 2010, Szatmari & Milani 2016, Kukla et al. 2018). On the other hand, in Santos Basin the margin is shaped like a concave circular cone and rift faults dip both land- and basinwards, due to an asymmetric rift that formed multiple basement highs, which strongly influence salt flow (Cobbold & Szatmari 1991, Demercian et al. 1993, Assine et al. 2008, Lentini et al. 2010, Pichel et al. 2019). On that regard, initial gliding in Santos Basin was probably radial, not parallel, forming radial folds on the lower slopes and complex fold pattern in contractional domains (Cobbold & Szatmari 1991, Demercian et al. 1993), so sedimentary systems were influenced by subsidence of the basin (Quirk et al. 2012), as well as by the eustatic rise of sea level (Assine et al. 2008). Therefore, raft tectonics (i.e., extensive faults separating the overburden into rafts that slide downslope on a thin salt décollement controlled by residual topography, becoming separated by younger synkinematic strata), which were defined in the African margin (Burollet 1975, Duval et al. 1992, Gaullier et al. 1993) and described in Campos (e.g. Amarante et al. 2021) and Espírito Santos (e.g. Piedade & Alves 2017) basins are not as well developed in northern Santos Basin.

Therefore, in the studied region, the initial focal point of salt rise was the IBSW (Fig. 4.13). This E/W feature and the E/W cartographic shape of minibasins points to an initial salt flow towards the south. Indeed, E/W-oriented well-layered salt bodies tend to have more symmetric and angular folds, which alongside the existence of

associated subbasins (i.e., contractional settings, Hudec et al. 2009 see Fig. 4.7a and 4.8c) in the IBSW may point that this northern area was initially a region of contraction (Cobbold et al. 1995), and perhaps a lower-slope in the initial gliding phase (Cobbold & Szatmari 1991). On the other hand, as salt tends to be thicker in pre-salt lows (Davison et al. 2012, Rodriguez et al. 2018), vertically stacked depocenters on these regions may have been developed by salt down building density-driven subsidence (Trusheim 1960, Hudec et al. 2009, Peel 2014, Zwaan et al. 2021).
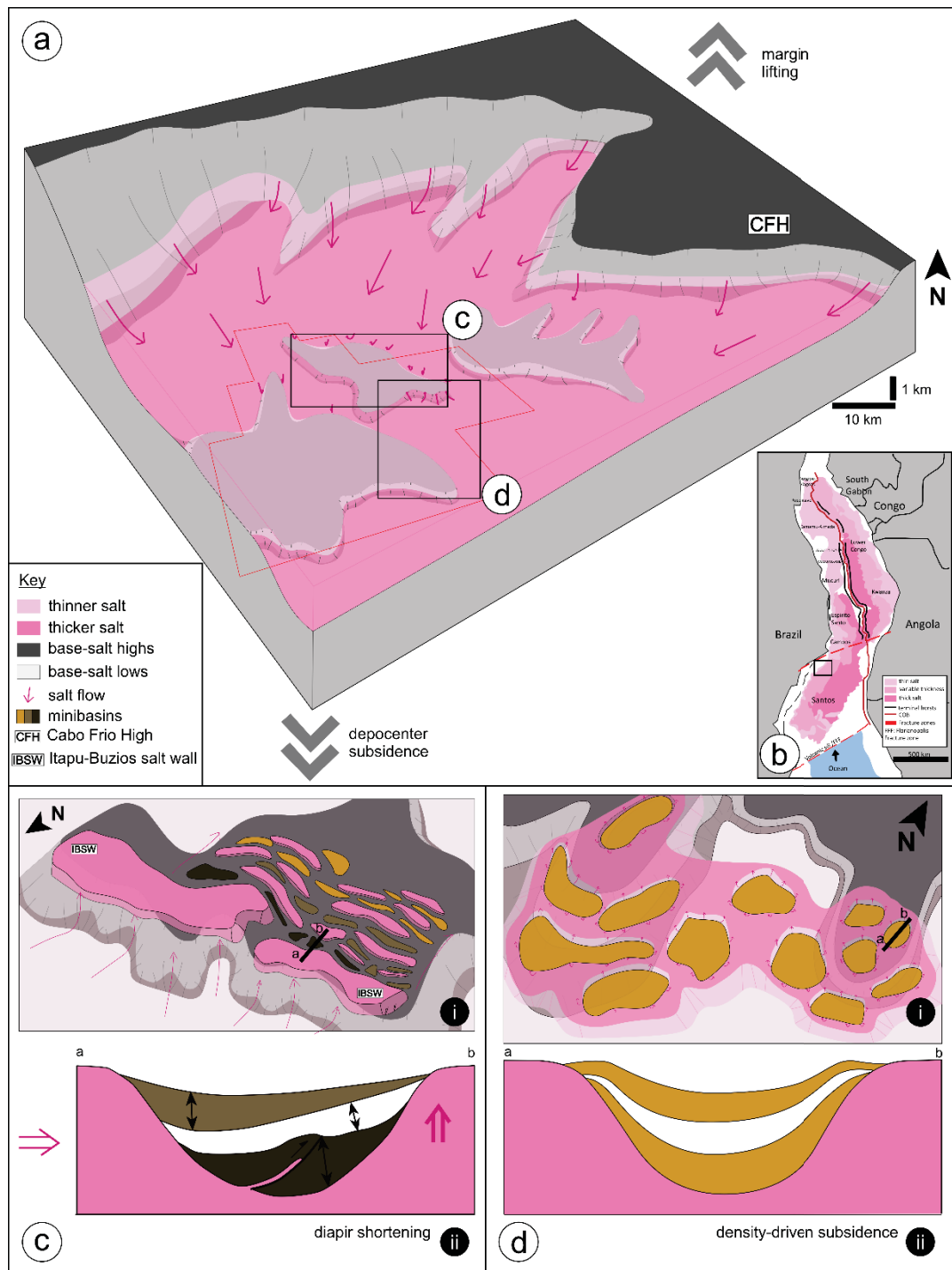

Figure 4.13: Proposed setting during Camburi Gr. Deposition. (a) Schematic model. Salt was deposited with variable thickness, increasing towards Santos Basin depocenter. The margin lift triggered a radial gliding, and in Northern Santos Basin salt migrated towards the South. In Franco Iara area base-salt

highs interfered in salt flow, creating a compressive zone which formed IBSW and diapir-shortening related minibasins. In the rest of the area, in relatively heterogeneous base-salt (i.e., either base-salt highs or lows) minibasins were formed due to density-driven subsidence. Where these different basement-types meet, shortening-related minibasins were formed. (b) Salt depositional thickness after Lentini et al. (2010) and Rodriguez et al. (2018). (c) In the IBSW area, (i) E/W elongated minibasins with predominantly (ii) subbasins point this was initially a salt contraction region, as salt migrated south. (d) In the rest of Franco Iara, (i) above thicker salt, the main (ii) minibasin-subsidence model (Hudec et al. 2009) for this time-period is density-driven subsidence.

4.1.5.2.2. Frade Group (Turonian-Maastrichian)

Salt tectonics was especially prevalent in the area during the Upper Cretaceous, highlighted by constant changes in depocenters' cross-sectional geometries. In the Frade Group, depocenters vary in cross-section (predominance of changing depocenters, followed by piled up but dipping depocenters, vertically stacked depocenters and, last, merging depocenters) and map shape (rounded to N/S elongated) and width (8-10 km). Significantly, piled but dipping depocenters were seen with different dipping angles and directions: dipping north with high angles near the IBSW, and dipping east with low angles in the rest of the area.

First, it is important to highlight that this was the thickest interval mapped, especially in the northern area near the IBSW (ca. 2.2 km thick). This is due to important changes in sedimentary input in this area in the Upper Cretaceous. According to Modica & Brush (2004), during the late Campanian–Maastrichtian, the re-organization of the Paraiba do Sul River system (see Fig. 4.1) increased input siliciclastic dispersal systems into northern and central Santos Basin. Similarly, according to Assine et al. (2008), from the Santonian to Maastrichtian, terrigenous sediment input was substantial (represented, as well, by the existence of Santos and Juréia Fm.), due to three recognized regressive sequences and significant increase in accommodation space resulted from increased subsidence rates, tectonic reactivation of the source area and salt movement downslope. As well, Guerra & Underhill (2012) describe NW-direction of sediment supply in the Late Cretaceous shifting to NNE in the Cenozoic. As a matter of fact, most stratal terminations were mapped in this time-interval (see Fig. 4.3), as well as influence of contourites and erosive features, may be due to these multiple varying sedimentary influences.

This significant increase in sedimentary load seems to be prevalent in the northern part of the studied area. In the asymmetric IBSW, Cretaceous post-salt units are displayed in a rollover anticline, followed by thickening Cretaceous and Cenozoic units (see Fig. 4.6b). This indicates its association to a normal-fault system, perhaps like the Albian Gap formation, as seen in Pichel & Jackson (2020). Also, piled but dipping depocenters dipping north with high angles occurred near this salt wall, being interpreted as due to sedimentary topographic loading (Hudec et al. 2009), also related to increasing sedimentary input in this time (Modica & Brush 2004, Assine et al. 2008). Therefore, there seems to be evidence that salt was moving from NNW to SSE in this period in the north of the studied area, prior to base-salt highs (see Fig. 4.5b).

However, there are three important features in the south and east of Franco Iara that indicate salt moving to east, which might have started with a fast salt rise early in the Turonian as evidenced by megaflaps in the West of Atapu minibasin (see Fig. 4.8c and Fig. 4.10b). First, the in-plan view of minibasins is mainly N/S elongated (see Fig.4.4b). Secondly, piled but dipping depocenters are dipping east with low angles (see Fig. 4.11b), and were interpreted as Ramp Syncline Basins (RSB), asymmetric basins formed when there are ramps in the salt base, causing units to translate above

salt layers as the movement generates a downwarp of the overburden, thereby creating accommodation space (Jackson & Hudec 2005). Such features were described and modeled by Pichel et al. (2018) in Central Santos Basin, recording a total 30 km (± 2 km) SE-directed translation (therefore, parallel to the regional gravity-driven tectonic transport) during the Late Cretaceous and Paleocene. Third, salt anticlines are more common in the southeast, with an N/S trend (Table 4.1 and Fig. 4.5a) and LES indicating fold-and-thrust-like systems (i.e., N/S asymmetric folds related to thrust-like faults) with an N/S direction, transported from west to east (Fig. 4.6d). These features might have been imposed by the Ilha Grande Gravitational Cell (IGGC, Fig. 4.14), indicating that the lateral edges of this cell were not thin-skinned transfer zones, but continued migration and further compression reworking nowadays curved shapes distal salt ridges (Guerra & Underhill 2012), alongside the main deformation phase of translation related to the Albian Gap (Pichel et al. 2018, Pichel & Jackson 2020).

Therefore, two salt movement trends seem to be recorded during the Upper Cretaceous in northern Santos Basin. The first one prevails northern as is mostly related to northern sedimentary input and related salt spreading towards the south. The second prevails in the south and southeast, and indicates a strong salt translation towards the east, as salt moved on base-salt highs forming RSB and contraction-related features within salt bodies. However, the second one still needs further research detailing the timing and its main influences.

4.1.5.2.3. Itamambuca Group (Cenozoic)

In the Cenozoic (Fig. 4.8a), depocenters are the largest (widths up to 15 km) but not the thickest, and predominantly rounded-shaped. An intriguing feature from the Itamambuca Gr. were MTDs found at the base of this succession dipping towards minibasins (Fig. 4.11a and b). The Cenozoic passage is a significant unconformity in Santos Basin, due to a global sea level drop and a crucial forced regression, and in the Paleocene deposition was confined to deep-water regions and deposits from gravitational flows formed in the northern part of the basin (Moreira & Carminatti 2004, Assine et al. 2008). This type of setting might have favored the formation of such deposits, and in basins characterized by complex bathymetries due to active salt tectonics mass failure may affect local slopes and trigger MTDs within minibasins (e.g., Biancardi et al. 2020, Poprawski et al. 2021).

As for stacking patterns, two main trends appear: a predominance of changing depocenters above base-salt highs, and vertically stacked depocenters and piled up but dipping north with high angles depocenters near the IBSW. This was also a period were northern parts (with dip angles up to ca. 20°) of the IBSW started collapsing (i.e., salt evacuation), forming mock-turtle anticlines.

During this period, northern salt bodies became mature, alongside salt welds (see Fig. 4.5a), minibasins also reached a mature development, and deposition became more influenced by sedimentary setting related to sea level fluctuations and consequent shifts in the coastline (e.g., Duarte & Viana 2007, Assine et al. 2008, Berton & Vesely 2016, Hercos et al. 2023, Assis et al. 2024). However, less mature salt bodies located above base-salt highs (see Fig. 4.5a) continue rising (see Fig. 4.6c).
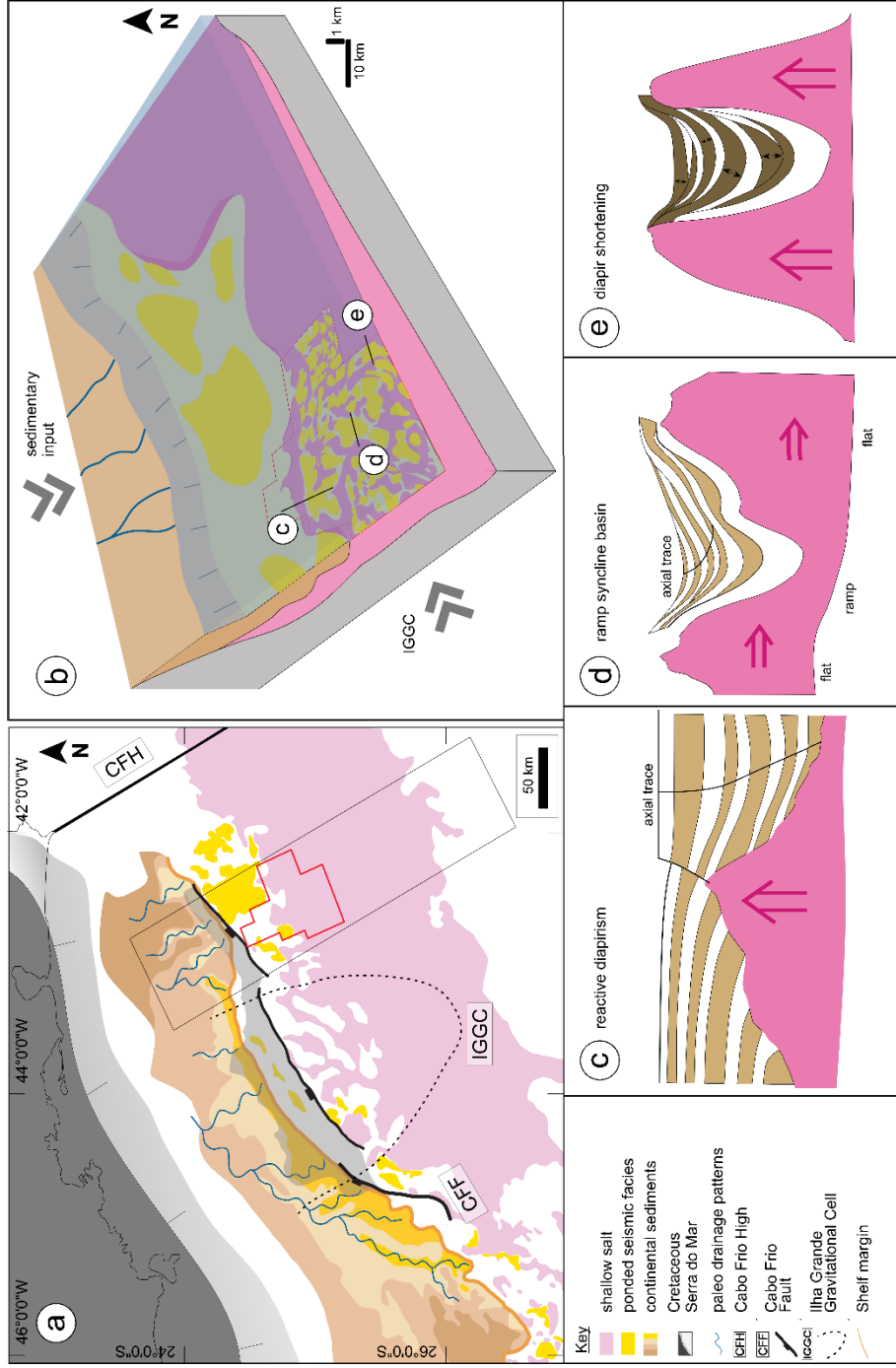
Figure 4.14: Proposed setting for the Frade Gr. deposition. (a) Regional setting, with features after Modica & Brush (2004), Zalan & Oliveira (2005) and Guerra & Underhill (2012). The Cretaceous Serra do Mar modified paleo drainage patterns, which started to input sediments also in northern Santos Basin. Also, the collapse of the IGGC as well as the formation of the Albin Gap in central Santos Basin influenced salt to migrate offshore in a radial pattern. (b) In the studied area, ponded seismic facies (i.e., minibasins) and salt migration were affected by northern sedimentary input and eastern salt migration, forming mostly three types of settings: (c) related to the northern sedimentary input, reative diapirism in response to normal faults (such as the CFF) was installed in the IBSW, as well as slightly dipping depocenters in the Itapu minibasin (see Fig. 4.9a); (d) related to eastern salt migration, ramp syncline basins formed above base-salt ramps in minibasins such as the Atapu minibasin (based on Fig. 4.11b and Pichel et al. 2018); and in the most distal part of Franco lara minibasins such as the West of Atapu minibasin present changing depocenters (after Fig. 4.10b and Hudec et al. 2009).

4.1.6. Final remarks

The Franco Iara area in northern Santos Basin records the intrinsic relationship between the evolution of salt tectonics and minibasins, as salt migrates in a passive margin basin highly affected by base-salt relief, slope instability, and variations in sedimentary inputs. Geometrical features of the well-layered Aptian salt and the post-salt minibasins analyzed both in plan-view and cross-sections presented genetic implications, which aligned with previous physical models, restorations and regional studies allowed for a 3D characterization of this studied area.

Results indicate that in this ca. 3,700 km^2 area there are significant differences in both salt bodies and minibasins. For the first, diapirs change trends, maturity, kinematics and internal deformation patterns. For the second, the analyzed stacked depocenters controlled by salt tectonics change size (i.e., width, thickness), in-plan shape and cross-view geometries (i.e., stacking patterns, end-member terminations) in three subdivided time intervals, implying different evolution.

In northern Santos Basin there was a non-plane salt base, which probably controlled Aptian salt deposition and later salt movement. An early Albian salt tectonics is recorded in the Camburi Gr., which includes a radially convergent salt tectonics towards the South (pointed out by EW-oriented well-layered salt bodies and EW-elongated minibasins) forming a contraction zone above base-salt highs leading to the rise of the E/W IBSW nearby subbasins, as well as density-driven subsidence forming minibasins with vertically stacked depocenters in base-salt low-relief areas. The apex of two salt tectonics trends is recorded in the Cretaceous Frade Gr.: a northern one is related to sedimentary input and salt spreading towards the south-southeast, indicated by reactive diapirism in the IBSW associated to piled but dipping north with high angles depocenters; and a southern one indicates salt E-directed translation, as pointed out by N/S elongated minibasins, RSB and contraction-related features within salt bodies with an N/S direction and might be related to the IGGC and Albian Gap formation. At last, during the Cenozoic the Itamambuca Gr. records a phase of decreasing salt tectonics interference (i.e., mature salt bodies started to collapse and salt bodies above base-salt high continue rising) and increasing influenced by sedimentary setting related to sea level fluctuations.

HALOKINETICALLY INDUCED MASS-TRANSPORT DEPOSITS IN MINIBASINS FROM NORTHERN SANTOS BASIN, BRAZIL

Author : Diório, Giovana Rebelo – giovanarebelo@ufpr.br – Laboratório de Análise de Bacias (LABAP), Universidade Federal do Paraná (UFPR)

Co Author: Assis, Vanessa da Silva Reis - vanessaassis7@gmail.com – LABAP, UFPR

Co Author: Dias, Sérgio Francisco Leon - sergio.leondias@hotmail.com – LABAP, UFPR

Co Author: Trzaskos, Barbara - barbaratrzaskos@ufpr.br –LABAP, UFPR

Co Author: Vesely, Fernando Farias - vesely@ufpr.br –LABAP, UFPR

MTDs (mass-transport deposits) are important features in deepwater environments that form because of subaqueous landslides and present characteristic patterns of internal deformation. Once formed by sediment failure in response to gravitational forces, the displaced mass flows down the regional slope towards basin's depocenter.

However, in basins characterized by complex bathymetries due to active salt tectonics, mass failure may affect local slopes and give rise to MTDs within minibasins. Minibasins are syn-kinematic features, a few tens of kilometers in diameter, and subside into relatively thick evaporites. Due to active topography, each minibasin has its individual setting and evolution, including MTDs that may diverge from trends found in the basin itself. In this contribution we describe MTDs filling salt-controlled minibasin in northern Santos Basin, offshore Brazil.

Santos Basin is a passive margin basin located in SE Brazil, and it is currently the largest oil producer in the country. The basin formed as a result of Gondwana breakup and opening of the Atlantic Ocean (Lower Cretaceous). Remarkable is a major evaporite stage during the Aptian (Ariri Formation) and expressive salt tectonics interfering in the deposition of the subsequent drift Sequence.

Four Cenozoic MTDs found in adjacent minibasins in northern Santos Basin (Fig. 4.15) were delimited in order to evaluate and compare their features. Seismic horizon slices (top salt; base and top of MTDs) were mapped using a ~3.700 km^2 3D seismic-reflection post-stack data (seismic survey Franco Iara). Lines and fault stick sets were traced using a spacing of ~250 m in in-lines and crosslines, interpolated using the inverse distance method, and followed by median and average filtering.

The MTDs (Fig. 4.16) are apart by less than 50km and aligned in a W-E trend (MTD1-MTD4). Their areal extent varies from 25-58 km^2 and their thickness ranges from 45-110 m. They all flow towards minibains' depocenters, diverging from and sometimes truncated due to rising diapirs. Internal features include ramps, blocks, compressive and distensive faults, frontal confinement, surface topography and basal erosion.

Halokinetically induced MTDs can help elucidate minibasins' structural evolution once they are related to the uplifting of bounding slopes. Moreover, they can form potential

seals for reservoir-quality deepwater sands that potentially accumulate in these minibasins.

Keywords: salt tecnonics, 3D seismic, seismic geomorphology
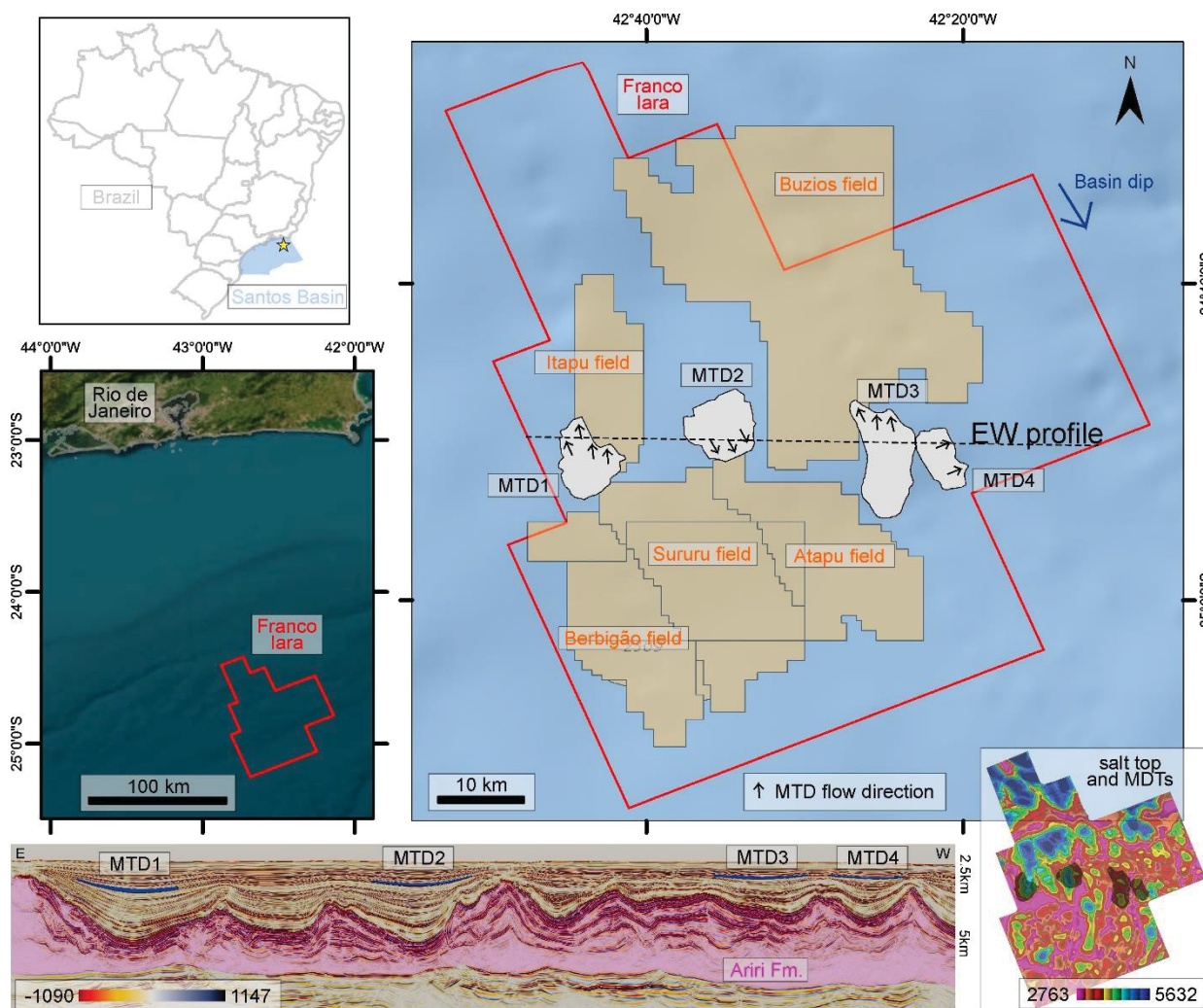
Figure 4.15: Setting of studied area, with Santos Basin location in offshore Brazil, Franco Iara's location ca. 220km from Rio de Janeiro, MTDs locations and paleoflows regarding Franco Iara and oil fields, E-W profile highlighting Ariri Formation and MTDs and salt top map (pink – highs; blue – lows, depth in meters) with MTDs diverging from rising diapirs.
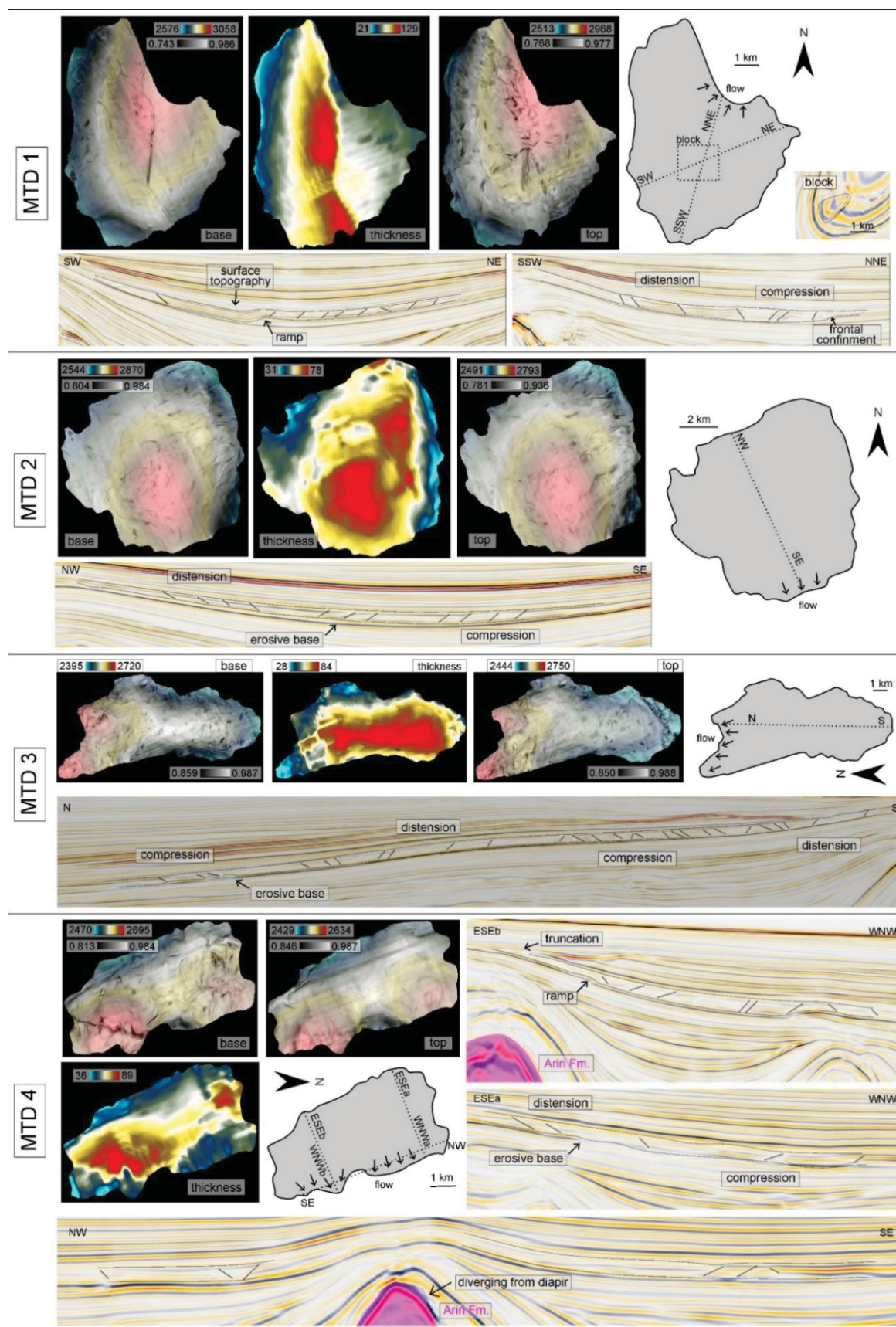
Figure 4.16: Thickness, MTD's base and top (similarity atribute with 30% transperency over depth in meters), paleoflow direction and profiles highlighting main features of each MTD.

SALT WALLS: WHAT CAN THEY TELL US ABOUT NORTHERN SANTOS BASIN HALOKINETIC EVOLUTION?

Giovana Rebelo Diório[1], Barbara Trzaskos[2]

[1] Laboratório de Análise de Bacias, Universidade Federal do Paraná, e-mail: g.rebelo.d@gmail.com
[2] Laboratório de Análise de Bacias, Universidade Federal do Paraná, e-mail: barbaratrzaskos@ufpr.br

Salt tectonics are responsible for remarkable deformations in sedimentary basins, even in ones that are not in active tectonic settings. In that sense, Santos Basin is a passive margin basin located in offshore Brazil, and currently the country's main oil and gas producer. Pre-salt reservoirs are covered and sealed by an Aptian evaporitic unit (Ariri Formation), that controlled the deposition and deformed the subsequent marine drift sequence. As different styles of deformation and multiple types of salt bodies can be found throughout the basin, this study focused on characterizing deformations related to major (>20 km wide) salt walls (i.e. discordant contact with overlaying rocks, with an elongated sinuous shape in plan view), with an NE/SW direction, that occur in northern Santos Basin, in the halokinetic transitional domain. To evaluate this, an area of ca. 800 km^2 where two salt walls connect was chosen. At first, faults in the drift sequence were mapped in the 3D seismic-reflection post-stack data (seismic survey Franco Iara), using the OpendTect 6.6 PRO software, and a spacing of ca. 620 m (50 steps) in both in-lines and crosslines, as well as application of the deep steering filter, followed by the dip attribute and the dip angle attribute, in the top of the salt to determinate the dip angle. These features were also detailed in the 3D seismic block BS-500, using a spacing of ca. 500 m in both in-lines and crosslines and seismic attributes, such as the fault enhancement filter (FEF, which tones down background in fault regions), and the thinned fault likelihood (TFL, which identifies faults and fractures with the highest possible resemblance). Intra-salt patterns within salt walls were also described, visible due to upper layered evaporitic sequences (LES). The most important faults related to these asymmetric salt walls – as dip angles reach up to ca. 20º towards the north and ca. 50º towards the south- are crestal grabens and mock-turtle anticlines. Crestal grabens are synthetic and antithetic conjugated faults directly above and following the crest of salt structures. As they are related to diapirs, the faults direction varies, but they are commonly perpendicular to the basin's dip direction forming anastomosed kilometric fault planes, highlighted by the TFL attribute in z-slice. All drift units are affected by these fault types. In the southern part of these salt walls, listric faults displacing sediments from the Itamambuca Group (Cenozoic) are commonly observed, dipping toward crestal grabens. *En échelon* (i.e. subparallel closely-spaced structures oblique to the main structural trend) faults dipping towards the north can be found where different salt walls connect. Additionally, mock-turtle anticlines, features formed by salt evacuation from a salt wall indicative of collapse, are frequently observed in some parts of these walls, particularly in their northern region, towards the extensive salt domain. Furthermore, there are some intra-salt features in these salt walls, such as shear and thrust zones, with eroded upper parts. This characterization aids in the interpretation of the evolution of salt tectonics in this area of the basin, once these features indicate an early shortening stage, followed by significant extension and collapse as salt migrated further into the basin.

Palavras-Chave: Salt tectonics, seimic mapping, mock-turtle anticlines, crestal grabens, listric faults.

5 CONCLUSIONS

The Franco Iara area in northern Santos Basin records the intrinsic relationship between the evolution of salt tectonics and minibasins, as salt migrates in a passive margin basin highly affected by salt-base relief and variations in sedimentary inputs. A seismostratigraphic mapping was done in this seismic block, emphasizing five key-surfaces (salt-base, top-salt, Turonian, top of Cretaceous, and seafloor) and four time-intervals isopaches (Aptian evaporitic Ariri Fm., Albian-Cenomanian Camburi Gr., Turonian-Maastrichian Frade Gr., and Cenozoic Itamambuca Gr.). With this, it was possible to identify intra-salt structures (i.e., faults, folds, and eroded tops) and geometry (i.e., kinematics and maturity), and minibasins' main characteristics in plan-view (shape, geometry, and thickness) and cross-sections (depocenters stacking patterns, divided into: vertically stacked depocenters, changing depocenters, subbasins, merging depocenters, and stacked but dipping depocenters), as well as some sedimentary systems (i.e., MTD and contornites). For minibasins, the analysis of depocenters stacking patterns was done for each mapped time-interval.

The evaporitic Ariri Fm. is heterogenous. Its thickness varies (ca. 340 to 3170 m), and there is a decrease in salt bodies' maturity basin ward (salt walls, stocks and welds prevail in the northwest, and salt anticlines in the southeast). In the north-eastern part there are salt walls and anticlines with an E/W direction and intra isoclinal folds, whereas in the south NNE/SSW salt anticlines with intra-salt fold-and-thrust prevail. In the salt-base, higher (>5°) dipping angles separate structural highs from lows in two main trends (NW/SE and a NE/SW), forming an "S-like" shape due to the influence of transfer zones or strike-slip faults.

The most prominent feature was named Itapu-Buzios salt wall, a major (>20 km wide) NE/SW asymmetric salt wall (dip angles up to ca. 20° towards the north and ca. 50° towards the south) with some important structural features. First, in its northern part there are features indicative of salt collapse such as mock-turtle anticlines. Second, also in the north, Cretaceous post-salt units are displayed in a rollover anticline, followed by thickening Cretaceous and Cenozoic units, indicating its association to a normal-fault system. Third, three types of fault systems were described: (i) prominent crestal grabens (offsets of ca. 350 m), synthetic and antithetic conjugated faults directly above and following the crest of salt structures, with varying direction but forming anastomosed kilometric fault planes which affect all drift units; (ii) listric faults displacing sediments from the Itamambuca Gr., dipping toward crestal grabens; and (iii) *en échelon* (i.e. subparallel closely-spaced structures oblique to the main structural trend) faults dipping towards the north, found where different salt walls connect. Last, although incipient, there are some intra-salt features, such as shear and thrust zones with eroded upper parts. These features indicate an early shortening stage, followed by significant extension and collapse as salt migrated further into the basin.

Camburi Gr. is the least thick (max. ca. 800 m) mapped interval, and depocenters are near-circular or E/W elongated in plan-view. There is a predominance of vertically stacked depocenters, followed by subbasins near the Itapu-Buzios salt wall. This Group records an Albian-Cenomanian initial phase of radially convergent of salt movement towards the south, as pointed out by E/W-oriented well-layered salt bodies and EW-elongated minibasins. This led to the rise of the E/W Itapu-Buzios salt wall nearby subbasins, indicating this was initially a region of contraction. Southern,

there is a predominance of vertically stacked depocenters in base-salt low-relief areas, areas where salt predominantly accumulates, indicating minibasin development by density-driven subsidence.

In the Frade Gr., the thickest one mapped (max. ca. 2.2 km), there are constant changes in depocenters' geometries both in plan-view (rounded to N/S elongated) and cross-section (predominance of changing depocenters, followed by stacked but dipping). It records the Upper Cretaceous apex of two salt tectonics trends. The first one prevails northern and is related to sedimentary input and related salt spreading towards the south-southeast, indicated by reactive diapirism in the Itapu-Buzios salt wall associated to piled but dipping north with high angles depocenters interpreted as due to sedimentary topographic loading. The second prevails in the south and southeast and indicates salt E-directed translation, as pointed out by N/S elongated minibasins, RSB and contraction-related features within salt bodies with an N/S direction and might be related to the IGGC and Albian Gap formation.

Depocenters of the Itamambuca Gr. are the largest (widths up to 15 km), predominantly rounded-shaped, with a majority of changing depocenters, followed by vertically stacked ones. It records a Cenozoic phase of decreasing salt tectonics (i.e., mature salt walls collapse and salt bodies above salt-base highs continue rising) and increasing influenced by sedimentary setting related to sea level fluctuations. As a matter of fact, the Cenozoic passage is marked by a global sea level drop and a forced regression, forming hallokinetic-influenced MTDs (i.e., flow towards minibains' depocenters, diverging from and sometimes truncated due to rising diapirs), apart by less than 50km, aligned in a W-E trend, with varying areal extents (25-58 km^2) and thickness (45-110 m). Internal features include ramps, blocks, compressive and distensive faults, frontal confinement, surface topography and basal erosion.

Results indicate that in this ca. 3,700 km^2 area there are significant differences in both salt bodies (i.e., trends, maturity, kinematics and internal deformation patterns) and minibasins, as these analyzed stacked depocenters controlled by salt tectonics change size (i.e., width, thickness), in-plan shape and cross-view geometries (i.e., stacking patterns, end-member terminations) in three subdivided time intervals, implying different evolution. These geometrical features of the well-layered Aptian salt and the post-salt minibasins present genetic implications, which aligned with previous physical models, restorations and regional studies allowed for a 3D characterization and interpretation: a non-plane salt base controlling Aptian salt deposition and later movement; an early Albian radially convergent salt tectonics towards the South; the apex of two Cretaceous salt tectonics trends (a northern one related to sedimentary input and salt spreading towards the south-southeast, and a southern one indicating salt E-directed translation that might be related to the IGGC and Albian Gap formation); and the Cenozoic decreasing salt tectonics interference and increasing influence of sedimentary deep-water setting related to sea level fluctuations. However, further studies are still needed to model and confirm such evolution and detail the Upper Cretaceous apex and its triggers.

REFERENCES

Alves, T.M., Fetter, M., Lima, C., Cartwright, J.A., Cosgrove, J., Gangá, A., Queiroz, C.L., Strugale, M. 2017. An incomplete correlation between pre-salt topography, top reservoir erosion, and salt deformation in deep-water Santos Basin (SE Brazil). Marine and Petroleum Geology, 79, 300-320. https://doi.org/10.1016/j.marpetgeo.2016.10.015

Amarante, F.B., Jackson, C.A.L., Pichel, L.M., Scherer, C.M.S., Kuchle, J. 2021. Pre-salt rift morphology controls salt tectonics in the Campos Basin, offshore SE Brazil. Basin Research, 33(5), 2837-2861. https://doi.org/10.1111/bre.12588

Andresen, K.J., Huuse, M., Schødt, N.H., Clausen, L.F., Seidler, L. 2011. Hydrocarbon plumbing systems of salt minibasins offshore Angola revealed by three-dimensional seismic analysis. American Association of Petroleum Geologists Bulletin, 95(6), 1039-1065. https://doi.org/10.1306/12131010046

ANP. 2020. Dados Técnicos. Agência Nacional do Petróleo, Gás Natural e Biocombustíveis, Ministério de Minas e Energia, Governo do Brasil. Available at: https://www.gov.br/anp/pt-br/assuntos/exploracao-e-producao-de-oleo-e-gas/dados-tecnicos (accessed March 18th 2023).

ANP. 2021. Panorama Exploratório das Bacias de Santos e Campos: Gigantes Nacionais. Marina Abelha, Superintendencia de Exploração, Agência Nacional do Petróleo, Gás Natural e Biocombustíveis. Available at: https://www.gov.br/anp/pt-br/centrais-de-conteudo/apresentacoes-palestras/2021/arquivos/Panorama_Exploratorio_das_Bacias_de_Santos_e_Campos_GigantesNacionais_Marina_Abelha.pdf (accessed May 17th 2023).

ANP. 2023. Boletim Mensal da Produção de Petróleo e Gás Natural: Dados da produção de petróleo e gás natural no Brasil. Agência Nacional do Petróleo, Gás Natural e Biocombustíveis, Ministério de Minas e Energia, Governo do Brasil. Available at: https://www.gov.br/anp/pt-br/centrais-de-conteudo/publicacoes/boletins-anp/boletins/boletim-mensal-da-producao-de-petroleo-e-gas-natural (accessed May 17th 2023).

Antunes, R.C., Guerrero, J.C., Jahnert, R.J. 2024. Coquina depositional model, Buzios Field, Brazil. Marine and Petroleum Geology, 160, 106607. https://doi.org/10.1016/j.marpetgeo.2023.106607

Arai, M. 1988. Geochemical reconnaissance of the mid-Cretaceous anoxic event in the Santos Basin, Brazil. Revista Brasileira de Geociências, 18(3), 273-282.

Araújo, C.C., Madrucci, V., Homewood, P., Mettraux, M., Ramnani, C.W., Spadini, A.R. 2022. Stratigraphic and sedimentary constraints on presalt carbonate reservoirs of the South Atlantic Margin, Santos Basin, offshore Brazil. AAPG Bulletin, 106(12), 2513-2546. https://doi.org/10.1306/08082219218

Assine, M.L., Corrêa, F.S., Chang, H.K. 2008. Migração de depocentros na Bacia de Santos: importância na exploração de hidrocarbonetos. Brazilian Journal of Geology, 38(2), 111-127.

Assis, V.D.S.R., Trzaskos, B., Vesely, F.F., Buso, V.V. 2024. Ramps as modifiers of deformation of mass-transport deposits flow cells: A case study in the Santos Basin, SE Brazil. Marine and Petroleum Geology, 160, 106632. https://doi.org/10.1016/j.marpetgeo.2023.106632

Berton, F., Vesely, F.F. 2016. Stratigraphic evolution of Eocene clinoforms from northern Santos Basin, offshore Brazil: evaluating controlling factors on shelf-margin growth and deep-water sedimentation. Marine and Petroleum Geology, 78, 356-372. https://doi.org/10.1016/j.marpetgeo.2016.09.007

Biancardi, C.A., Alves, T.M., Martins-Ferreira, M.A.C. 2020. Unpredictable geometry and depositional stacking patterns of mass-transport complexes in salt minibasins. Marine and Petroleum Geology, 120, 104522. https://doi.org/10.1016/j.marpetgeo.2020.104522

Booth, J.R., Dean, M.C., DuVernay III, A.E., Styzen, M.J. 2003. Paleo-bathymetric controls on the stratigraphic architecture and reservoir development of confined fans in the Auger Basin: central Gulf of Mexico slope. Marine and Petroleum Geology, 20(6-8), 563-586. https://doi.org/10.1016/j.marpetgeo.2003.03.008

Bose, S., Sullivan, M. 2022. Structural analysis of layered evaporites using internal deformation patterns: Examples from Santos and Campos basins, Brazil. Journal of Structural Geology, 161, 104661. https://doi.org/10.1016/j.jsg.2022.104661

Bradshaw, M., Rees, S., Wang, L., Szczepaniak, M., Cook, W., Voegeli, S., Boreham, C., Wainman, C., Wong, S., Southby, C., Feitz, A. 2023. Australian salt basins–options for underground hydrogen storage. The APPEA Journal, 63(1), 285-304. https://doi.org/10.1071/AJ22153

Brun, J.P., Fort, X. 2011. Salt tectonics at passive margins: Geology versus models. Marine and Petroleum Geology, 28(6), 1123-1145. https://doi.org/10.1016/j.marpetgeo.2011.03.004

Burollet, P.F. 1975. Tectonique en radeaux en Angola. Bulletin de la Société Géologique de France, 7(4), 503-504. https://doi.org/10.2113/gssgfbull.S7-XVII.4.503

Caldas, M.F., Zalán, P.V. 2009. Reconstituição cinemática e tectono-sedimentação associada a domos salinos nas águas profundas da Bacia de Santos, Brasil. Boletim de Geociências da Petrobras, 17(2), 227-248.

Callot, J.P., Salel, J.F., Letouzey, J., Daniel, J.M., Ringenbach, J.C. 2016. Three-dimensional evolution of salt-controlled minibasins: Interactions, folding, and megaflap development. American Association of Petroleum Geologists Bulletin, 100(9), 1419-1442. https://doi.org/10.1306/03101614087

Castro A.S., Holz M. 2005. A tectônica de sal e a deposição de sedimentos em águas profundas na região sul da Bacia de Santos. In: Anais do III Congresso Brasileiro de Pesquisa e Desenvolvimento em Petróleo e Gás, Salvador, Brasil. Available at: http://www.portalabpg.org.br/PDPetro/3/trabalhos/IBP0211_05.pdf (accessed March 18th 2020).

Catuneanu, O. 2002. Sequence stratigraphy of clastic systems: concepts, merits, and pitfalls. Journal of African Earth Sciences, 35(1), 1-43. https://doi.org/10.1016/S0899-5362(02)00004-0

Chang, H.K., Assine, M.L., Corrêa, F.S., Tinen, J.S., Vidal, A.C., Koike, L. 2008. Sistemas petrolíferos e modelos de acumulação de hidrocarbonetos na Bacia de Santos. Brazilian Journal of Geology, 38(2), 29-46.

Chang, H.K. 2023. Mapeamento e Interpretação dos Sistemas Petrolíferos da Bacia de Santos. Lebac, Universidade Estadual Paulista, Campus de Rio Claro. Available at: https://www.gov.br/anp/pt-br/rodadas-anp/rodadas-concluidas/concessao-de-blocos-exploratorios/5a-rodada-licitacoes-blocos/arquivos/seminarios/r5_santos.pdf (accessed May 17th 2023)

Cobbold, P.R., Rossello, E., Vendeville, B. 1989. Some experiments on interacting sedimentation and deformation above salt horizons. Bulletin de la Société Géologique de France, (3), 453-460.

Cobbold, P.R., Szatmari, P. 1991. Radial gravitational gliding on passive margins. Tectonophysics, 188(3-4), 249-289. https://doi.org/10.1016/0040-1951(91)90459-6

Cobbold, P.R., Szatmari, P., Demercian, L.S., Coelho, D., Rossello, E.A. 1995. Seismic and experimental evidence for thin-skinned horizontal shortening by convergent radial gliding on evaporites, deep-water Santos Basin, Brazil. In Jackson, M.P.A., Roberts, D.G., Snelson, S. (eds.) Salt tectonics: a global perspective, AAPG Memoir, 65, 305–321.

Cobbold, P.R., Meisling, K.E., Mount, V.S. 2001. Reactivation of an obliquely rifted margin, Campos and Santos basins, southeastern Brazil. American Association of Petroleum Geologists Bulletin, 85(11), 1925-1944. https://doi.org/10.1306/8626D0B3-173B-11D7-8645000102C1865D

Cohen, K.M., Finney, S.C., Gibbard, P.L. Fan, J.-X. (2013; updated) The ICS International Chronostratigraphic Chart. Episodes 36: 199-204. International Commission on Stratigraphy. Available at: http://www.stratigraphy.org/ICSchart/ChronostratChart2022-10.pdf (accessed May 23rd 2023).

Corrêa, F.S. 2009. Evolução halocinética da região centro-norte da Bacia de Santos, Brasil. Doctorate Thesis, Programa de Pós-graduação em Geociências e Meio Ambiente, Instituto de Geociências e Ciências Exatas, Universidade Estadual Paulista, 308p.

Crameri, F. 2018. Scientific colour maps. Zenodo. http://doi.org/10.5281/zenodo.1243862

Cumberpatch, Z.A., Kane, I.A., Soutter, E.L., Hodgson, D.M., Jackson, C.A., Kilhams, B.A., Poprawski, Y. 2021. Interactions between deep-water gravity flows and active salt tectonics. Journal of Sedimentary Research, 91(1), 34-65. https://doi.org/10.2110/jsr.2020.047

Davison, I. 2007. Geology and tectonics of the South Atlantic Brazilian salt basins. Geological Society London Special Publications, 272(1), 345-359. https://doi.org/10.1144/GSL.SP.2007.272.01.18

Davison, I., Anderson, L., Nuttall, P. 2012. Salt deposition, loading and gravity drainage in the Campos and Santos salt basins. Geological Society London Special Publications, 363(1), 159-174. https://doi.org/10.1144/SP363.8

de Mio, E.D., Chang, H.K., Corrêa, F.S. 2005. Integração de métodos geofísicos na modelagem crustal da Bacia de Santos. Revista Brasileira de Geofísica, 23, 275-284. https://doi.org/10.1590/S0102-261X2005000300006

Dehler, N.M., Magnavita, L.P., Gomes, L.C., Rigoti, C.A., de Oliveira, J.A.B., Sant'Anna, M.V., da Costa, F.G.D. 2016. The 'Helmut' geophysical anomaly: a regional left-lateral transtensional shear zone system connecting Santos and Campos basins, southeastern Brazil. Marine and Petroleum Geology, 72, 412-422. https://doi.org/10.1016/j.marpetgeo.2016.01.012

Demercian L.S. 1996. A halocinese na evolução do sul da Bacia de Santos do Aptiano ao Cretaceo superior. Masters Thesis, Instituto de Geociências, Universidade Federal do Rio Grande do Sul, 201p.

Demercian, S., Szatmari, P., Cobbold, P.R. 1993. Style and pattern of salt diapirs due to thin-skinned gravitational gliding, Campos and Santos basins, offshore Brazil. Tectonophysics, 228(3-4), 393-433. https://doi.org/10.1016/0040-1951(93)90351-J

dGB. 2024a. 4.5.2 Dip. https://doc.opendtect.org/6.6.0/doc/dgb_userdoc/content/dip-steering/attributes_with_steering/dip.htm (acceded March 01st 2024).

dGB. 2024b. 4.5.3 Dip Angle. https://doc.opendtect.org/6.6.0/doc/dgb_userdoc/content/dip-steering/attributes_with_steering/dip_angle.htm (acceded March 01st 2024).

Diório, G.R. 2021. Halocinese e Sedimentação na Porção Sudeste do Bloco BS-500, Bacia De Santos. Undergraduate Thesis, Departamento de Geologia, Universidade Federal do Paraná, 45p.

Diório, G.R.; Assis, V.S.R.; Dias, S.F.L.; Trzaskos, B.; Vesely, F.F. 2023a. Halokinetically induced mass-transport deposits in minibasins from northern Santos Basin, Brazil. In Mixed/Hybrid Systems (Turbidites, MTDs and Contourites) on Continental Margins, Lisboa. Programme & Book of Abstracts, 2023.

Diório, G.R., Trzaskos, B. 2023b. Salt walls: what can they tell us about northern Santos Basin halokinetic evolution?. In XII Simpósio Sul Brasileiro de Geologia, 2023, Florianópolis. Anais XII Simpósio Sul Brasileiro de Geologia, p. 101

Dooley, T.P., Jackson, M.P., Hudec, M.R. 2007. Initiation and growth of salt-based thrust belts on passive margins: Results from physical models. Basin Research, 19(1), 165-177. https://doi.org/10.1111/j.1365-2117.2007.00317.x

Dooley, T.P., Jackson, M.P., Jackson, C.A.L., Hudec, M.R., Rodriguez, C.R. 2015. Enigmatic structures within salt walls of the Santos Basin—Part 2: Mechanical explanation from physical modelling. Journal of Structural Geology, 75, 163-187. https://doi.org/10.1016/j.jsg.2015.01.009

Dooley, T.P., Hudec, M.R., Carruthers, D., Jackson, M.P., Luo, G. 2017. The effects of base-salt relief on salt flow and suprasalt deformation patterns—Part 1: Flow across simple steps in the base of salt. Interpretation, 5(1), SD1-SD23. https://doi.org/10.1190/INT-2016-0087.1

Duarte, C.S., Viana, A.R. 2007. Santos Drift System: stratigraphic organization and implications for late Cenozoic palaeocirculation in the Santos Basin, SW Atlantic Ocean. Geological Society London Special Publications, 276(1), 171-198. https://doi.org/10.1144/GSL.SP.2007.276.01.09

Duffy, O., Hudec, M., Peel, F., Apps, G., Bump, A., Moscardelli, L., Dooley, T., Fernandez, N., Bhattacharya, S., Wisian, K., Shuster, M. 2023. The role of salt tectonics in the energy transition: An overview and future challenges. Tektonika, 1(1). https://doi.org/10.55575/tektonika2023.1.1.11

Duval, B., Cramez, C., Jackson, M.P.A. 1992. Raft tectonics in the Kwanza basin, Angola. Marine and Petroleum Geology, 9(4), 389-404. https://doi.org/10.1016/0264-8172(92)90050-O

Fiduk, J.C., Rowan, M.G. 2012. Analysis of folding and deformation within layered evaporites in Blocks BM-S-8 &-9, Santos Basin, Brazil. Geological Society London Special Publications, 363(1), 471-487. https://doi.org/10.1144/SP363.22

Fossen, H. 2010. Structural Geology. Cambridge University Press, New York, 481 p.

Freitas, J.T.R. 2006. Cliclos deposicionais evaporíticos da Bacia de Santos: uma análise cicloestratigráfica a partir de dados de 2 poços e de traços de sísmica. Masters Thesis, Instituto de Geociências, Universidade Federal do Rio Grande do Sul, 160p.

Freitas, V.A. 2019. 4.5.3 Bacia de Santos. Apresentação de Seminário da ANP na 16ª Rodada de Licitações. https://www.gov.br/anp/pt-br/rodadas-anp/rodadas-concluidas/concessao-de-blocos-exploratorios/16a-rodada-licitacoes-blocos/seminarios (acceded March 26th 2024).

Freitas, V.A., Vital, J.C.S., Rodrigues, B.R., Rodrigues, R. 2022. Source rock potential, main depocenters, and CO2 occurrence in the pre-salt section of Santos Basin, southeast Brazil. Journal of South American Earth Sciences, 115, 103760. https://doi.org/10.1016/j.jsames.2022.103760

Gamboa, L.A., Machado, M.P., Silveira, D.P., Freitas, J.T., Silva, S.P., Mohriak, W., Szatmari, P., Anjos, S. 2008. Evaporitos estratificados no Atlântico Sul: interpretação

sísmica e controle tectono-estratigráfico na Bacia de Santos. In: Mohriak, W. U., Szatmari, P., Anjos, S. C. (eds) Sal: Geologia e Tectônica, Exemplos nas Bacias Brasileiras. Editora Beca, São Paulo, 340-359.

Garcia, S.F.D.M. 2012. Restauração estrutural da halotectônica na porção central da bacia de Santos e implicações para os sistemas petrolíferos. Doctorate Thesis, Programa de Pós-Graduação em Evolução Crustal e Recursos Naturais, Departamento de Geologia, Escola de Minas, Universidade Federal de Ouro Preto, 206p.

Garcia, S.F.M., Letouzey, J., Rudkiewicz, J.L., Danderfer Filho, A., de Lamotte, D.F. 2012. Structural modeling based on sequential restoration of gravitational salt deformation in the Santos Basin (Brazil). Marine and Petroleum Geology, 35(1), 337-353. https://doi.org/10.1016/j.marpetgeo.2012.02.009

Gaullier, V., Brun, J.P., Gue, G., Lecanu, H. 1993. Raft tectonics: the effects of residual topography below a salt décollement. Tectonophysics, 228(3-4), 363-381. https://doi.org/10.1016/0040-1951(93)90349-O

Ge, Z., Gawthorpe, R.L., Rotevatn, A., Zijerveld, L., Jackson, C.A.L., Oluboyo, A. 2020. Minibasin depocentre migration during diachronous salt welding, offshore Angola. Basin Research, 32(5), 875-893. https://doi.org/10.1111/bre.12404

Ge, Z., Gawthorpe, R.L., Zijerveld, L., Oluboyo, A.P. 2021. Spatial and temporal variations in minibasin geometry and evolution in salt tectonic provinces: Lower Congo Basin, offshore Angola. Basin Research, 33(1), 594-611. https://doi.org/10.1111/bre.12486

Ge, Z., Rosenau, M., Warsitzka, M., Gawthorpe, R.L. 2019. Overprinting translational domains in passive margin salt basins: insights from analogue modelling. Solid Earth, 10(4), 1283-1300. https://doi.org/10.5194/se-10-1283-2019

Giles, K.A., Druke, D.C., Mercer, D.W., Hunnicutt-Mack, L. 2008. Controls on Upper Cretaceous (Maastrichtian) heterozoan carbonate platforms developed on salt diapirs, La Popa Basin, NE Mexico. In Lukasik, J., Simo, J.A. (eds) Controls on Carbonate Plataform and Reef Development. https://doi.org/10.2110/pec.08.89.0107

Giles, K.A., Lawton, T.F. 2002. Halokinetic sequence stratigraphy adjacent to the El Papalote diapir, northeastern Mexico. AAPG bulletin, 86(5), 823-840. https://doi.org/10.1306/61EEDBAC-173E-11D7-8645000102C1865D

Giles, K.A., Rowan, M.G. 2012. Concepts in halokinetic-sequence deformation and stratigraphy. Geological Society London Special Publications, 363(1), 7-31. https://doi.org/10.1306/61EEDBAC-173E-11D7-8645000102C1865D

Gomes, P.O., Kilsdonk, B., Grow, T., Minken, J., Barragan, R. 2013. Tectonic evolution of the outer high of Santos Basin, Southern São Paulo Plateau, Brazil, and implications for hydrocarbon exploration. In: Gao, D. (eds) AAPG Memoir 100: Tectonics and Sedimentation: Implications for Petroleum Systems, AAPG Special Volumes, https://doi.org/10.1306/13351550M1003530

Grunau, H.R. 1987. A worldwide look at the cap-rock problem. Journal of Petroleum Geology, 10(3), 245-265. https://doi.org/10.1111/j.1747-5457.1987.tb00945.x

Guerra, M.C., Underhill, J.R. 2012. Role of halokinesis in controlling structural styles and sediment dispersal in the Santos Basin, offshore Brazil. Geological Society London Special Publications, 363(1), 175-206. https://doi.org/10.1144/SP363.9

Hardie, L.A. 1991. On the significance of evaporites. Annual Review of Earth and Planetary Sciences, 19(1), 131-168. https://doi.org/10.1146/annurev.ea.19.050191.001023

Hercos, C.M., Schreiner, S., Ferreira, E.T.I. 2023. Deep-water seafloor geomorphic features of the Santos Basin, Southeastern Brazilian Margin, shown by analyses and integration of an extensive 3-D seismic data set. Ocean and Coastal Research, 71, e23059. https://doi.org/10.1590/2675-2824071.22067cmh

Hite, R.J. 1972. Shelf carbonates sedimentation controlled by salinity in the Paradox basin southeast Utah. Mountain Geology, 27, 329–349.

Hite, R.J., Anders, D.E. 1991. Chapter 4: Petroleum and evaporites. In: Melvin, J.L. (eds) Developments in Sedimentology, 50, Elsevier, 349. https://doi.org/10.1016/S0070-4571(08)70262-0

Hudec, M.R., Jackson, M.P. 2007. Terra infirma: Understanding salt tectonics. Earth-Science Reviews, 82(1-2), 1-28. https://doi.org/10.1016/j.earscirev.2007.01.001

Hudec, M.R., Jackson, M.P., Schultz-Ela, D.D. 2009. The paradox of minibasin subsidence into salt: Clues to the evolution of crustal basins. Geological Society of America Bulletin, 121(1-2), 201-221. https://doi.org/10.1130/B26275.1

Hudec, M.R., Jackson, M.P. 2012. De Re Salica: Fundamental principles of salt tectonics. In Roberts, D.G., Bally, A.W. (eds.) Regional geology and tectonics: Phanerozoic passive margins, cratonic basins and global tectonic maps, 1, 19-41. https://doi.org/10.1016/B978-0-444-56357-6.00001-9

Hudec M.R., Dooley T.P., Peel F.J., Soto J.I. 2020. Controls on the evolution of passive-margin salt basins: Structure and evolution of the Salina del Bravo region, northeastern Mexico. Geological Society of America Bulletin, 132(5-6), 997-1012. https://doi.org/10.1130/B35283.1

Hudec, M.R., Jackson, M.P. 2022. Salt tectonics in deepwater settings. In Rotzien, J.R., Yeilding, C.A., Sears, R.A., Hernández-Molina, F.J., Catuneanu, O. (eds) Deepwater Sedimentary Systems. Elsevier, 149-177. https://doi.org/10.1016/B978-0-323-91918-0.00020-7

Ingersoll, R.V. 2012. Tectonics of sedimentary basins, with revised nomenclature. In Busby, C., Azro, A. (eds.), Tectonics of Sedimentary Basin: Recent advances. Blackwell Publishing Ltd, 3–46.

Jackson, C.A.L., Rodriguez, C.R., Rotevatn, A., Bell, R.E. 2014. Geological and geophysical expression of a primary salt weld: An example from the Santos Basin, Brazil. Interpretation, 2(4), SM77-SM89. https://doi.org/10.1190/INT-2014-0066.1

Jackson, C.A.L., Jackson, M.P., Hudec, M.R., Rodriguez, C.R. 2015a. Enigmatic structures within salt walls of the Santos Basin—Part 1: Geometry and kinematics from 3D seismic reflection and well data. Journal of Structural Geology, 75, 135-162. https://doi.org/10.1016/j.jsg.2015.01.010

Jackson, C.A.L., Jackson, M.P., Hudec, M.R. 2015b. Understanding the kinematics of salt-bearing passive margins: A critical test of competing hypotheses for the origin of the Albian Gap, Santos Basin, offshore Brazil. Bulletin, 127(11-12), 1730-1751. https://doi.org/10.1130/B31290.1

Jackson, M.P., Talbot, C.J. 1986. External shapes, strain rates, and dynamics of salt structures. Geological Society of America Bulletin, 97(3), 305-323. https://doi.org/10.1130/0016-7606(1986)97%3C305:ESSRAD%3E2.0.CO;2

Jackson, M.P.A., Talbot, C.J., 1991. A glossary of salt tectonics. Geological Circular, vol. 91-4. The University of Texas at Austin, Bureau of Economic Geology. 44 pp.

Jackson, M.P.A., Vendeville, B.C. 1994. Regional extension as a geologic trigger for diapirism. Geological Society of America Bulletin, 106(1), 57-73. https://doi.org/10.1130/0016-7606(1994)106%3C0057:REAAGT%3E2.3.CO;2

Jackson, M.P., Vendeville, B.C., Schultz-Ela, D.D. 1994. Structural dynamics of salt systems. Annual Review of Earth and Planetary Sciences, 22(1), 93-117. https://doi.org/10.1146/annurev.ea.22.050194.000521

Jackson, M.P., Hudec, M.R. 2005. Stratigraphic record of translation down ramps in a passive-margin salt detachment. Journal of Structural Geology, 27(5), 889-911. https://doi.org/10.1016/j.jsg.2005.01.010

Jackson, M.P., Hudec, M.R. 2017. Salt tectonics: Principles and practice. Cambridge University Press, 510p. https://doi.org/10.1017/9781139003988

Karner, G.D., Gambôa, L.A.P. 2007. Timing and origin of the South Atlantic pre-salt sag basins and their capping evaporites. Geological Society London Special Publications, 285(1), 15-35. https://doi.org/10.1144/SP285.2

Kukla, P.A., Strozyk, F., Mohriak, W.U. 2018. South Atlantic salt basins–witnesses of complex passive margin evolution. Gondwana Research, 53, 41-57. https://doi.org/10.1016/j.gr.2017.03.012

Kumar, N., Gamboa, L.A.P. 1979. Evolution of the São Paulo Plateau (southeastern Brazilian margin) and implications for the early history of the South Atlantic. Geological Society of America Bulletin, 90(3), 281-293. https://doi.org/10.1130/0016-7606(1979)90%3C281:EOTSPP%3E2.0.CO;2

Leite, C.O.N., Silva, C.M.A., De Ros, L.F. 2020. Depositional and diagenetic processes in the pre-salt rift section of a Santos Basin area, SE Brazil. Journal of Sedimentary Research, 90(6), 584-608. https://doi.org/10.2110/jsr.2020.27

Lentini, M.R., Fraser, S.I., Sumner, H.S., Davies, R.J. 2010. Geodynamics of the central South Atlantic conjugate margins: implications for hydrocarbon potential. Petroleum Geoscience, 16(3), 217-229. https://doi.org/10.1144/1354-079309-909

Magee, C., Pichel, L.M., Madden-Nadeau, A.L., Jackson, C.A.L., Mohriak, W. 2021. Salt–magma interactions influence intrusion distribution and salt tectonics in the Santos Basin, offshore Brazil. Basin Research, 33(3), 1820-1843. https://doi.org/10.1111/bre.12537

Magoon, L.B., Dow, W.G. 1994. The petroleum system: chapter 1: Part I. Introduction. In: Magoon, L.B., Dow, W.G. (eds) AAPG Memoir 60: The Petroleum System-From Source to Trap, AAPG Special Publication, 3-24p.

Marinha do Brasil. 2023. New Brazilian Digital Terrain Model (DTM). https://www.marinha.mil.br/dhn/?q=node/249 (acceded March 26th 2024).

Martins, G.S. 2016. Evolução tectono-estratigráfica dos evaporitos Horizonte e Paripueira na porção alagoana da Bacia de Sergipe-Alagoas e suas implicações na abertura do Oceano Atlântico Sul. Masters Thesis, Pós Graduação em Análise de Bacias,Tectônia, Petrologia e Recursos Minerais, Universidade do Estado do Rio de Janeiro, 258p.

Mayall, M., Lonergan, L., Bowman, A., James, S., Mills, K., Primmer, T., Pope, D., Rogers, L., Skeene, R. 2010. The response of turbidite slope channels to growth-induced seabed topography. American Association of Petroleum Geologists Bulletin, 94(7), 1011-1030. https://doi.org/10.1306/01051009117

Meisling, K.E., Cobbold, P.R., Mount, V.S. 2001. Segmentation of an obliquely rifted margin, Campos and Santos basins, southeastern Brazil. American Association of Petroleum Geologists Bulletin, 85(11), 1903-1924. https://doi.org/10.1306/8626D0A9-173B-11D7-8645000102C1865D

Mello, U.T., Karner, G.D., Anderson, R.N. 1995. Role of salt in restraining the maturation of subsalt source rocks. Marine and Petroleum Geology, 12(7), 697-716. https://doi.org/10.1016/0264-8172(95)93596-V

Mello, M.R., Peres, W., Rostirolla, S.P., Pedrosa Jr, O.A., Piquet, A., Becker, S., Yilmaz, P.O. 2021. The Santos Basin Pre-Salt Super Giant Petroleum System: An Incredible Journey from Failure to Success. In Mello, M.R., Yilmaz, P.O., Katz, B.J. (eds) AAPG Memoir 124: The Supergiant Lower Cretaceous Pre-Salt Petroleum Systems of the Santos Basin, Brazil, AAPG Special Volumes, 1-34p. https://doi.org/10.1306/13722313MSB.1.1853

Milani, E.J., Brandão, J.A.S.L., Zalán, P.V., Gamboa, L.A.P. 2000. Petróleo na margem continental brasileira: geologia, exploração, resultados e perspectivas. Revista Brasileira de Geofísica, 18, 352-396. https://doi.org/10.1590/S0102-261X2000000300012

Mindat.org. 2023. mindat.org and the Hudson Institute of Mineralogy: minerals and their localities, deposits, and mines worldwide. Available at: https://www.mindat.org/ (accessed April 14th 2023).

Modica, C.J., Brush, E.R. 2004. Postrift sequence stratigraphy, paleogeography, and fill history of the deep-water Santos Basin, offshore southeast Brazil. American Association of Petroleum Geologists Bulletin, 88(7), 923-945. https://doi.org/10.1306/01220403043

Mohriak, W.U., Macedo, J.M., Castellani, R.T., Rangel, H.D., Barros, A.Z.N., Latgé, M.A.L., Ricci, J.A., Mizusaki, A.M.P., Szatmari, P., Demercian, L.S., Rizzo, J.G., Aires, J.R., 1995. Salt tectonics and structural styles in the deep-water province of the Cabo Frio region, Rio de Janeiro, Brazil. In: Jackson, M.P.A., Roberts, D.G., Snelson, S. (eds.) Salt Tectonics: A Global Perspective. American Association of Petroleum Geologists Memoir 65, 273-304.

Mohriak, W. U. 2003. Bacias sedimentares da margem continental Brasileira. In: L. A. Bizzi, L.A., Schobbenhaus, C., Vidotti, R.M., Gonçalves, J.H. (eds) Geologia, tectônica e recursos minerais do Brasil, Brazil, CPRM, 87-165.

Mohriak, W.U., Szatmari, P., Anjos, S.C. 2008. Sal: Geologia e Tectônica, Exemplos nas Bacias Brasileiras. Editora Beca, São Paulo, 2008p.

Mohriak, W.U., Nóbrega, M., Odegard, M.E., Gomes, B.S., Dickson, W.G. 2010. Geological and geophysical interpretation of the Rio Grande Rise, south-eastern Brazilian margin: extensional tectonics and rifting of continental and oceanic crusts. Petroleum Geoscience, 16(3), 231–245. https://doi.org/10.1144/1354-079309-910

Moreira, J.L.P., Carminatti, M. 2004. Sistemas deposicionais de talude e de bacia no Eoceno da Bacia de Santos. Boletim de Geociências da Petrobras, 12(1), 73-87.

Moreira, J.L.P., Madeira, C.V., Gil, J.A., Machado, M.A.P. 2007. Bacia de Santos. Boletim de Geociências da Petrobras, 15(2), 531-549.

Museu Heinz Ebert. 2023. Banco de Dados de Rochas e Minerais. Museu de Minerais, Minérios e Rochas Heinz Ebert. Available at: https://museuhe.com.br/ (accessed April 14th 2023).

Nalpas, T., Brun, J.P. 1993. Salt flow and diapirism related to extension at crustal scale. Tectonophysics, 228(3-4), 349-362. https://doi.org/10.1016/0040-1951(93)90348-N

Paleomap Project. 2003. Download data. PALEOMAP PaleoAtlas for GPlates. Available at: https://www.earthbyte.org/paleomap-paleoatlas-for-gplates/ (accessed May 28th 2023).

Peel, F.J. 2014. How do salt withdrawal minibasins form? Insights from forward modelling, and implications for hydrocarbon migration. Tectonophysics, 630, 222-235. https://doi.org/10.1016/j.tecto.2014.05.027

Pereira, M.J., Barbosa, C.M., Agra, J., Gomes, J.B., Aranha, L.G.F., Saito, M., Ramos, M.A., Carvalho, M.D., Stamato, M. Bagni, O. 1986. Estratigrafia da Bacia de Santos: análise das sequências, sistemas deposicionais e revisão litoestratigráfica. In: Anais do Congresso Brasileiro de Geologia, 34(1), 65-79p.

Pereira, M.J., Feijó, F.J. 1994. Bacia de Santos. Boletim de Geociências da Petrobras, 8.

Pereira, C.E.L., Gomes, C.J.S., de Araujo, M.N.C. 2021. A influência de estruturas preexistentes na formação de riftes oblíquos: o uso da modelagem física e sua comparação com a fase Pré-sal da Bacia de Santos, Brasil. Geologia USP. Série Científica, 21(4), 103-124. https://doi.org/10.11606/issn.2316-9095.v21-181314

PETROBRAS. 2023. Bacia de Santos. PETROBRAS. Available at: https://petrobras.com.br/pt/nossas-atividades/principais-operacoes/bacias/bacia-de-santos.htm (accessed May 17th 2023).

Pichel, L. M., Peel, F., Jackson, C. A., Huuse, M. 2018. Geometry and kinematics of salt-detached ramp syncline basins. Journal of Structural Geology, 115, 208-230. https://doi.org/10.1016/j.jsg.2018.07.016

Pichel, L.M., Jackson, C.A.L., Peel, F., Dooley, T.P. 2019. Base-salt relief controls salt-tectonic structural style, São Paulo Plateau, Santos Basin, Brazil. Basin Research, 32(3), 453-484. https://doi.org/10.1111/bre.12375

Pichel, L.M., Jackson, C.A.L. 2020. The enigma of the Albian Gap: spatial variability and the competition between salt expulsion and extension. Journal of the Geological Society, 177(6), 1129-1148. https://doi.org/10.1144/jgs2020-055

Pichel, L.M., Jackson, C.A.L., Peel, F., Ferrer, O. 2021. The Merluza Graben: How a failed spreading center influenced margin structure, and salt deposition and tectonics in the Santos Basin, Brazil. Tectonics, 40(10), e2020TC006640. https://doi.org/10.1029/2020TC006640

Pichel, L.M., Ferrer, O., Jackson, C.A.L., Roca, E. 2022. Physical modelling of the interplay between salt-detached gravity gliding and spreading across complex rift topography, Santos Basin, offshore Brazil. Basin Research, 34(6), 2042-2063. https://doi.org/10.1111/bre.12695

Piedade, A., Alves, T.M. 2017. Structural styles of Albian rafts in the Espírito Santo Basin (SE Brazil): Evidence for late raft compartmentalisation on a 'passive'continental margin. Marine and Petroleum Geology, 79, 201-221. https://doi.org/10.1016/j.marpetgeo.2016.10.023

Pilcher, R.S., Kilsdonk, B., Trude, J. 2011. Primary basins and their boundaries in the deep-water northern Gulf of Mexico: Origin, trap types, and petroleum system implications. American Association of Petroleum Geologists Bulletin, 95, 219–240. https://doi.org/10.1306/06301010004

Pontes, R.L.B., Maul, A.R., Silva, C.G. 2021. Seismic characterization of internal salt cycles: a case study in the Santos Basin, Brazil. Brazilian Journal of Geophysics, 39(2), 181-195. http://dx.doi.org/10.22564/rbgf.v38i4.2082

Poprawski, Y., Basile, C., Cumberpatch, Z., Eude, A. 2021. Mass transport deposits in deep-water minibasins: Outcropping examples from the minibasins adjacent to the Bakio salt wall (Basque Country, Northern Spain). Marine and Petroleum Geology, 132, 105194. https://doi.org/10.1016/j.marpetgeo.2021.105194

Pré-sal Petróleo. 2023. Bacia de Santos: A casa do pré-sal. Empresa Brasileira de Administração de Petróleo e Gás Natural S.A., Pré-Sal Petróleo S.A., Ministério de Minas e Energia. Available at: https://www.presalpetroleo.gov.br/bacia-de-santos/ (accessed May 17th 2023).

Quirk, D.G., Schødt, N., Lassen, B., Ings, S.J., Hsu, D., Hirsch, K.K., Von Nicolai, C. 2012. Salt tectonics on passive margins: examples from Santos, Campos and Kwanza basins. Geological Society London Special Publications, 363(1), 207-244. https://doi.org/10.1144/SP363.10

Rigoti, C.A. 2015. Evolução tectônica da Bacia de Santos com ênfase na geometria crustal: Interpretação integrada de dados de sísmica de reflexão e refração, gravimetria e magnetometria. Doctorate Thesis, Programa de Pós-Graduação em Análise de Bacias e Faixas Móveis, Centro de Tecnologia e Ciências, Faculdade de Geologia, Universidade do Estado do Rio de Janeiro, 135p.

Rodriguez, C.R., Jackson, C.L., Rotevatn, A., Bell, R.E., Francis, M. 2018. Dual tectonic-climatic controls on salt giant deposition in the Santos Basin, offshore Brazil. Geosphere, 14(1), 215-242. https://doi.org/10.1130/GES01434.1

Rowan, M.G., Jackson, M.P., Trudgill, B.D. 1999. Salt-related fault families and fault welds in the northern Gulf of Mexico. American Association of Petroleum Geologists Bulletin, 83(9), 1454-1484. https://doi.org/10.1306/E4FD41E3-1732-11D7-8645000102C1865D

Rowan, M.G., Vendeville, B.C. 2006. Foldbelts with early salt withdrawal and diapirism: Physical model and examples from the northern Gulf of Mexico and the Flinders Ranges, Australia. Marine and Petroleum Geology, 23(9-10), 871-891. https://doi.org/10.1016/j.marpetgeo.2006.08.003

Rowan, M.G. 2014. Passive-margin salt basins: Hyperextension, evaporite deposition, and salt tectonics. Basin Research, 26(1), 154-182. https://doi.org/10.1111/bre.12043

Rowan, M.G., Giles, K.A., Hearon IV, T.E., Fiduk, J.C. 2016. Megaflaps adjacent to salt diapirs. AAPG Bulletin, 100(11), 1723-1747. https://doi.org/10.1306/05241616009

Rowan, M.G., Urai, J.L., Fiduk, J.C., Kukla, P.A. 2019. Deformation of intrasalt competent layers in different modes of salt tectonics. Solid Earth, 10(3), 987-1013. https://doi.org/10.5194/se-10-987-2019

Rowan, M.G., Muñoz, J.A., Giles, K.A., Roca, E., Hearon IV, T.E., Fiduk, J.C., Ferrer, O., Fischer, M.P. 2020. Folding and fracturing of rocks adjacent to salt diapirs. Journal of Structural Geology, 141, 104187. https://doi.org/10.1016/j.jsg.2020.104187

Rowan, M.G., Tilton, J., Lebit, H., Fiduk, J.C. 2022. Thin-skinned extensional salt tectonics, counterregional faults, and the Albian Gap of Brazil. Marine and Petroleum Geology, 137, 105478. https://doi.org/10.1016/j.marpetgeo.2021.105478

Santos, C.H.O., Silva, F.C.A., Pichel, L.M. 2022. Analogical simulation of salt flow and associated structures in different extensional conditions. Journal of South American Earth Sciences, 120, 104052. https://doi.org/10.1016/j.jsames.2022.104052

Santos, C.H.O., Pichel, L.M., Silva, F.C.A. 2023. The effects of subsalt relief on gravity-driven salt tectonics: Results from analogue modelling. Journal of Structural Geology, 174, 104919. https://doi.org/10.1016/j.jsg.2023.104919

Santos, P.T., Gordon, A.C. 2021. Búzios Field: Geological setting of the largest pre-salt field, Santos Basin, Brazil. In: Mello, M.R., Yilmaz, P.O., Katz, B.J. (eds) AAPG Memoir 124: The Supergiant Lower Cretaceous Pre-Salt Petroleum Systems of the Santos Basin, Brazil, AAPG Special Volumes, 375-394p. https://doi.org/10.1306/13722365MSB.14.1853

Seni, S.J., Jackson, M.P.A. 1983. Evolution of salt structures, east Texas diapir province, part 1: Sedimentary record of halokinesis. American Association of Petroleum Geologists Bulletin, 67(8), 1219-1244. https://doi.org/10.1306/03B5B731-16D1-11D7-8645000102C1865D

Sobiesiak, M.S., Kneller, B., Alsop, G.I., Milana, J.P. 2018. Styles of basal interaction beneath mass transport deposits. Marine and Petroleum Geology, 98, 629-639. https://doi.org/10.1016/j.marpetgeo.2018.08.028

Souza, I.A.D. 2008. Falhas de transferência da porção norte da Bacia de Santos interpretadas a partir de dados sísmicos: sua influência na evolução e deformação da bacia. Doctorate Thesis, Curso de Pós-Graduação em Geociências, Instituto de Geociências e Ciências Exatas, Universidade Estadual Paulista, 202p.

Souza, L.S., Sgarbi, G.N.C. 2019. Bacia de Santos no Brasil: geologia, exploração e produção de petróleo e gás natural. Boletín de Geología, 41(1), 175-195. http://dx.doi.org/10.18273/revbol.v41n1-2019009

Szatmari, P. 2000. Habitat of petroleum along the South Atlantic margins. In: Mello, M.R., Katz, B.J. (eds.), Petroleum Systems of South Atlantic Margins. AAPG Memoir, 69-75.

Szatmari, P., Guerra, M.C.M., Pequeno, M.A. 1996. Genesis of large counter-regional normal fault by flow of Cretaceous salt in the South Atlantic Santos Basin, Brazil. Geological Society London Special Publications, 100(1), 259-264. https://doi.org/10.1144/GSL.SP.1996.100.01.16

Szatmari, P., Milani, E.J. 2016. Tectonic control of the oil-rich large igneous-carbonate-salt province of the South Atlantic rift. Marine and Petroleum Geology, 77, 567-596. https://doi.org/10.1016/j.marpetgeo.2016.06.004

Tarkowski, R., Uliasz-Misiak, B., Tarkowski, P. 2021. Storage of hydrogen, natural gas, and carbon dioxide–Geological and legal conditions. International Journal of Hydrogen Energy, 46(38), 20010-20022. https://doi.org/10.1016/j.ijhydene.2021.03.131

Trusheim, F. 1960. Mechanism of salt migration in northern Germany. American Association of Petroleum Geologists Bulletin, 44(9), 1519-1540. https://doi.org/10.1306/0BDA61CA-16BD-11D7-8645000102C1865D

Van Gent, H., Urai, J.L., De Keijzer, M. 2011. The internal geometry of salt structures–a first look using 3D seismic data from the Zechstein of the Netherlands. Journal of Structural Geology, 33(3), 292-311. https://doi.org/10.1016/j.jsg.2010.07.005

Vendeville, B.C., Jackson, M.P.A. 1991. The fall of diapirs during thin-skinned extension. Marine and Petroleum Geology, 9(4), 354-371. https://doi.org/10.1016/0264-8172(92)90048-J

Vendeville, B.C., Jackson, M.P. 1992. The rise of diapirs during thin-skinned extension. Marine and Petroleum Geology, 9(4), 331-354. https://doi.org/10.1016/0264-8172(92)90047-I

Vendeville, B.C. 2005. Salt tectonics driven by sediment progradation: Part I—Mechanics and kinematics. American Association of Petroleum Geologists Bulletin, 89(8), 1071-1079. https://doi.org/10.1306/03310503063

Vital, J.C.S., Ade, M.V.B., Morelatto, R., Lupinacci, W. 2023. Compartmentalization and stratigraphic-structural trapping in pre-salt carbonate reservoirs of the Santos Basin: A case study in the Iara complex. Marine and Petroleum Geology, 106163. https://doi.org/10.1016/j.marpetgeo.2023.106163

Waltham, D. 1997. Why does salt start to move?. Tectonophysics, 282(1-4), 117-128. https://doi.org/10.1016/S0040-1951(97)00215-1

Warren, J.K. 2006. Evaporites: Sediments, Resources and Hydrocarbons. Springer Berlin, Heidelberg, 1036p. https://doi.org/10.1007/3-540-32344-9

Warren, J.K. 2016. Evaporites: A Geological Compendium. 2nd Edition, Springer International Publishing, Berlin, 1813 pp.

Weijermars, R., Jackson, M.P.A., Dooley, T.P. 2014. Quantifying drag on wellbore casings in moving salt sheets. Geophysical Journal International, 198(2), 965-977. https://doi.org/10.1093/gji/ggu174

Williams, B. G., Hubbard, R. J. 1984. Seismic stratigraphic framework and depositional sequences in the Santos Basin, Brazil. Marine and Petroleum Geology, 1(2), 90-104. https://doi.org/10.1016/0264-8172(84)90079-5

Worrall, D.M., Snelson, S. 1989. Evolution of the northern Gulf of Mexico, with emphasis on Cenozoic growth faulting and the role of salt. In Bally, A., Palmer, A. (eds.) The geology of North America—An overview, Boulder, Colorado, Geological Society of America, v. A, 97–138.

Ysaccis, R., El-Toukhy, M., Moreira, L. 2019. Maximizing the value of seismic data for a better regional understanding and exploration assessment in the Santos Basin, Brazil: Brazilian Geophysical Society, 16th International Congress, Proceedings, p. 1–6.

Zalán, P.V., Oliveira, J.A. 2005. Origem e evolução estrutural do Sistema de Riftes Cenozóicos do Sudeste do Brasil. Boletim de Geociências da Petrobras, 13(2), 269-300.

Zalán P.V., Severino M.C.G., Oliveira J.A.B., Magnavita L.P., Mohriak W.U., Gontijo R.C., Viana A.R., Szatmari P. 2009. Stretching and thinning of the upper lithosphere and continental-oceanic crustal transition in Southeastern Brazil. In AAPG International Conference and Exhibition, AAPG, Houston.

Zalán, P.V., Severino, M.D.C.G., Rigoti, C.A., Magnavita, L.P., Oliveira, J.A.B., Vianna, A. R., 2011. An entirely new 3D-view of the crustal and mantle structure of a South Atlantic passive margin–Santos, Campos and Espírito Santo basins, Brazil. In: AAPG Annual Conference and Exhibition, 13.

Zuo, G., Wang, H., Lan, L., Zhang, Y., Zuo, Y., Yang, L., Wang, C., Pang, X., Song, X., Yang, M. 2023. Present geothermal field of the Santos Basin, Brazil. Scientific Reports, 13, 12369. https://doi.org/10.1038/s41598-023-39702-5

Zwaan, F., Rosenau, M., Maestrelli, D. 2021. How initial basin geometry influences gravity-driven salt tectonics: Insights from laboratory experiments. Marine and Petroleum Geology, 133, 105195. https://doi.org/10.1016/j.marpetgeo.2021.105195

SUPPLEMENTARY MATERIAL 1

Halokinetically induced mass-transport deposits in minibasins from northern Santos Basin, Brazil

Authors: Diório, G. R.; Assis, V. S. R.; Dias, S. F. L.; Trzaskos, B.; Vesely, F. F.
Affiliation: Laboratório de Análise de Bacias (LABAP), Universidade Federal do Paraná (UFPR)

Keywords: salt tecnonics, 3D seismic, seismic geomorphology

Introduction

MTDs (mass-transport deposits) are important features in deepwater environments that form because of subaqueous landslides and present characteristic patterns of internal deformation (Sobiesiak et al., 2018). Once formed by sediment failure in response to gravitational forces, the displaced mass flows down the regional slope towards basin's depocenter.
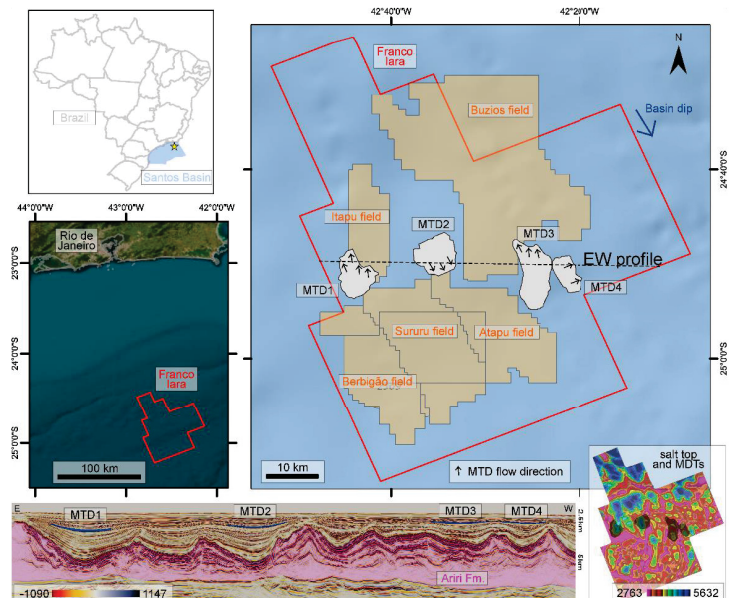
However, in basins characterized by complex bathymetries due to active salt tectonics, mass failure may affect local slopes and give rise to MTDs within minibasins (e.g., Biancardi et al., 2020; Poprawski et al., 2021). Minibasins are syn-kinematic, a few tens of kilometers in diameter, and subside into relatively thick evaporites (Jackson & Talbot 1991, Hudec et al. 2009, Hudec & Jackson 2022). Due to active topography, each minibasin has its individual setting and evolution, including MTDs that may diverge from trends found in the basin itself.

Santos Basin is a passive margin basin located in SE Brazil, and it is currently the largest oil producer in the country (Moreira et al. 2007, Assine et al. 2008, ANP 2023). The basin formed as a result of Gondwana breakup and opening of the Atlantic Ocean in the Lower Cretaceous (Assine et al. 2008, Chang et al. 2008, Kukla et al. 2018). Remarkable is a major evaporite stage during the Aptian (Ariri Formation) and expressive salt tectonics interfering in the deposition of the subsequent drift Sequence (e.g., Modica & Brush 2004, Assine et al. 2008, Caldas e Zalán 2009, Guerra & Underhill 2012, Garcia et al. 2012).

In this contribution we describe four Cenozoic MTDs filling salt-controlled adjacent minibasins in northern Santos Basin, offshore Brazil, in order to evaluate and compare their features.

Methodology

Seismic horizons (top salt; base and top of MTDs) were mapped in a ca. 3,700 km2 3D seismic-reflection post-stack data (seismic survey Franco Iara), using the OpendTect PRO software. Lines and fault stick sets were traced using a spacing of ca. 250 m (20 steps) in in-lines and crosslines, interpolated using the inverse distance method, and followed by median and average filtering. Similarity attribute was employed to highlight internal features, and isopach maps were created to evaluate thickness.

Figure 1: Setting of studied area, with Santos Basin location in offshore Brazil. Franco Iara's location ca. 220km from Rio de Janeiro, MTDs locations and paleoflows regarding Franco Iara and oil fields. E-W profile highlighting Ariri Formation and MTDs and salt top map (pink – highs; blue – lows, depth in meters) with MTDs diverging from rising diapirs.
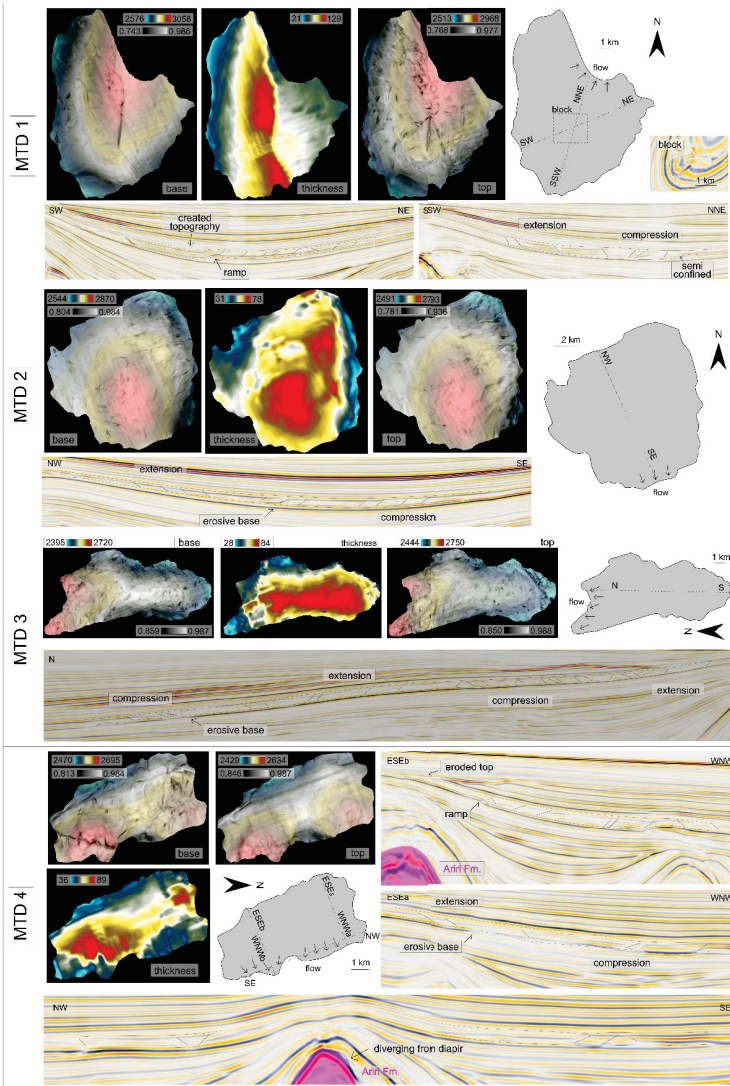

Figure 2: Thickness, MTD's base and top (similarity attribute with 30% transparency over depth in meters), paleoflow direction and profiles highlighting main features of each MTD.

Results & Discussions

Four MTDs were identified in neighboring minibasins in the northern Santos Basin (see Fig. 1). These MTDs (Fig. 2) are located within a distance of less than 50 km and aligned in a west-east trend (MTD1-MTD4). Their main characteristics are summarized in Table 1 and Figure 2. The MTDs have an areal extent ranging from 25 to 58 km2, with thicknesses ranging from 45 to 110 m. They exhibit a common flow pattern towards the depocenters of the minibasins, diverging from and occasionally being truncated due to rising diapirs. All MTDs display proximal extensional and distal compressional features, as well as additional characteristics such as ramps, blocks, frontal confinement, surface topography and basal erosion.

Table 1: Summary of main characteristics of tracked MTDs.

MTD	Flow directi on	Base depth Min.	Base depth Max.	Top depth Min.	Top depth Max.	Thickness Min.	Thickness Max.	Internal features
1	N	2576	3058	2513	2968	21	129	Blocks (ca. 1km²), created topography, ramps, frontal confinement
2	SSE	2544	2870	2491	2793	31	78	Erosive base
3	NNW	2395	2420	2444	2750	28	84	Erosive base, two extensional and compressional domains
4	ENE	2470	2695	2429	2634	36	89	Diverges from rising diapir, ramp, erosive base, truncation

Conclusions

Halokinetically induced MTDs can help elucidate minibasins' structural evolution once they are related to the uplifting of bounding slopes. Moreover, they can form potential seals for reservoir-quality deepwater sands that potentially accumulate in these minibasins.

References

ANP. 2023. Boletim Mensal da Produção de Petróleo e Gás Natural: Dados da produção de petróleo e gás natural no Brasil. Agência Nacional do Petróleo, Gás Natural e Biocombustíveis, Ministério de Minas e Energia, Governo do Brasil. Available at: https://www.gov.br/anp/pt-br/centrais-de-conteudo/publicacoes/boletins-anp/boletins/boletim-mensal-da-producao-de-petroleo-e-gas-natural (accessed May 17th 2023).

Assine, M. L., Corrêa, F. S., Chang, H. K. 2008. Migração de depocentros na Bacia de Santos: importância na exploração de hidrocarbonetos. Brazilian Journal of Geology, 38(2), 111-127.

Biancardi, C. A., Alves, T. M., Martins-Ferreira, M. A. C. 2020. Unpredictable geometry and depositional stacking patterns of mass-transport complexes in salt minibasins. Marine and Petroleum Geology, 120, 104522. https://doi.org/10.1016/j.marpetgeo.2020.104522

Caldas, M. F., Zalán, P. V. 2009. Reconstituição cinemática e tectono-sedimentação associada a domos salinos nas águas profundas da Bacia de Santos, Brasil. Boletim de Geociências da Petrobras, 17(2), 227-248.

Chang, H. K., Assine, M. L., Corrêa, F. S., Tinen, J. S., Vidal, A. C., Koike, L. 2008. Sistemas petrolíferos e modelos de acumulação de hidrocarbonetos na Bacia de Santos. Brazilian Journal of Geology, 38(2), 29-46.

Garcia, S. F.M., Letouzey, J., Rudkiewicz, J. L., Danderfer Filho, A., de Lamotte, D. F. 2012. Structural modeling based on sequential restoration of gravitational salt deformation in the Santos Basin (Brazil). Marine and Petroleum Geology, 35(1), 337-353. https://doi.org/10.1016/j.marpetgeo.2012.02.009

Guerra, M. C., Underhill, J. R. 2012. Role of halokinesis in controlling structural styles and sediment dispersal in the Santos Basin, offshore Brazil. Geological Society, London, Special Publications, 363(1), 175-206. https://doi.org/10.1144/SP363.9

Hudec, M. R., Jackson, M. P. 2022. Salt tectonics in deepwater settings. In: Rotzien, J. R., Yeilding, C.A., Sears, R.A., Hernández-Molina, F.J., Catuneanu, O. (eds) Deepwater Sedimentary Systems. Elsevier, 149-177p. https://doi.org/10.1016/B978-0-323-91918-0.00020-7.

Hudec, M. R., Jackson, M. P., Schultz-Ela, D. D. 2009. The paradox of minibasin subsidence into salt: Clues to the evolution of crustal basins. Geological Society of America Bulletin, 121(1-2), 201-221. https://doi.org/10.1130/326275.1

Jackson, M.P.A., Talbot, C.J., 1991. A glossary of salt tectonics. Geological Circular, vol. 91-4. The University of Texas at Austin, Bureau of Economic Geology. 44 pp.

Kukla, P. A., Strozyk, F., & Mohriak, W. U. 2018. South Atlantic salt basins – witnesses of complex passive margin evolution. Gondwana Research, 53, 41-57. https://doi.org/10.1016/j.gr.2017.03.012

Modica, C. J., Brush, E. R. 2004. Postrift sequence stratigraphy, paleogeography, and fill history of the deep-water Santos Basin, offshore southeast Brazil. AmericanAssociation of Petroleum Geologists Bulletin, 88(7), 923-945. https://doi.org/10.1306/01220403043

Moreira, J.L.P., Madeira, C.V., Gil, J.A., Machado, M.A.P. 2007. Bacia de Santos. Boletim de Geociências da PETROBRAS, 15(2), 531-549.

Poprawski, Y., Basile, C., Cumberpatch, Z., Eude, A. 2021. Mass transport deposits in deep-water minibasins: Outcropping examples from the minibasins adjacent to the Bakio salt wall (Basque Country, Northern Spain). Marine and Petroleum Geology, 132, 105194. https://doi.org/10.1016/j.marpetgeo.2021.105194

Sobiesiak, M. S., Kneller, B., Alsop, G. I., Milana, J. P. 2018. Styles of basal interaction beneath mass transport deposits. Marine and Petroleum Geology, 98, 629-639. https://doi.org/10.1016/j.marpetgeo.2018.08.023

SUPPLEMENTARY MATERIAL 2

SALT WALLS
what can they tell us about northern Santos Basin halokinetic evolution?

Giovana Rebelo Diório, Barbara Trzaskos
g.rebelo.d@gmail.com
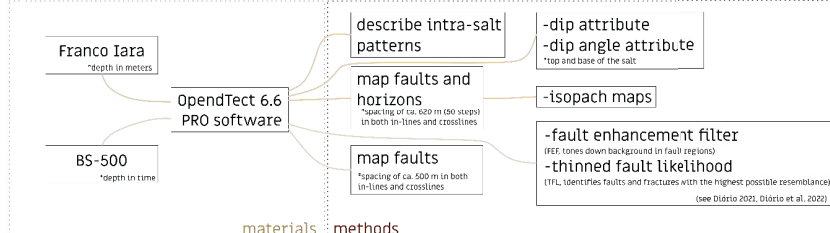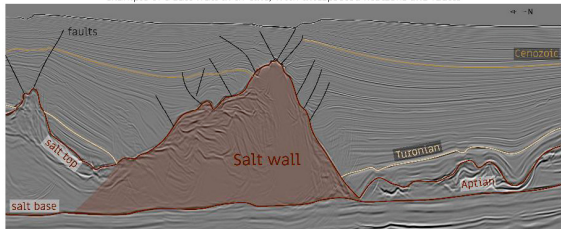barbaratrzaskos@ufpr.br
LABAP, UFPR

Keywords: Salt tectonics, seimic mapping, mock-turtle anticlines, crestal grabens, listric faults.

XII Simpósio Sul-Brasileiro de Geologia - Florianópolis

LABAP — Laboratório de Análise de Bacias
PÓS-GRADUAÇÃO GEOLOGIA - UFPR
UFPR — UNIVERSIDADE FEDERAL DO PARANÁ

INTRODUCTION

Salt tectonics are responsible for remarkable deformations in sedimentary basins (Hudec & Jackson 2007, Jackson & Hudec 2017). One is Santos Basin, located in offshore Brazil (Moreira et al. 2007). The Aptian evaporitic unit (Ariri Formation) controlled the deposition and deformed the subsequent marine drift sequence, and multiple studies analyze the halokinetic evolution of the area using regional data (e.g. Assine et al. 2008, Caldas & Zalán 2009, Guerra & Underhill 2012). But can a single salt body help in this interpretation?

This study focused on **characterizing deformations related to major** (>20 km wide) **salt walls** (i.e. diapirs that have a discordant contact with overlaying rocks, with an elongated sinuous shape in plan view), with an NE/SW direction, that occur in northern Santos Basin, in the halokinetic transitional domain.

Cabo Frio Fault (CFF) system

example of a salt wall in in-line, with interpreted horizons and faults

faults
Cenozoic
salt top
Salt wall
salt base
Turonian
Aptian

METHODOLOGY

Franco Iara
*depth in meters

BS-500
*depth in time

OpendTect 6.6 PRO software

describe intra-salt patterns
-dip attribute
-dip angle attribute
*top and base of the salt

map faults and horizons
*spacing of ca. 620 m (50 steps) in both in-lines and crosslines
-isopach maps

map faults
*spacing of ca. 500 m in both in-lines and crosslines
-fault enhancement filter
(FEF, tones down background in fault regions)
-thinned fault likelihood
(TFL, identifies faults and fractures with the highest possible resemblance)
(see Diório 2021, Diório et al. 2022)

materials | methods

RESULTS

① Salt walls

Salt thickness
-ENE/WSW direction
-ca. 3 km thick

Salt top
-depth of ca. 2.7 km to

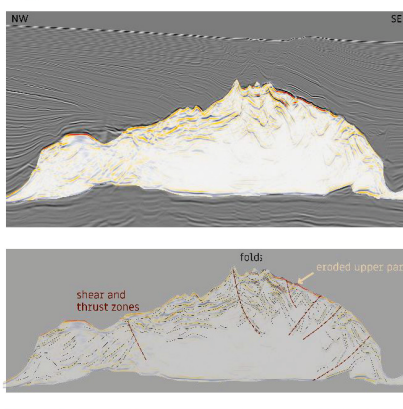-dip angles up to ca. 20 degrees towards the north and ca. 50 degrees towards the south

-asymmetric
modified from Diório (2021)

Salt base
-varying depth, anges up to 20 degrees

② Intra-salt

NW | SE

folds
eroded upper part
shear and thrust zones

Listric faults
-southern part of salt walls
-displace Cenozoic sediments
-dip towards crestal grabens

Mock-turtle anticlines
-formed by salt evacuation and indicative of collapse
-observed mostly in northern region, towards the extensive salt domain

En échelon faults
-subparallel closely-spaced structures oblique to the main structural trend
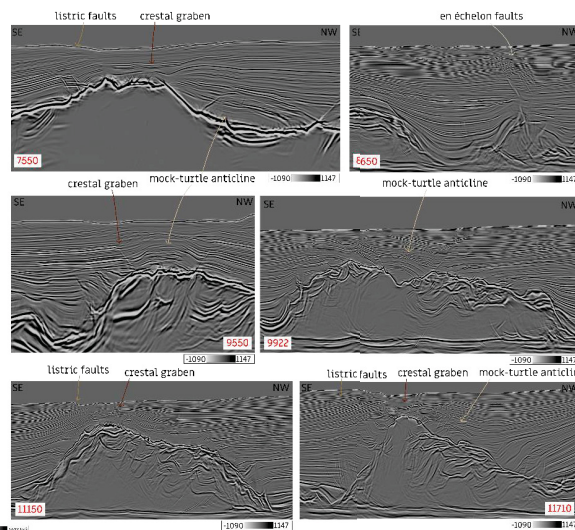-dip towards the north
-found where salt walls connect

③ Faults

Crestal grabens
-synthetic and antithetic conjugated faults
-directly above and following the crest of salt structures
-commonly perpendicular to the basin's dip
-anastomosed kilometric fault planes
-affect all drift units

(TFL) z-slice
Basin dip
in-line 9375
5 km
-3318
3359 (ms)
modified from Diório (2021)

SE | NW — listric faults, crestal graben | en échelon faults
7550 | 6650
crestal graben, mock-turtle anticline | mock-turtle anticline
9550 | 9922
listric faults, crestal graben | listric faults, crestal graben, mock-turtle anticline
11150 | 11710
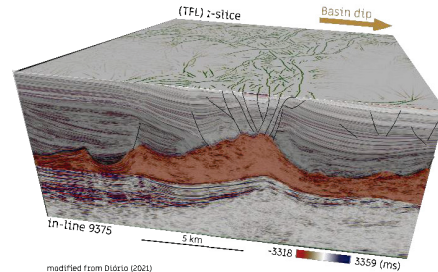
DISCUSSION

Based on the features discribed above and other references, we were able to propose a schematic evolution model for these salt walls:

initial salt movement
Progradation of the overburden pushed salt basinward and formed a landward-dipping fault, where salt served as detachement (Mohriak et al., 1995).
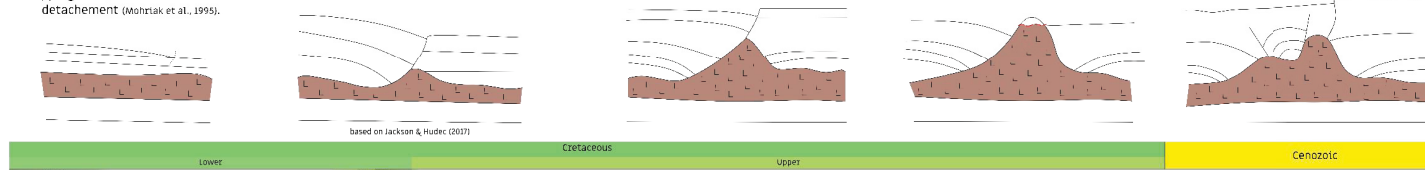
reactive and latter active diapirism
Salt rise initially related to the development of the Cabo Frio Fault System, forming intra-salt contractional features and its asymetric shape
based on Jackson & Hudec (2017)

erosion

salt colapse
mock-turtle anticlines

Aptian | Turonian | Lower | Upper | Cretaceous | Cenozoic

CONCLUSION

This characterization aids in the interpretation of the evolution of salt tectonics in this area of the basin, once these features indicate an early shortening stage, followed by significant extension and collapse as salt migrated further into the basin.

REFERENCES

Assine, M. L., Corrêa, F. S., Chang, H. K. 2008. Migração de depocentros na Bacia de Santos: importância na exploração de hidrocarbonetos. Brazilian Journal of Geology, 38(2), 111-127.

Caldas, M. F., Zalán, P. V. 2009. Reconstituição cinemática e tectono-sedimentação associada a domos salinos nas águas profundas da Bacia de Santos, Brasil. Boletim de Geociências da Petrobras, 17(2), 227-248.

Diório, G. R. 2021. Halorinese e Sedimentação na Porção Sudeste do Bloco BS-500. TCC, Curso de Geologia, UFPR.

Diório, G. R., Trzaskos, B., Assis, V. S. R. 2022. Use of seismic attributes to support fault tracing in Santos Basin Post-Salt sequences. In: Resumos expandidos do IX SBGeof, 2022. Curitiba.

Guerra, M. C., Underhill, J. R. 2012. Role of halokinesis in controlling structural styles and sediment dispersal in the Santos Basin, offshore Brazil. Geological Society, London, Special Publications, 363(1). 175-206. https://doi.org/10.1144/SP363.9

Hudec, M. R., Jackson, M. P. 2007. Terra infirma: Understanding salt tectonics. Earth-Science Reviews, 82(1-2), 1-28. https://doi.org/10.1016/j.earscirev.2007.01.001

Jackson, M. P., Hudec, M. R. 2017. Salt tectonics: Principles and practice. Cambridge University Press, 510p. https://doi.org/10.1017/9781139003988

Mohriak, W. U., J. M. Macedo, R. T. Castellani, H. D. Rangel, A. Z. N. Barros, M. A. L. Latgé, J. A. Ricci, A. M. P. Mizusaki, P. Szatmari, L. S. Demercian, J. G. Rizzo, J. R. Aires, 1995, Salt tectonics and structural styles in the deep water province of the Cabo Frio region, Rio de Janeiro, Brazil. inM. P. A. Jackson, D. G. Roberts, and S. Snelson, eds. Salt tectonics: a global perspective: AAPG Memoir 65, p. 273–304.

Moreira, J. L. P., Madeira, C. V., Gil, J. A., Machado, M. A. P. 2007. Bacia de Santos. Boletim de Geociências da PETROBRAS, 15(2), 531-549.